Development of *Debaryomyces hansenii* as a Host for Biotechnology

Sondos Abdullah Alhajouj

This Thesis is Submitted to the University of Sheffield for the degree of Doctor of Philosophy

Faculty of Science

Department of Bioscience

September 2022

Abstract

This study undertakes an analysis of the yeast *Debaryomyces hansenii* and its potential in biotechnology. Biotechnology is the process of using living organisms in technology. Bacteria and yeasts are some of the microorganisms used in biotechnology, and the reasons why are discussed herein. The focus will be on *Debaryomyces hansenii*, a stress-resistant organism that has a strong potential for use in biotechnology, and which can grow at high salinity and a low pH. *D. hansenii* produces toxic chemicals which kill other yeasts, this is important for the prospective control of yeast infections. In biotechnology*, D. hansenii* is used for the production of compounds such as xylitol, ethanol, bioflavour products, and meat fermentation. Peroxisomes play an essential role in fatty acid β-oxidation (Wanders, 2004); fatty acids have a range of industrial applications. Peroxisomes are small yet important organelles found in most eukaryotic cells, and they have different functions in the different organisms of plants, animals, and fungi. The absence of peroxisomes causes Zellweger's syndrome in humans. There are two peroxins, Pex3 and Pex19, which are required for the import of peroxisomal membrane proteins (PMPs). The absence of Pex3 and Pex19 will cause the yeast's corresponding absence of peroxisomes. The aims of the study are (i) to establish an efficient genome modification approach (ii) to describe some physiological aspects important for biotechnology with the goal of identifying strains valuable for industry; (iii) to gain a better understanding of fatty acid metabolism. The lack of molecular tools is the main challenge in studying *D. hansenii*: in this study, a set of molecular tools were developed that allow targeted genome modifications in *D. hansenii*. This study is the first to describe a PCR-mediated gene targeting method that uses short homology flanks (50bp) for homologous recombination (HR) in *D. hansenii*. Analysis of 13

different isolates identifies NCYC 3363 as a promising strain to use in metabolic engineering and Biotechnology. In addition, various factors affecting the growth of *D. hansenii* were tested. Finally, lipid accumulation was examined in two strains of *D. hansenii* that are deficient in fatty acid breakdown and channel glycerol into triacylglycerol biosynthesis. These mutants display increased neutral lipid accumulation, and our findings are interesting for future biotechnological applications.

Acknowledgements

I am extremely grateful to Dr Ewald Hettema for his help and support. He was kind and supportive. His office was open to us all the time. He was a remarkable supervisor; my thesis would not be the way it is today if it is not for him. I am deeply indebted to Dr Donald Watts for his valuable advice throughout my thesis. I would like to extend my sincere thanks to my second supervisor Dr Stephane Mesnage he was supportive whenever I needed him.

Special thanks to the members of the E28 lab, for their help, encouragement, and friendship: Dr Lakhan Ekal, Dr Georgia Hulmes, Abdulaziz Alqahtani, Afroza Begum, Ibrahim Sumaily, Jenny Harris, Nourah Nayef, Quentin Levicky, Selva Turkolmez, Tarad Abalkhail, and Yousef Alhammad.

I gratefully acknowledge the University of Sheffield for allowing me to use their laboratory, and equipment, the staff were friendly and helpful.

Thanks, should also go to Jouf University for sponsoring my education and giving me this opportunity to complete my PhD, if it is not for them, I would not be here.

I would like to thank my spouse Ahmed for his effort and love, and my lovely children: Hussain, Zainab, Mohammed, and Doaa for their patience with me.

I would also like to thank my friends, and neighbours for their assistance and inspiration, especially during the pandemic.

I appreciate my parents' support and love throughout my PhD journey. They were always there for me when I needed them.

Table of Contents

Abbreviations

ACT1 – Actin structural protein in cytoskeleton

C. albicans – *Candida albicans*

C/N – carbon-nitrogen ratio

D. hansenii – *Debaryomyces hansenii*

DMSO – dimethyl sulfoxide

E. coli – *Escherichia coli*

EDTA – Ethylenediamine tetraacetic acid

ER – Endoplasmic reticulum

FADH – flavin adenine dinucleotide

GFP – green fluorescence protein

G3P – glycerol 3 phosphate

HCL – hydrochloric acid

HR – homologous recombination

LB – lipid bodies

MCS – multiple cloning site

NaCl – sodium chloride

NADH – nicotinamide adenine dinucleotide

OD – optical density

ORF – open reading frame

PCR – polymerase chain reaction

PMP – peroxisomal membrane protein

PTS – peroxisomal targeting signal

PTS1 – peroxisomal targeting signal I

PTS2 – peroxisomal targeting signal II

SAT1 – gene coding for nourseothricin resistance marker

S. cerevisiae – *Saccharomyces cerevisiae*

S. stipitis – *Scheffersomyces stipitis*

TAG – triacylglycerol

TEF1 – translational elongation factor EF-1 alpha

Y. lipolytica – Yarrowia lipolytica

YM deb – yeast media for *Debaryomyces hansenii*

YPD – yeast extract peptone dextrose media

List of Figures

List of Tables

Chapter1

Introduction and Literature Review

1. Background:

Biotechnology uses microorganisms to produce other materials. One of the reasons for the increasing interest in using microbial metabolic activities in the biotechnological production of chemicals is the finite supply of mineral oil resources (Mattanovich, Sauer and Gasser, 2014). One group of microorganisms is bacteria. They are used in biotechnology to produce many different resources. Some examples of the biotechnological processes carried out by bacteria are milk fermentation, pyruvate formation, and the production of proteins, drugs, and enzymes (McKay and Baldwin, 1990; Vieira Gomes *et al.*, 2018). Some bacteria such as *Lactococcus lactis* are responsible for flavour and aroma production in cultured dairy products (McKay and Baldwin, 1990).

Another group of microorganisms used in biotechnology are yeasts. Yeasts are preferred in biotechnology over bacteria in certain processes because they have low nutritional requirements, and the ability to achieve the post-translational adaptations needed for producing biologically active proteins (Vieira Gomes *et al.*, 2018). In addition, yeasts are used in biotechnology in the production of metabolites, and the production of recombinant proteins (Mattanovich, Sauer and Gasser, 2014). *Saccharomyces cerevisiae* has been the most studied yeast in food and drink production. *S. cerevisiae's* remarkable molecular genetic characterization allows the yeast to be used for many years to produce heterologous proteins such as insulin, and the hepatitis B surface antigen (Mattanovich, Sauer and Gasser, 2014). Moreover, *S. cerevisiae* has been used for thousands of years for production of alcohol and later leavening bread (Zhang *et al.*, 2015). *S. cerevisiae* is not always the preferred host to

use in biotechnology, so industries have started to look for other yeasts which are more stress resistant, and which have a high potential in biotechnology. Several yeasts are found to be more efficient in the production of many recombinant proteins (Mattanovich, Sauer and Gasser, 2014). *Debaryomyces hansenii* is another stress-resistant yeast that has a strong potential for biotechnology. In this study, the biotechnological potential of *D. hansenii* is considered, and the emphasis will be on constructing new molecular tools, the factors affecting *D. hansenii* and fatty acid metabolism.

2. The Advantages of *Debaryomyces hansenii*:

Debaryomyces hansenii is an extremophile, osmotolerant, and non-pathogenic yeast from the family of *Saccharomycetaceae. D. hansenii* is an ascomycetous yeast, which reproduces by multilateral budding (Mishra and Baranwal, 2009). It is found in salty environments such as the sea and in salted food (Prista *et al.*, 2005). *D. hansenii* can grow in high amounts of salt such as 4 M NaCl, on the other hand, *S. cerevisiae* can grow up to 1.7 M NaCl (Aggarwal and Mondal, 2009). *D. hansenii* is found in cheese, sausages, soy sauce, and brines. In these food environments, *D. hansenii* is exposed to additional stress conditions that are more impactful than the high salt content, such as low pH, high and low temperatures, and the presence of preservatives. *D. hansenii* can tolerate all these stresses (Almagro *et al.*, 2000). The osmo-tolerance of *D. hansenii* is important in biotechnology because it resists contamination (Johnson, 2011). Gientka et al., (2017) state that *D. hansenii* is one of the oleaginous yeasts, which can store more than 20% of its biomass as neutral lipids. The ability to store large amounts of lipids enables the profitable potential of biodiesel generation and production of lipids or lipid derivatives. In addition, *D. hansenii* produces toxic chemicals which kill other yeasts, important for the prospective control

of yeast infections (Johnson, 2011). The review of the literature shows that *D. hansenii* has the ability to bear high levels of nitrite and to also utilise it as a nitrogen source (Vigliotta *et al.*, 2007). It also has the ability to resist the powerful biocide chlorine dioxide (CIO2) (Ramírez-Orozco, Hernández-Saavedra and Ochoa, 2001).

D. hansenii is a favoured host for biotechnology in some cases, however, and unlike *S. cerevisiae,* it usually reads CTGs codons, a common codon for leucine, as serine (Jeffries and Cregg, 2010). In addition, little research has been done on *D. hansenii*, so there are few molecular tools available to use when studying this yeast. The whole genome of *D. hansenii* has been sequenced and annotated by the consortium Genolevures and is now available at http://cbi.labri.fr/Genolevures/ (Dujon *et al.*, 2004; Aggarwal and Mondal, 2009).

Even though most *D. hansenii* isolates are thought to be haploid, further studies have shown heterogeneity in genome size and genome duplication. The examination of the genome showed that diploid heterozygous strains had a significant loss of heterozygosity (Petersen and Jespersen, 2004; Jacques *et al.*, 2015). Further translocation can generate multiple alleles of different sizes, and some strains are diploid or even aneuploid (Petersen and Jespersen, 2004). Chromosome number variations have also been reported in many other yeast species. (Petersen and Jespersen, 2004; Jacques, Mallet and Casaregola, 2009; Jacques *et al.*, 2010). The size of the genome varies among different *D. hansenii* strains.

3. Biotechnology:

D. hansenii can be used in different production processes. This section will summarize six of these different processes.

3.1 Xylitol production:

Gírio et al.(2000) point out that *D. hansenii* produces polyols (xylitol, arabitol) from pentose sugar. Xylitol was the major polyol produced by *D. hansenii* in all the

culture conditions tested. Domínguez et al.(1999) demonstrate that *D. hansenii* is one of the best xylitol-producing yeasts. Xylitol is a natural sweeter; a five-carbon polyols (Converti, Perego and Domínguez, 1999; Domínguez *et al.*, 1999). Xylitol is important in biotechnology because it is currently being used in marketable products such as mouthwash, chewing gum, toothpaste, sweets, and medicines (Leathers and Gupta, 1997). Xylitol can be gained by several technologies, including (i) abstraction from some fruits and vegetables, a technique which is costly because of its low concentrations. (ii) Chemical demotion of xylose; this procedure is reasonably expensive because of the vast purification and segregation steps needed. (iii) Biotechnological alteration of xylose solutions which is a selective and promising method for the production of xylitol (Domínguez *et al.*, 1999). Xylitol is also used to treat various diseases such as diabetes, hemolytic anemia, and inflammatory processes (López-Linares *et al.*, 2018). Several studies provided information on how *D. hansenii* xylose reductase converts xylose into xylitol using wood hydrolysates as feedstock (Converti, Perego and Domínguez, 1999; Converti and Dominguez, 2001; Rivas *et al.*, 2003; López-Linares *et al.*, 2018).

3.2 Ethanol production:

Brooks (2008) research tended to show the ability of *D. hansenii* to produce ethanol from banana peels. *D. hansenii* was able to produce ethanol under high respiratory activity and under the fermentation of glucose (Gírio *et al.*, 2000; Sánchez *et al.*, 2006). The existing literature found that *D. hansenii* produced more ethanol under anaerobic conditions than under aerobic conditions (Sánchez *et al.*, 2006). Empirical evidence appears to confirm the notion that *D. hansenii* has the capability to produce ethanol because it is essential in biotechnology. Ethanol is used in the laboratory to sterilize benches to prevent bacteria and other fungal growth. It is also

used in car fuel, and it is one of the building blocks for ethylene and acetaldehyde when it is fermented (Danner and Braun, 1999).

3.3 Bioflavour production:

A previous study has demonstrated that *D. hansenii* can produce flavour compounds from tomato and pepper pomaces (Güneşer *et al.*, 2015). Flavour compounds are natural flavours produced by the metabolic pathway of the microorganism. (Güneşer *et al.*, 2015) noted some examples of flavour compounds are esters, aldehydes, ketones, and acids, and also that *D. hansenii* has the ability to produce fruity and rose-like flavours by microbial fermentation from certain wastes in the food industry. Bioflavour production is important in biotechnology because people prefer natural flavourings for their health over artificial flavourings, which is why studies about bioflavour production have increased (Güneşer *et al.*, 2015).

3.4 Meat fermentation:

D. hansenii is found in different types of meat such as dry fermented pork and llama sausages, pork fat, dry meat products (Spanish fermented sausages, loin pork) (Sørensen, 1997; Durá, Flores and Toldrá, 2004; Flores *et al.*, 2017; Ramos *et al.*, 2017). All these different types of meat have high salt concentrations. In the literature on *D. hansenii,* there seems to be general agreement that *D. hansenii* can hydrolyse fat to fatty acids. To achieve this, certain conditions need to be considered such as the time of incubation, temperature, and pH: all of these affect the breakdown of lipids (Sørensen, 1997). *D. hansenii* increases the lipolytic activity in meat, and it gives the typical flavour of sausages (Durá, Flores and Toldrá, 2004; Ramos *et al.*, 2017). *D. hansenii* has the ability to hydrolyse meat proteins, produce volatile compounds, and influence the sensory properties of the meat (Mishra and Baranwal, 2009).

3.5 Dairy products:

D. hansenii is generally found in cheese brine and raw milk cheese (Seiler and Busse, 1990; Padilla, Manzanares and Belloch, 2014). The high salt in the cheese brines and sausages shows the resistance of *D. hansenii* to NaCl. Some papers stress the importance of *D. hansenii* as a producer for Danablu, which is blue mould cheese, and the ability of *D. hansenii* to inhibit the germination of undesired microorganisms in cheese brines (Van Den Tempel and Jakobsen, 2000; Mishra and Baranwal, 2009). *D. hansenii* can produce proteolytic and lipolytic enzymes that can metabolize milk, proteins, and fat (Mishra and Baranwal, 2009). Boekhout, (2003) notes that cheese ripening affects the structure flora of *D. hansenii* and that the presence of *D. hansenii* increases both the pH value and the proteolytic activity in the cheese ripening pathway: the ability of *D. hansenii* to lower the concentration of lactic and acetic acids in cheese may prevent the growth of other microorganisms. In addition, *D. hansenii* generates a fruity, cheesy, acidic, and alcoholic aroma (Boekhout, 2003). Dairy products are important in biotechnology because they serve the increased demand of worldwide consumption of dairy products (Coffey, Daly and Fitzgerald, 1994). People use dairy products every day, they support the body with calcium.

3.6 Protein:

One study identifies the characteristics of *D. hansenii* as being a host for producing heterologous proteins (Jeffries and Cregg, 2010). Their research design involved proteolysis of protein to form free amino acids in *D. hansenii* (Durá, Flores and Toldrá, 2004). *D. hansenii* has the ability to produce a protein which is important in biotechnology because they serve as a source of biocatalysts for the production of high-value sufficient chemicals and protein medications (Johnson and Echavarri-Erasun, 2011b).

So far, this section has focused upon the use of *D. hansenii* in biotechnology, now the next section will discuss the importance of peroxisomes in cell metabolism and how that is important in producing more fatty acids in *D. hansenii*.

4. Peroxisomes:

Peroxisomes play a significant role in the fatty acid synthesis and cellular lipid metabolism (Wanders *et al.*, 2010). Peroxisomes are ubiquitous organelles found in many eukaryotic cells. They arise from the endoplasmic reticulum (ER) (Joshi *et al.*, 2018), and they enlarge and bud to produce new peroxisomes by growth and division (Motley and Hettema, 2007). Their functions differ from one organism to another. For example, in plants, peroxisomes play an important role in fatty acid β-oxidation, catalyse H_2O_2 to water and molecular oxygen, and photorespiration (Kao, Gonzalez and Bartel, 2017). Also, in mammals, peroxisomes play a role in several metabolic pathways such as plasmalogen biosynthesis, alpha and beta-oxidation of fatty acids, glyoxylate metabolism, lysine metabolism, oxygen metabolism, and polyamine metabolism (Wanders and Waterham, 2006).

In addition, in humans, peroxisomes have other pathways such as bile acid synthesis, cholesterol metabolism, purine and amino acid catabolism, and glyoxylate utilization (Subramani, 1992). Moreover, in yeasts, fatty acid β-oxidation and the glyoxylic acid cycle are the main pathways that occur only in peroxisomes (van Roermund *et al.*, 2003). Peroxisomes disorders can be classified into three classes: (i) Zellweger's syndrome is the loss of all peroxisomal function; (ii) β-oxidation enzyme deficiency, in which some, but not all, peroxisomal enzymes are absent; and (iii) thiolase deficiency results from the loss of individual peroxisomal enzymes (Subramani, 1992).

There are two types of protein targeting signals (PTS) for peroxisomal soluble proteins, the PTS1 and PTS2. The PTS1 is located at the carboxy-terminus, or the C-

terminus of proteins; the conserved sequence used by PTS1 is (S/A/C)-(K/R/H)-(L/M). On the contrary, the PTS2 is located at the amino-terminus or N-terminus, and the sequence is(R/K)-(L/I/V)-X5-(Q/H)-(L/I/V) (Wanders and Waterham, 2006). A PTS1 protein is recognized by a specific cytosolic receptor protein Pex5, (Figure 1). Meanwhile, a PTS2 uses the protein Pex7 as a receptor. These receptors (Pex5, and Pex7) bind cargo in the cytoplasm and transport it to the peroxisomal membrane, where there are specific docking sites containing Pex14 for PTS1 and Pex18 for PTS2, for the cargo-receptor complex. The Pex5 and Pex14 forms a pore through which cargo is transported. Once their cargo is delivered to the peroxisomal lumen, the receptors return back to the cytoplasm (Hettema *et al.*, 2014; Kim and Hettema, 2015). There are data on matrix proteins that cross the peroxisomal membrane but which do not contain PTS1 or PTS2 signals, these are in fact transported by binding to a protein with a PTS (Sibirny, 2016).

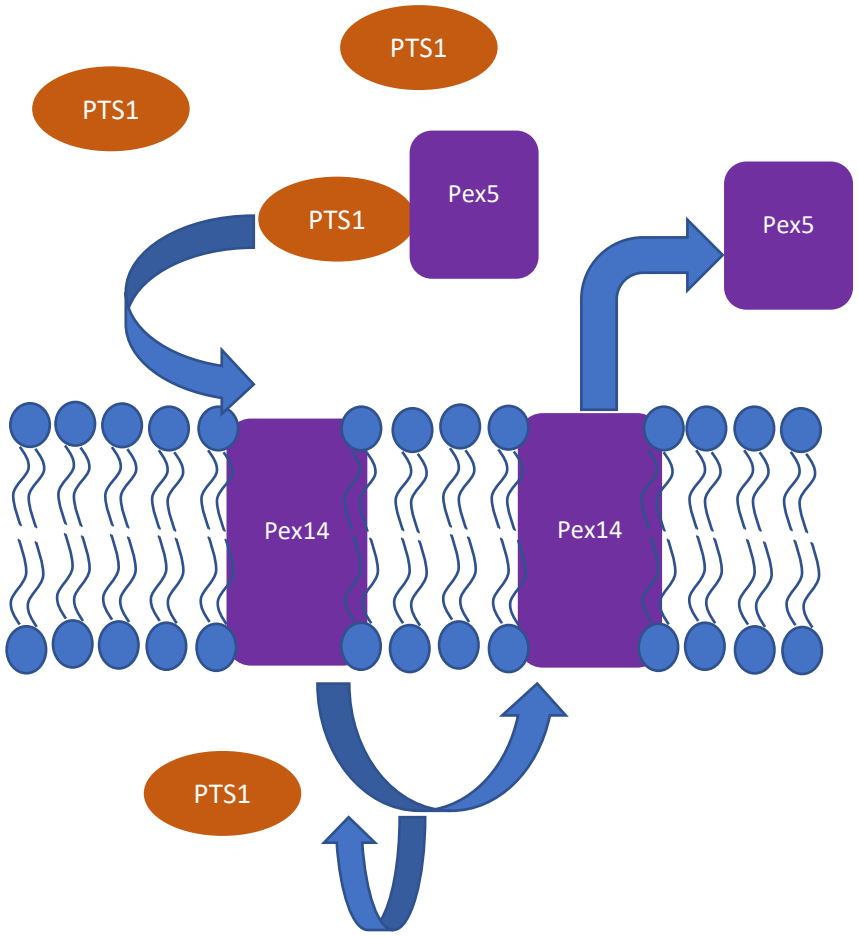

Figure 1 A model for the process of the PTS1 import pathway. A PTS1 protein is recognised by Pex5 in the cytosol and complex docks onto the peroxisomal membrane to a protein complex containing Pex14. Pex5 together with Pex14 form a pore through which the PTS1 containing cargo protein crosses the membrane and is released inside peroxisomes. Pex5 is then recycled. The PTS1 protein is represented in the orange oval, while the Pex5 and Pex14 are in purple.

In yeasts, there are two peroxins Pex3 and Pex19 which are required for the import of peroxisomal membrane proteins (PMPs) (Hettema *et al.*, 2000). Pex3 buds from the ER in a pre-peroxisomal vesicle (Hoepfner *et al.*, 2005) and functions as a docking receptor for Pex19 (Jones, Morrell and Gould, 2004). Pex3 is also required for peroxisome membrane biogenesis (Fang *et al.*, 2004). When knocking out *PEX3*

formation of peroxisomes will be blocked thereby disabling fatty acid β-oxidation in yeasts.

5. Fatty Acid β-oxidation:

In plants and most of the fungi, β-oxidation occurs only in peroxisomes, but in other eukaryotics, β-oxidation occurs in both peroxisomes and mitochondria (Wanders and Waterham, 2006). Fatty acid β-oxidation is the breakdown of lipids to acetyl-CoA in four different steps. At the beginning of the β-oxidation the activation of fatty acids to acyl-CoA by acyl-CoA synthetase is required as shown in Figure 2 (van Roermund *et al.*, 2003). The first step is dehydrogenation, which is removing a hydrogen atom from the alpha and beta carbons and forming a double bond between them. The compound formed is 2-trans-enoyl-CoA which is catalyzed by acyl-CoA oxidase as in Figure 3 (van Roermund *et al.*, 2003). Electrons from $FADH_2$ are transferred directly to O_2 creating H_2O_2, and the energy is released as heat because peroxisomes do not have a respiratory chain (Lodhi and Semenkovich, 2014).

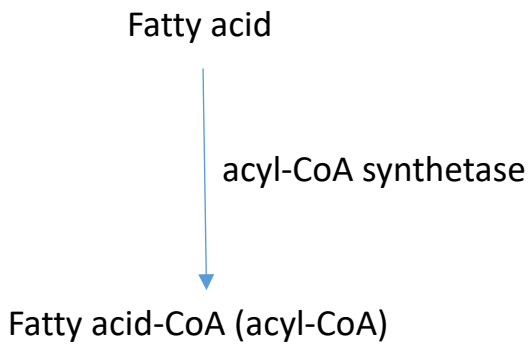

Figure 2 The activation of fatty acid to acyl-CoA by Acyl-CoA synthetase.

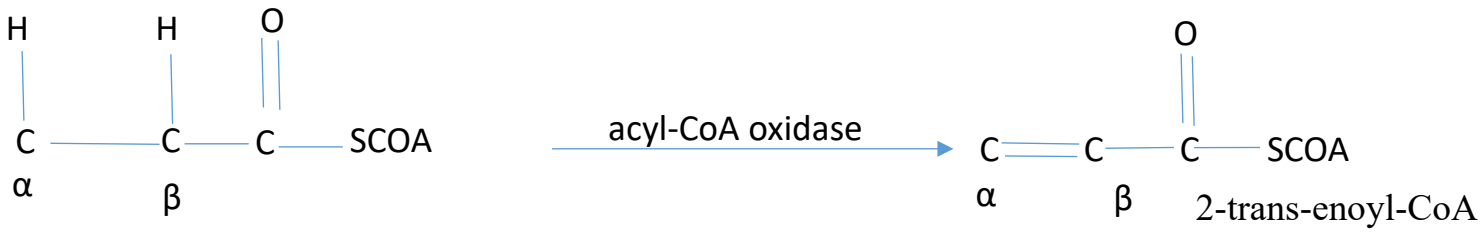

Figure 3 The first step in β-oxidation which is dehydrogenation, which is removing a hydrogen atom from the alpha and beta carbons and forming a double bond between them.

The second and third steps are catalyzed by a multifunction enzyme called FOX2, which performs a hydration process first to form 3- hydroxyl acyl-CoA. The enzyme used in this step is the 2-enoyl-CoA hydratase. Then a dehydrogenation process, which is catalyzed with 3 -hydroxyl acyl-CoA dehydrogenase, forming 3-keto acyl-CoA as in Figures 4, and 5 (van Roermund *et al.*, 2003; Lodhi and Semenkovich, 2014). During this step, $NADH+H^+$ is reoxidised to NAD^+ by redox shuttles (Al-Saryi *et al.*, 2017).

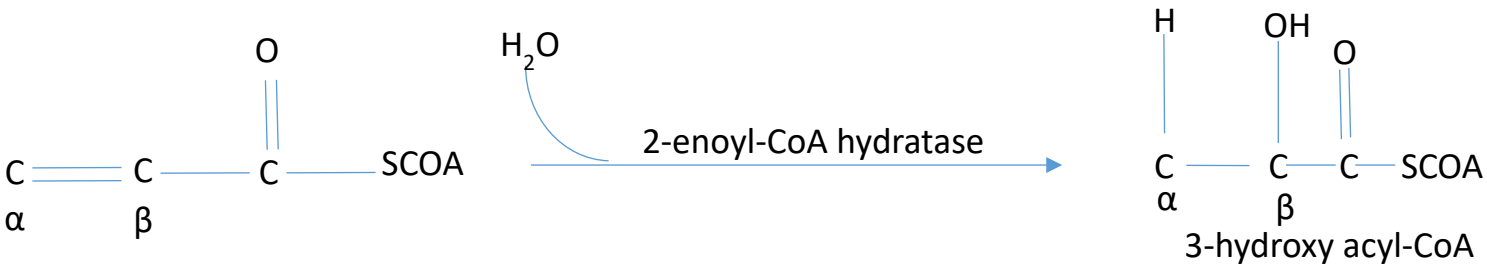

Figure 4 The second step in the fatty acid β-oxidation, the FOX2 multifunctional enzyme, which does a hydration process first to form 3- hydroxyl acyl-CoA. The enzyme used in this step is 2-enoyl-CoA hydratase.

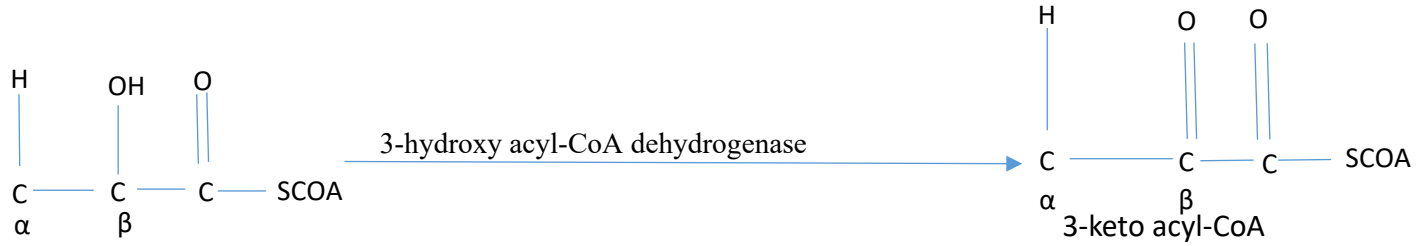

Figure 5 The third step in the fatty acid β-oxidation, the FOX2 multifunctional enzyme, which does a dehydrogenation process, which is catalyzed with 3 -hydroxyl acyl-CoA dehydrogenase forming 3- keto acyl-CoA.

The last step in β-oxidation is thiolysis, which breaks down 3- keto acyl-CoA to acetyl-CoA and fatty acid-CoA by thiolase as in Figure 6 (van Roermund *et al.*, 2003). The fatty acid-CoA enters β-oxidation again until it is entirely broken down into acetyl-CoA (Allenbach and Poirier, 2000). Figure 7 gives an overview of the whole β-oxidation process. β-oxidation is essential in cell metabolism because it generates energy and carbon for the cell, and it is dedicated to fatty acid degradation (Poirier *et al.*, 2006).

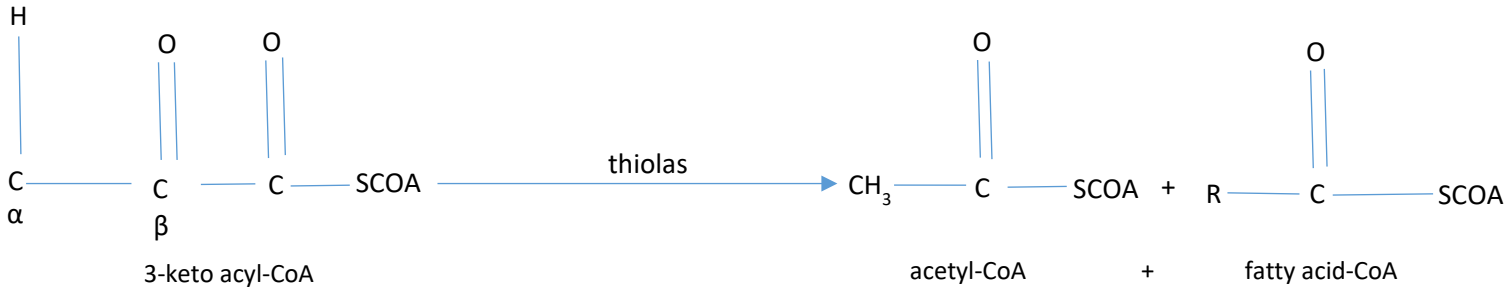

Figure 6 The last step in β-oxidation is thiolysis, which breaks down 3- keto acyl-CoA to acetyl-CoA and fatty acid-CoA by thiolase.

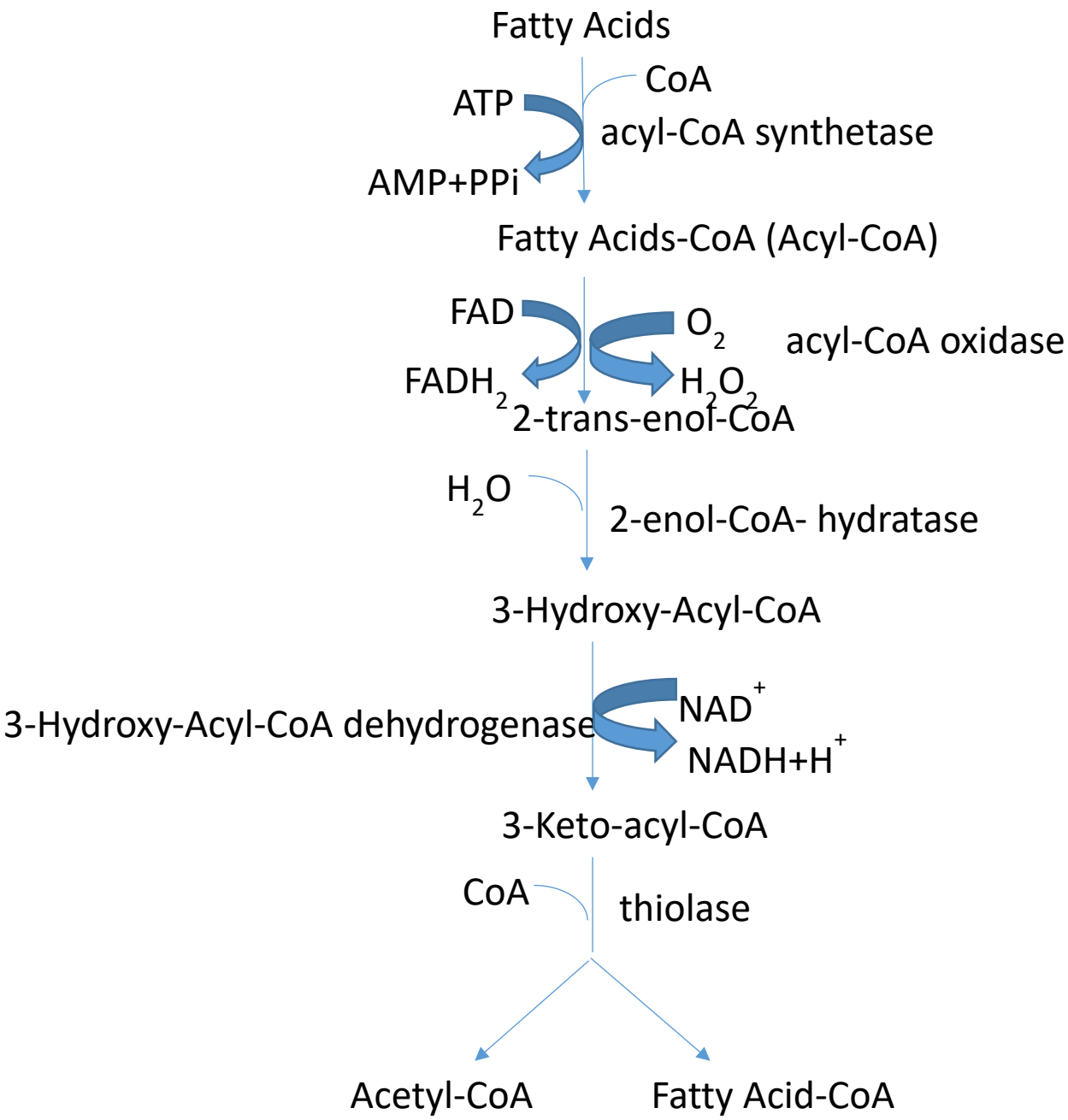

Figure 7 Fatty acid β-oxidation in peroxisomes. The process consists of 4 enzymatic reactions. oxidase, hydratase, dehydrogenase, and thiolase. The fatty acid-CoA enters β-oxidation again until it is entirely broken down into acetyl-CoA.

From the information mentioned above, β-oxidation consists of four enzymatic reactions which comprise oxidase, hydratase, dehydrogenase, and thiolase activity. Another oxidation occurs in peroxisomes which is α-oxidation. This happens when the fatty acid contains 3-methyl groups which interfere with β-oxidation. Hence, α-oxidation shortens the fatty acid, to give a free fatty acid, which can be further processed by β-oxidation. α-oxidation contains three reactions which are hydroxylation, lysis, and aldehyde dehydrogenation (Wanders and Waterham, 2006). In the literature, some papers gave information about how fatty acids enter peroxisome, via several pathways one is for free fatty acids by a protein-facilitated process or by passive flip-flopping, and the second is for activated fatty acids by Pat proteins, which are peroxisomal ABC transporters, and one by porin Pxmp2 (Hettema *et al.*, 1996; Hettema and Tabak, 2000; Visser *et al.*, 2007; Van Roermund *et al.*, 2012).

The previous section focused upon the functions of peroxisomes, the important pathways carried within them, and how deleting the *PEX3* gene causes the production of fatty acids. The next part of this study will be concerned with the literature review on knocking out genes in other yeasts, and the CRISPR/Cas9 system in *D. hansenii*.

6. The literature review on gene deletion, and CRISPR/Cas9

Baudin *et al.*, (1993) describes that in *S. cerevisiae* gene disruption was accomplished by PCR amplification for the selectable marker and two flanked regions away from the ORF. In addition, Kaur, Ingavale and Bachhawat, (1996) explains in *Schizosaccharomyces pombe* the gene deletion was conducted by PCRing the oligonucleotides with 40bp flank from both sides of the targeted gene. . Hegemann *et al.*, (2014) defines that the one step deletion method in *S. cerevisiae* and *S. pombe* is integrated with a LoxP sit if the marker needed to be used again for

another gene deletion a Cre-recombinase reaction will happen. In this study, it was desirable to set the same system in *D. hansenii*. Reuß *et al.*, (2004) explains that in *Candida albicans* the SAT1 marker with *ACT1* promoter and *URA3* terminator can be used in gene deletion by homologous recombination. This marker was used in this study for the deletion of *PEX3* gene. Moreover, Nett *et al.*, (2005) defines that since in *Pichia pastoris* there is few selectable markers they set to develop some auxotrophic markers by deleting *ARG1* and *HIS1* genes. *The ARG1* gene was deleted in this study to generate a new deletion method in *D. hansenii*. A number of studies (Spasskaya *et al.*, 2021; Strucko *et al.*, 2021) investigated the CRISPR/ Cas9 in *D. hansenii*, they were able to generate the CRISPR/Cas9 system in this yeast. To do that some steps needed to be taken care off first, (i) replace all the CTG codons in Cas9 gene to leucine. (ii) small RNAs and heterologous proteins, and the corresponding optimal promoters need to be identified, (iii) to transform *D. hansenii* usage of a highly effective conversion system is recommended. Spasskaya *et al.*, (2021) explains that the Cas9 gene was under the control of different promoters, *TEF1* promoter gave the highest efficiency in *D. hansenii*; Cas9 was also stimulated at 20-22^{o}C.The CRISPR system was able to delete genomic regions to completely inactivate genes that encodes the proteins and long noncoding RNAs. It was also, used to regulate transcription of proteasomal genes. The CRISPR/Cas9 method was verified by the deletion of *ADE2* gene because by deleting of *ADE2* gene the cells will be red in colour. By further analysis, most of the *D. hansenii* genes are CRISPR targeted (Spasskaya *et al.*, 2021). This system allowed scientists to modify the genome of *D. hansenii* easily.

The following section will discuss the literature review on lipid accumulation in *Yarrowia lipolytica*.

7. Lipid accumulation:

The review of the literature shows that *Yarrowia lipolytica* is used as a model microorganism as one of the oleaginous yeasts for producing lipid because it can store more than 20% of its biomass as neutral lipids and the availability of its genomic tools. The lipids in *Y. lipolytica* were stored in the form of triacylglycerol (TAG) (Beopoulos *et al.*, 2009; Ledesma-Amaro and Nicaud, 2016; Fakas, 2017; Gálvez-López *et al.*, 2019; Kamineni *et al.*, 2021). Lipids are essential for starting materials in the food, cosmetics, biodiesel, raw materials for the fuel, and biochemical industries (Qiao *et al.*, 2017; Kamineni *et al.*, 2021). Lipid synthesis in *Y. lipolytica* take place in the cytosol. First, the glucose is phosphorylated to glucose-6-phosphate by hexokinase using ATP. Glucose-6-phosphate is isomerized to fructose-6-phosphate by phosphoglucoisomerase. Fructose-6-phosphate is catalyzed by phosphofructokinase-1 to produce fructose-1,6-bisphosphate. The aldolase enzyme catalyzes the fructose-1,6-bisphosphate to glyceraldehyde-3-phosphate and dihydroxyacetone phosphate (DHAP) (Miesfeld and McEvoy, 2017)**.** DHAP is phosphorylated to glycerol-3-phosphate (G3P) by G3P dehydrogenase. G3P is acylated to lysophosphatidic acid (LPA) by G3P acyltransferase (SCT1), and then further acylated to phosphatidic acid (PA) by LPA acyltransferase (SLC1). This is followed by dephosphorylation of PA with PA phosphohydrolase (pAp) which releases diacylglycerol (DAG). In the final step, DAG is acylated by phospholipid DAG acyltransferase (LRO1 containing the glycerophospholipids as an acyl donor) to produce the TAG (Beopoulos *et al.*, 2009) (Figure 8). Similar to *Y. lipolytica*, *D. hansenii* is an oleaginous yeast, which can store more than 20% of its biomass as neutral lipids (Gientka *et al.*, 2017): fatty acids are used in industry, cosmetics, and in cleaning products such as mouthwashes, and soaps.

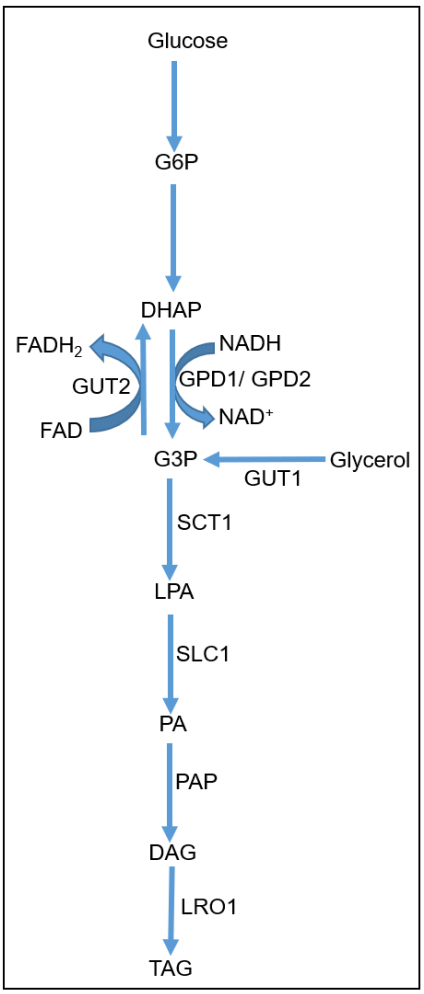

Figure 8 lipid synthesis in the yeast Yarrowia lipolytica, showing the pathway of TAG triacylglycerids synthesis.

The previous section discussed the literature review on lipid accumulation in *Y. lipolytica.* The next part will examine the aims of this study.

8. Aims:

The lab aims to establish *D. hansenii* as a host for biotechnology, particularly as a production host for fatty acids. My aims within this research group are (i) to establish an efficient genome modification approach, (ii) to describe some physiological aspects important for biotechnology with the goal of identifying strains valuable for industry; (iii) to gain a better understanding of fatty acid metabolism.

The following Chapter will be about the Materials and Methods used in this study. After that, Chapter 3 will discuss the development of new molecular tools used to work with *D. hansenii* and the foundation of the new PCR-mediated gene deletion method with a 50bp flank size for homologous recombination (HR). Chapter 4 will then describe some of the factors affecting growth of *D. hansenii*, while Chapter 5 will describe lipid accumulation and Chapter 6 will discuss the thesis.

Chapter2:

Materials and Methods

2.1 Bioinformatics analysis

Uniprot, National Center for Biotechnology Information (NCBI) nucleotide database, Saccharomyces Genome Database (SGD), add gene, the Kyoto Encyclopedia of Genes and Genomes (KEGG), and Scan Prosite were researched for gene and protein functions, regulations, expressions, and interactions. These websites were used to get the sequence of the *ARG1, PEX3*, *GUT2, and FOX2* genes. Multiple DNA sequence alignments we performed using ClustalW and Clustal Omega (Lassmann T., 2009).

2.2 Chemicals, Enzymes, DNA molecules, and growth media

Most chemicals and, materials used in this study were supplied by Sigma-Aldrich. DNA polymerases and buffers were supplied by Bioline and the restriction enzymes and buffers were supplied by New England Biolabs. Miniprep Kits for plasmid DNA isolation were supplied by Biobasic, and the gel extraction kits were supplied by Qiagen. DNA sequence was ordered from Genscript. Growth media components were supplied by Formedium.

2.3 Strains, Primers, and Plasmids

2.3.1 Strains

Yeast strains

The yeast strains used in this study are shown in Table 1.

Yeast strains	**Description or Genotype**	**Yeast strain source**	**Purpose**
Debaryomyces hansenii DebEHOO2 (*YEH750*)	NCYC 102 (national collection of yeast culture)	Lab stock	Strain used in the study.
Saccharomyces cerevisiae (WT *YEH703*) *BY4741*	*MATα his3-Δ1, leu-2ΔO, met15-ΔO, ura3-ΔO*	Lab stock	To compare the strain with *D. hansenii*
Saccharomyces cerevisiae ∆ *pex3*	*MATα his3-Δ1, leu-2ΔO, met15-ΔO, ura3-ΔO, ydr329c::kanMX4*	Lab stock	To compare the strain with *D. hansenii*
Hansenula polymorpha (*YEH154*)		Lab stock	To compare the strain with *D. hansenii*
Kluyveromyces lactis (*YEH156*)		Lab stock	To compare the strain with *D. hansenii*
Yarrowia lipolytica (*YEH 993*)	NCYC 2904	Lab stock	To compare the strain with *D. hansenii*

Pichia pastoris (*YEH155*)		Lab stock	To compare the strain with *D. hansenii*
Cryptococcus curvatus (*YEH992*)	NCYC 476	Lab stock	To compare the strain with *D. hansenii*
D. hansenii DebEH009 (*YEH1076*)	NCYC3363	Lab stock	Main strain used in this study
D. hansenii DebEH011 (*YEH1078*)	NCYC3981	Lab stock	Strain used in this study
D. hansenii DebEH034	CBS 13215	Lab stock	Strain used in this study
D. hansenii DebEH036	CBS 767	Lab stock	Strain used in this study
D. hansenii DebEH037	CBS 7848	Lab stock	Strain used in this study
D. hansenii DebEH038	CBS 13202	Lab stock	Strain used in this study
D. hansenii DebEH039	CBS 1102	Lab stock	Strain used in this study

D. hansenii DebEH040	CBS 5139	Lab stock	Strain used in this study
D. hansenii DebEH041	CBS 5307	Lab stock	Strain used in this study
D. hansenii DebEH042	CBS 13195	Lab stock	Strain used in this study
D. hansenii DebEH043	CBS 1142	Lab stock	Strain used in this study
D. hansenii DebEH044	CBS 1099	Lab stock	Strain used in this study

Table 1 Yeast strains.

***E. coli* strains**

E. coli strains used in this study are shown in Table 2.

***E. coli* strain**	**Genotype**	**Purpose**	**Source**
Chemically competent (RbCl) DH5α	*supE44 ΔlacU169 (ϕ80 lacZ ΔM15) hsdR17 recA1 endA1 gyrA96 thi-relA1*	Plasmid transformation	Lab stock

Table 2 E. coli strains.

2.3.2 Plasmids

Plasmids used in this study are listed in Table 3.

Plasmid name	Marker	Parental plasmid	Source
pSA1(upstream homology arm for *PEX3* knockout)	SAT1	pbluescript SK(+)	This study
pSA2 (downstream homology arm for *PEX3* knockout)	SAT1	pbluescript SK(+)	This study
pSA3(upstream homology arm for *ARG1* knockout)	KanR	pUC19	This study
pSA4(downstream homology arm for *ARG1* knockout)	KanR	pUC19	This study
pZA1(*PEX3* knockout)	SAT1	pbluescript SK(+)	Lab stock
pSA5 (upstream and downstream homology arms for *ARG1* knockout)	HygroB	pUC19+*ARG1* upstream and downstream	This study
pSA6 (pSA5+*ACT1* promoter from *Scheffersomyces*	HygroB	pUC19+ *ARG1* upstream and downstream	This study

stipitis+ *GFPPTS1*)			
pDEB21 (*ACT1* promoter from *Scheffersomyces stipitis*+ *GFPPTS1*)	SAT1	pDEB15	Lab stock

Table 3 Plasmids in this study.

2.3.3 Primers

To design a primer five rules were followed:(i) each primer was ~20 nucleotides long; (ii) the sequence of each primer ended with a G or C nucleotide at the 3'end; (iii) the GC content of the primer was approximately 50%; (iv) the forward and reverse primers did not show complementarity; (v) the primer did not have more than 3 copies of the same nucleotide repeatedly. (vi) the primer temperature (Tm) was calculated using the formula:

$$Tm= 4(G+C) +2(A+T)$$

The temperature used for annealing was 5^{o}C below the Tm.

Table 4 presents the primers used in this study.

Name	Primer sequence 5' ⟶ 3'	Description
VIP3856	CACTGGTACCTGAAGCACTC GAGTTGAAG	Forward primer with *Kpn*1 site annealing 927bp upstream of *D.hPEX3*.
VIP3857	CAATGAATTCGCATGCTTAGT AGTTTTGCTTG	Reverse primer with *EcoR*1 annealing just upstream of ATG of *D.hPEX3* ORF.
VIP3858	CAGTTCTAGACTTAATGACCT CTTCACATCG	Forward primer with *Xba*1 site annealing 948bp downstream of *D.hPEX3.*
VIP3859	CAATGAGCTCTTCCTACTACC AGACCTACC	Reverse primer with *Sac*1 annealing just downstream of ATG of *D.hPEX3* ORF.
VIP3872	CGCTGAAGCTGATGTAGATC	Forward primer annealing 200bp away from the upstream region of *D.hPEX3*.
VIP3873	GTGATTAATCCTGGCGACTC	Reverse primer annealing 200bp away from the downstream region of *D.hPEX3*.
VIP3889	CTTCTTTACGGGTATGTCGC	Reverse primer annealing 32bp away from the downstream region of *D.hPEX3*.

VIP3901	AGACAGCTCCTTGGCATACG	Forward primer inside SAT1 marker to check the presence of downstream of *D.hPEX3*. (Alternative to Zeena's VIP3375)
VIP 3397	TAGCACACACCCACAACAAC	Reverse primer inside SAT1 marker to check the presence of upstream of *D.hPEX3.*
VIP3967	CAATGAATTCCCTGTAGTTGTAGATGCCAC	Forward primer with *EcoRI* site annealing 929bp upstream of *D.hARG1*.
VIP3968	CAATGGATCCGGCAATAGTGATCGGATTG	Reverse primer with *BamHI* annealing just upstream of ATG of *D.hARG1* ORF.
VIP3969	CAATGTCGACTAATCAGCAGTCCAGTACTC	Forward primer with *SALI* site annealing 959bp downstream of *D.hARG1*.
VIP3970	CAATGCATGCATGGGGACAAGTTGGCTAGATG	Reverse primer with *SPHI* annealing just downstream of ATG of *D.hARG1* ORF.
VIP4016	AGGAGCGCGGTATATAGATC	Forward primer annealing 200bp away from upstream region of *D.hARG1*.

VIP4026	CGCGAGCCCATTTATACCCA	Reverse primer inside the kanamycin marker to check the presence of the upstream of *D.hARG1*.
VIP4027	CTAATCTGGCAAACGAACCC	Forward primer inside kanamycin marker to check the presence of the downstream of *D.hARG1*.
VIP4019	CAGCGGGTATAGTTGGAATG	Reverse primer annealing 200bp from downstream region of *D.hARG1.*
VIP4065	TTACCCGTAGGACATATCCAC G	Reverse primer inside the hygromycin B marker to check the presence of the upstream of *D.hARG1*.
VIP4066	CTATCAGAGCTTGGTTGACG	Forward primer inside hygromycin B marker to check the presence of the downstream of *D.hARG1*.
VIP 4161	CCTTCTTCCAATAACCAAGC	Reverse primer inside the *ARG1* ORF to check the presence of a second copy of the *D.hARG1* gene.

VIP4223	GAATTCGTAGGCTATGTACATCACTG	Forward primer annealing at 750bp upstream of *D.hARG1.*
VIP4224	GCATGCCTTCATTGTGATGTATCCAG	Reverse primer annealing at 750bp downstream of *D.hARG1.*
VIP4225	GAATTCGAGCAGTGAGAAGATGTTCA	Forward primer annealing at 500bp upstream of *Dh.ARG1.*
VIP4226	AAGCTTGAACCAGAATTTTGGGTACC	Reverse primer annealing at 500bp downstream of *D.hARG1.*
VIP4227	GAATTCCAATGACTATCTATACATTCGG	Forward primer annealing at 250bp upstream of *D.hARG1.*
VIP4228	AAGCTTGTCGATGAAGGTGAAAGTTTGC	Reverse primer annealing at 250bp downstream of *D.hARG1*.
VIP 4262	CAAGACTATGGCACTTGATG	Forward primer annealing at 200bp upstream of *D.hARG1*.
VIP 4263	CGATGAAGGTGAAAGTTTGC	Reverse primer annealing at 200bp downstream of *D.hARG1*.

VIP 4260	GGTAATCATACACATAAAGG	Forward primer annealing at 150bp upstream of *D.hARG1.*
VIP 4261	CTGATGGCCAATGTAATATC	Reverse primer annealing at 150bp downstream of *D.hARG1.*
VIP4258	TTCCTGTGAACCTGGCTCAG	Forward primer annealing at 100bp upstream of *D.hARG1.*
VIP4259	TACAGACGTCTTGATGAATC	Reverse primer annealing at 100bp downstream of *D.hARG1*.
VIP4298	GAGCGCAAAGCGAGCTTGTA	Forward primer annealing at 63bp upstream of *D.hARG1*.
VIP4299	GTACGATTTTGATTATACCG	Reverse primer annealing at 63bp downstream of *D.hARG1*.
VIP4383	GAGCTTGTAAGAACAATCCG ATCACTATTGCCGGTTTCATG TTGAATTGAGTGAATTCGAGC TCGGTACC	Forward primer annealing at 50bp upstream of *D.hARG1.*
VIP4384	TATACCGTATTCGACGATGAA TACGAAAATGAGTACTGGACT	Reverse primer annealing at 50bp downstream of *D.hARG1.*

	GCTGATTAAAGCTTGCATGCC TGCAGGTC	
VIP4489	ATAGAATTAGTGTTATTTTAC GTTAATCAGTTACATATTATTA TAAAAGAGTGAATTcGAGCTC GGTACC	Forward primer annealing at 50bp upstream of *D.hARG1* ORF.
VIP4490	TATTTTAGATTCCCTATTTAAT TATCTTTATAGTTAGTCGAGT GCAACAAAGCTTGCATGCCT GCAGGTC	Reverse primer annealing at 50bp downstream of *D.hARG1* ORF.
VIP4491	ATAGAATTAGTGTTATTTTAC GTTAATCAGTTACATATTATTA TAAAAGACGAAGTTATGGAAT GATCCAGAGG	Forward primer annealing at 50bp upstream *D.hARG1* GFP-PTS1.
VIP4492	TATTTTAGATTCCCTATTTAAT TATCTTTATAGTTAGTCGAGT GCAACAAGTCGACCTAGAGT TTTGAGTGCAGTGG	Reverse primer annealing at 50bp downstream *D.hARG1* GFP-PTS1.
VIP 4493	TATAGACAGTAAGAACACCCT AGAAAGATTTTAGAAAGTTTG TCTCGAGAGTGAATTCGAGC TCGGTACC	Forward primer annealing at 50bp upstream of *D.hGUT2*.
VIP 4494	ACAAAAATTATACTTAGCAAT ATACAAATACAAACAAATTATT	Reverse primer annealing at 50bp downstream of *D.hGUT2.*

	AATCATAAGCTTGCATGCCTGCAGGTC	
VIP 3396	GCATTGTCTCGCTGATGAAC	Forward primer annealing 650bp away from upstream region of *D.hGUT2*.
VIP 3408	GAATTGATGGTCACGGAGAAGG	Reverse primer annealing 640bp away from downstream region of *D.hGUT2*.
VIP 4018	GTCCGTGCCATTAGAGATCA	Forward primer inside *ARG1* ORF to check the presence of a second copy of *D.hARG1* gene.
VIP 4474	GACTTCCAACGTATTTAAATTCTCTAAACAAGCAAAACTACTAAGCATGCTATCGAATTCCTGCAGGTCG	Forward primer annealing at 50bp upstream of *D.hPEX3*.
VIP 4476	AAGATGATTAATACTATATGAAAGTTGAACGATGTGAAGAGGTCATTAAGAACTAGTGGATCCATGCAGG	Reverse primer annealing at 50bp downstream of *D.hPEX3*.

Table 4 Primers used in this study.

2.4 *Debaryomyces hansenii* protocols

2.4.1 Growth and maintenance

The components of the media used in this study are described in Table 5, and all the media were dissolved in Millipore water to a final volume of 1000ml, mixed with a magnetic follower and then autoclaved. To prepare the agar plates 10ml (100x) of leucine (0.3g leucine in 100ml H_2O), and 10ml (100x) of uracil (0.2g uracil in 100ml H_2O) were added after autoclaving. Liquid cultures and plates were incubated at 25^oC.

D. hansenii cells were grown on media containing different carbon sources to conduct the growth curves. Cell growth was measured using optical density at 600nm ($OD_{600)}$ every half an hour for glucose, galactose, and glycerol media for the duration of 6 hours at 25^oC shaking at 200rpm. For growth on oleate medium YM2glucose and YM2 glycerol, measurements were taken every 3 days, one reading in the morning and one reading in the afternoon. The initial inoculation was at OD_{600}=0.05 for all growth curves.

Media	**Media ingredients to prepare 1L**
YPD	20g peptone, 10 g yeast extract, and 20g glucose.
Yeast minimal media 1(YM1)	5g ammonium sulphate, 1.9g yeast nitrogen base, and NaOH was added to adjust pH to 6.5.
Yeast minimal media 2 (YM2)	5g ammonium sulphate, 1.9g yeast nitrogen base, 10 g casamino acid, and NaOH was added to adjust pH to 6.5.

Yeast media for *D. hansenii* (YM deb)	3g yeast extract, 3g malt extract, 5g peptone, 10g glucose, and 15g Agar. When antibiotic resistance was required, nourseothricin, geneticin, and Hygromycin B were added to the autoclaved media to final concentrations of 1.5µg/ml and 5µg/ml for nourseothricin (50µg/ml and 80µg/ml for HygroB, 300µg/ml for geneticin). (For liquid media, the agar and glucose were omitted, and the required carbon source was added).
Oleate liquid media	1.2ml oleate + 2ml Tween 40, 1g yeast extract, 5g peptone, 100ml 500 mM KPI (potassium phosphate buffer) buffer pH=6.
Oleate agar plates	6.25ml oleate+ Tween 40, 1g yeast extract, 20g agar, 1.9g yeast nitrogen base, 5g ammonium sulphate, and 10g casamino acids.
Arginine (-) plate media	YM1 media, 20g agar,20g glucose, 0.74g CSM Arginine dropout.
Glucose agar plate	YM2 media, 20g agar, 20g glucose.

Table 5 The components of the different carbon source media used in this study. Glucose was substituted with glycerol (3%) and galactose (2%) for glycerol and galactose plates.

2.4.2 Genomic DNA isolation

D. hansenii cells (3ml) were grown overnight in a YM deb media in 5ml tube at 25^{o}C while shaking at 200rpm. Next, the cells were harvested by centrifugation in 2ml screw cap tubes, pellet on pellet at 13400rcf for 1 min. After that, the cells were washed with 1ml water. The supernatant was then poured away, and the cells were re-suspended in the remaining volume. After that, 200μl of TENTS solution (20mM TRIS-HCl pH8.0, 1mM EDTA, 100mM NaCl, 2% (v/v) Triton X100, and 1% (w/v) SDS), 200μl of 425-600μm glass beads (BioSpec Products), and 200μl phenol/chloroform were added to the samples. The samples were then lysed by bead beating for 45seconds at high speed in the bead beater (MiniBeadBeater-16 BioSpec Products). After that, the tubes were centrifuged at 13400rcf, for 30 seconds. Then 200μl TENTS solution was added, and tubes were vortexed and then centrifuged at 13400rcf for 5 minutes. Subsequently, 350μl supernatant was transferred to a new Eppendorf tube, where 200μl phenol/chloroform was added, and the samples were vortexed and centrifuged at 13400rcf for 5 minutes. 300μl of the supernatant was taken, and to precipitate the DNA, 30μl (1/10 volume) of 3 M sodium acetate pH 5.2 and 750μl (2.5x volume) of 100% ethanol were added. After that, the tubes were vortexed and left on ice for 15 minutes, to allow the nucleic acids to precipitate. The tubes were centrifuged at 13400rcf for 15 minutes, and the pellets were washed in 70% ethanol and centrifuged at 13400rcf for 5 minutes. After removal of 70% ethanol, the pellets were dissolved in 200μl 1X TE (1ml of 10X TE (0.1M Tris-HCl,0.01M EDTA, pH 7.4) and 9ml H_2O) + 2μl RNase (10mg/ml) and incubated at room temperature for 10 minutes. Subsequently, the DNA was precipitated as described above. After the 70% wash step, the dried pellets were dried at 50^{o}C and re-suspended in 50μl 1XTE.

2.4.3 *Debaryomyces hansenii* transformation

This protocol is only for one transformation, it is possible to multiply the volumes as necessary for multiple transformations (Minhas, Biswas and Mondal, 2009) modified by (Alwan, 2017).

Two days before: *D. hansenii* cells were inoculated in 5ml YM deb media and incubated overnight at 25^{o}C while shaking at 200rpm.

One day before: cells from the overnight culture were transferred to a fresh 5ml of YM deb medium at OD_{600}=0.1 and grown to OD_{600}= 0.6, Subsequently, the cells were diluted in 50 ml of YM deb medium to OD_{600}= 0.0125 and grown overnight.

On the day of transformation: when the overnight culture had reached OD_{600} 2.6-2.8 by the next morning, a sterile 50ml Falcon tube was used to transfer the cells (10ml/transformation), then the cells were centrifuged for 5 minutes at 1610rcf. The pellet was re-suspended, after discarding the supernatant, in 1ml (per transformation) of 50mM sodium phosphate buffer, pH7.5, containing 25mM DTT (500µl 1M sodium phosphate buffer (pH7.5), 250µl 1M DTT, 9.25ml distilled water). Then the cells were incubated at 25^{o}C for 15 minutes, centrifuged for 5 minutes at 1610rcf, the supernatant was removed, and the pellet re-suspended in 8ml sterile cold (4^{o}C) water and centrifuged for a further 5 minutes at 1610rcf. After removing the supernatant, the cell pellets were re-suspended in a 200µl sterile ice-cold 1M sorbitol (per transformation) and centrifuged as before and 160µl (per transformation) of supernatant was discarded and the cells were re-suspended in the remaining volume. 1µl (2.0µg) of each DNA sample was mixed with 40µl of the cell suspension to be transformed and placed in a precooled 0.2cm electroporation cuvette (Geneflow Electroporation Cuvettes 2mm). As a negative control, a transformation was performed without the addition of DNA. Subsequently, the

cuvettes were incubated on ice for 5 minutes, then quickly wiped dry with a tissue and placed into the Equibio electroporator (a BioRad Gene Pulser) and electroporated at 11.5 $kVcm^{-1}$ (2.3kV, 50µFd and 1000 for 0.2cm cuvettes), after which they were placed on ice. After electroporation, a mixture of 0.1M sorbitol and 1ml YM deb medium was added to the cells immediately, mixed, and the cells were transferred to a 2ml Eppendorf tube. The samples were incubated for 4 hours at 25°C with shaking at 120rpm. Following this, the samples were centrifuged for 5 minutes at 800rcf, the supernatant was discarded, and the pellets were re-suspended in the remaining volume. The cells were then spread on YM deb plates containing the appropriate amount of antibiotic and then incubated at 25°C for 3-4 days. Single colonies were picked and grown up on the YM plates containing a high amount of antibiotic.

2.4.4 Antibiotic assay

Different concentrations of geneticin (G418), Hygromycin B, and nourseothricin were analysed with the wild type of *D. hansenii* on the YM deb media. The antibiotics were added to the medium after it had cooled down and were mixed well. The concentrations were 200 to 500µg/ml, 25 to 80µg/ml, and 1.5 to 5µg/ml) respectively. The cells were checked after incubation for 5 days at 25°C.

2.4.5 Spot assay protocol

The cells were grown for 24 hours on YM deb media, then the OD_{600} was measured. Next, the cells were inoculated in YM deb until the OD reached 1. After that, to a 96-well plate, 200µl of the cell suspensions were added to the second row of plate B2. The organization of the cells had to be the WT first, the mutants, and then the WT again. In the B3, B4, and B5 rows 180µl YM1 media was added. Then with the multichannel pipette 20µl from the undiluted B2 row was taken and moved to the B3

row where it was resuspended, then 20µl from B3 to B4 was resuspended again, and after that 20µl from B4 to B5 was resuspended again. These actions were carried out on the rest of the mutants respectively Figure 9. Then a manual pinner was used to place the cells from the 96-well plate onto a petri dish containing agar medium.

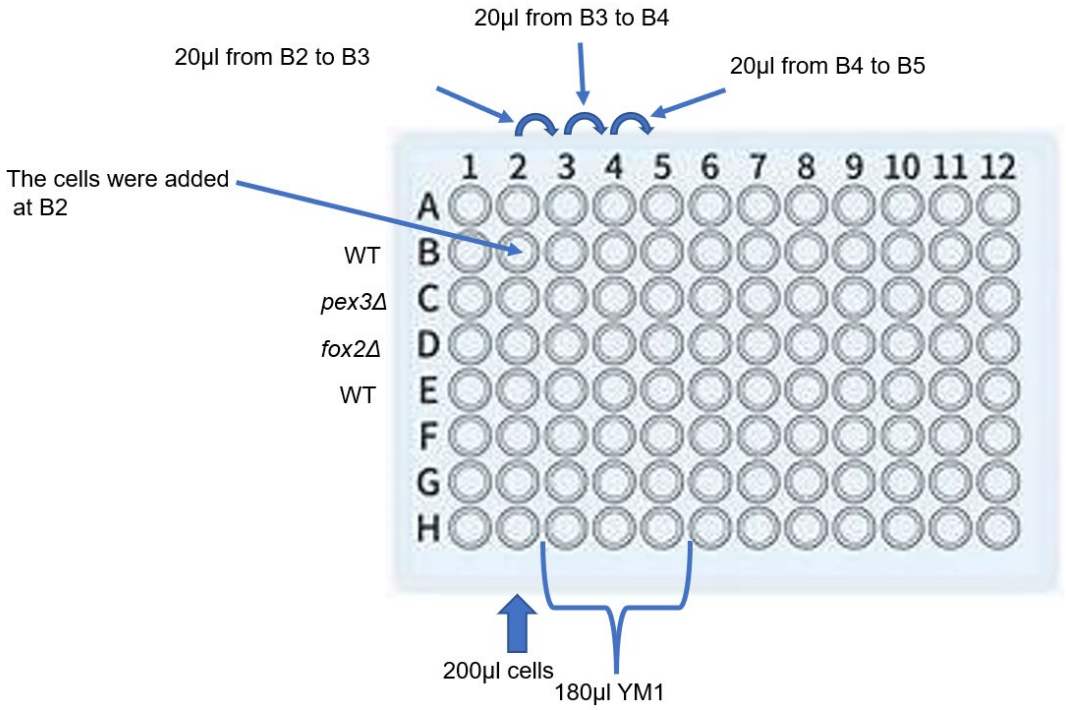

Figure 9 explains the spot assay procedure by showing the WT and mutants orders and the B2 where the cells are placed, and how the dilutions are made in the 96 well plates using a multichannel pipette, via transferring the cells from B2 to B3 and from B3 to B4 and B4 to B5 to get the dilutions 1/10 in B3, 1/100 in B4, and 1/1000 in B5.

2.5 *Escherichia coli* protocols

2.5.1 2TY media with ampicillin

16g of tryptone, 10g of Yeast Extract, 5g NaCl, and 15g of Agar were dissolved in 1L of H_2O. The media was autoclaved and cooled down to about 50ºC. 1500µl of ampicillin (75µg/ml) was added, mixed and media was immediately poured. For liquid media agar was omitted. Then the cells were grown at 37ºC for 24 hours.

2.5.2 *E. coli* transformation for chemical competent cells

The chemical competent cells in the lab were prepared by Dr Donald Watts. The competent *E. coli* cells (DH5α) were thawed on ice. The tube with the ligation mixture

or plasmid was placed on ice for 1 minute. 1µl of plasmid or 10µl of ligation mixture was added to the 100µl cells, and the cells were left on ice for 30 minutes. After that, the cells were heat-shocked in a water bath at 42°C for 2 minutes and then placed on ice for 5 minutes. 900µl 2TY media was added, and it was then incubated for 30-45 minutes at 37°C. The cells were centrifuged at 5900rcf for 1 minute, and 900µl of the supernatant was discarded. The cells were re-suspended in the remaining volume and plated out onto a 2TY plate with the appropriate antibiotic (ampicillin). The last step was incubating the plates at 37°C.

2.6 DNA procedures

2.6.1 Polymerase chain reaction

The polymerase chain reaction (PCR) was performed to amplify specific regions of DNA. For colony PCR, DNA templates were obtained by using a sterile pipette tip to pick individual colonies and inoculate the PCR reaction mixture. The PCR reactions are listed in Table 6 and the PCR conditions are shown in Table 7.

Component	**My Taq polymerase**	**Velocity polymerase**	**My Fi polymerase**
Reaction Buffer	5µl 5x buffer	5µl Hi-Fi buffer velocity	5µl My Fi buffer
Forward primer	2.5µl of 5µM	2.5µl of 5µM	2.5µl of 5µM
Reverse primer	2.5µl of 5µM	2.5µl of 5µM	2.5µl of 5µM
DNA template	1µl	1µl	1µl
DNA polymerase	0.5µl of 5U/1µl	0.5µl of 5U/1µl	1µl of 5U/1µl
d.H_2O	13.5µl	11µl	13µl

dNTP's		2.5µl of 2.5mM	
Total per reaction	25µl	25µl	25µl

Table 6 The PCR reaction components.

Conditions	**My Taq polymerase**	**Velocity polymerase**	**My Fi polymerase**
1.initial denaturation of DNA	2mins at 95^{o}C	2mins at 98^{o}C	2mins at 95^{o}C
2. denaturation step of DNA	30 seconds at 95^{o}C	30 seconds at 98^{o}C	30 seconds at 95^{o}C
3. annealing step of the primers	30 seconds at (----) depends on the primers used in the PCR reaction.	30 seconds at (----) depends on the primers used in the PCR reaction.	30 seconds at (----) depends on the primers used in the PCR reaction.
4. elongation	1min/1kb at 72^{o}C	15 seconds/1kb at 72^{o}C	10 minutes at 65^{o}C
5.final extension	10 minutes at 72^{o}C	5-10 minutes at 72^{o}C	10 minutes at 72^{o}C

Table 7 PCR conditions were set up as detailed above. Steps 2-4 were repeated for 30 cycles in each PCR reaction.

The annealing temperature was occasionally changed depending on the base composition of the primers. An approximation of the Tm was calculated using the formula:

$$Tm= 4(G+C) +2(A+T)$$

The temperature used for annealing was 5^{o}C below the Tm.

2.6.2 Agarose gel electrophoresis

DNA samples were examined by agarose gel electrophoresis. 1% agarose gel was prepared by dissolving 0.5g agarose in 1xTAE buffer solution (40mM Tris, 20mM acetic acid, 1mM EDTA, pH 8.3), and adding 3µl of ethidium bromide to a final concentration of 0.5µg/ml. Samples were loaded after mixing the DNA with Gel Loading Dye Purple (6x) from New England Bio Labs. A DNA ladder (GeneRuler ™ 1kb DNA Ladder, and a Bioline HyperLadder 1kb) was run alongside the DNA samples to determine the size of the DNA fragment. Agarose gels were run in a 1xTAE buffer solution at 95V for 30 minutes: for gel extraction, the gel runs for 45 minutes at 95V. The gels were examined under a Gene Genius ultraviolet transilluminator imaging system.

2.6.3 DNA gel extraction

The QIAquick Gel Extraction Kit (Qiagen) was used to perform the gel extraction, in accordance with the manufacturer's instructions.

2.6.4 DNA purification for PCR product

DNA purification was used to purify the PCR product, to do that the QIAquick Gel Extraction Kit (Qiagen) was used as per the manufacturer's instructions.

2.6.5 Restriction Digest

A restriction digest reaction was prepared of 1µg plasmid DNA, 1µl first restriction enzyme (20000u/ml), 1µl second restriction enzyme (20000u/ml), and 2.5µl Cutsmart ™ Buffer. Its volume was made up to 25µl with sterile H_2O; the reactions were incubated at 37°C for 4 hours.

2.6.6 Ligation

For the ligation 4 components are required, a vector, an insert, 0.5µl T4 DNA ligase (400,000 U/ml; New England Biolabs), and 1µl of 10xT4 ligase buffer. All the components were added in one tube and sterile H_2O was added up to a volume of

10µl. The amount of the insert was calculated by 3:1 insert: vector molar ratio. The reaction tubes were left overnight at room temperature and transformed to competent *E. coli* the next day.

2.6.7 Plasmid miniprep preparation

E. coli cells with plasmid were grown overnight in 5ml TY containing 7.5µl ampicillin (75µg/ml). Plasmid DNA was isolated from the cells using a Bio Basic Plasmid DNA minipreps Kit, following the manufacturer's instructions.

2.6.8 DNA sequencing

The plasmids were diluted to120ng/µl and 5µl for each sequencing reaction was sent to Source Bioscience for sequencing. The plasmids were sequenced using M13 forward and M13 reverse primers and the data was analysed by using a SNAP GENE viewer program.

2.6.9 DNA precipitation

(1/10 volume) of 3 M sodium acetate pH 5.2 and (2.5x volume) of 100% ethanol were added to the test tube. After that, the tubes were vortexed and left at -20^{o}C for one hour. Following this, the tubes were centrifuged at 13400rcf for 15 minutes. The pellets were next washed in 70% ethanol, centrifuged as before, supernatant removed, and the pellets were air-dried before being dissolved in 1XTE.

2.7 Lipid assay procedures

2.7.1 Nile Red preparation

A primary stock was prepared first by adding 10mg Nile Red (Fluorochem) to 10 ml DMSO (Dimethyl sulphoxide) resulting in a concentration of 3.14 mM. Then, 128µl from the primary stock was added to 872µl DMSO to obtain the concentration of 0.4 mM which was recommended to use for *D. hansenii* (Alwan, 2017).

2.7.2 Growth conditions used to induce intracellular lipid storage

First, the cells were grown on a YM deb media for 24 hours, then they were centrifuged for 5 minutes at 1610rcf. After that, the supernatant was discarded, and the pellet was washed with 10ml water. The cells were then transferred to 7 different starvation media shown in the table 8 below, at the same OD_{600} and incubated at 25^{o}C shaking at 200rpm for 24 hours.

Components per 1L/ media#	**YNB**	**glucose**	**ammonium sulphate**	**yeast extract**	**diluted 10x YNB**	**500mM KPI potassium phosphate buffer pH=6.**
Media#1	1.9g	60g	1.25g			
Media#2		60g	1.25g		1.7g	50ml
Media#3		60g		3g	1.7g	
Media#4		60g	1.25g		1.7g	
Media#5		60g		3g		50ml
Media#6	1.9g	60g	1.25g			50ml
Media#7	1.9g	60g	0.5g			

Table 8 shows the 7 different media used in lipid accumulation; all media was dissolved in a final volume of 1L H_2O.

2.7.3 Triolein standard curve

A triolein standard curve was generated to measure the quantification of natural lipid levels in *D. hansenii*. A 96 well plate format was used to create the standard curve. Several lipid concentrations were applied using the ratio 1:20 polar (PC-

phosphatidylcholine (L-lecithin Type XVI-E, from fresh egg yolk ˜99%)) to neutral (TO-Triolein) lipids, isopropanol, and distilled water. To stabilize the triolein, a primary solution needed to be created. The primary solution was achieved by adding 12.5µl (125µg) of PC (with chloroform) to 500µl (2500µg) of triolein in a 1.5ml Eppendorf tube to obtain 512.5µl of balanced triolein. In 2ml Eppendorf tubes seven secondary lipid standards were prepared by adding distilled water, isopropanol, and the primary solution of Triolein in different quantities as shown in Table 9 below.

Triolein (mg/ml)	**0.1**	**0.08**	**0.06**	**0.04**	**0.02**	**0.01**	**0**
Sterilized water	1959.5	1959.5	1959.5	1959.5	1959.5	1959.5	1959.5
1:20 Triolein (µl)	40.5	32.8	24.6	16.4	8.2	4.05	0
Isopropanol (µl)	0	7.7	15.9	24.1	32.3	36.4	40.5

Table 9 seven triolein secondary standards.

The tubes were sealed and placed on ice and in darkness to prevent degradation. In the 96 plates well, the first row from A to D were the unstained cells of 4x 200µl. They had been accumulated from the reservoir which had 1ml of cells in each wall. The other row from E to H were for the stained cells of 4x 200µl, the staining being with Nile Red for 7 minutes (Alwan, 2017). All wells were read using a Varioskan plate reader at an excitation wavelength of 485nm and an emission of 580nm, and the standard curve was conducted between the lipid concentration and the fluorescent intensity (Figure 10).

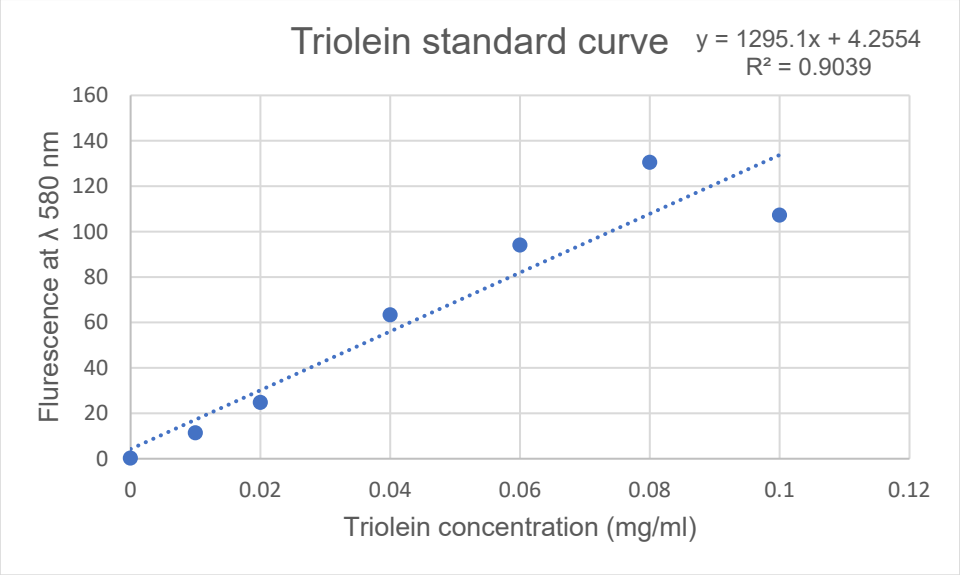

Figure 10 shows the Triolein standard curve between the lipid concentration (mg/ml) and the fluorescence intensity.

2.7.4 Nile Red procedure for *D. hansenii*

The cells were grown at the minimal media as mentioned in section 2.7.2. The culture began at the same OD_{600} for 24 hours and 48 hours. 20ml cells were taken in a 50ml Falcon tube and were centrifuged for 5min at 1610rcf. The supernatant was removed, the OD_{600} was calculated, and then the cells were moved to 10ml water with the same OD_{600} for all samples. From each falcon tube, 6ml of cells were taken each 2ml in one Eppendorf tube. From the Eppendorf tube, 1ml was added to the reservoir plate and 4x200µl was gathered with a multichannel pipette and added to the 96-plate wall from A to D as unstained cells. From E to H another 4x200µl were added to the plate as stained cells, which were stained with Nile Red for 7 minutes (Alwan, 2017). The 96-plate wall was taken to the Varioskan plate reader which was set at an excitation wavelength of 485nm and emission wavelength of 580nm.

2.7.5 Dry-weight procedure

To calculate the dry weight, 30ml of cells were centrifuged at 1610rcf for 5 minutes, the supernatant was then removed. The pellet was resuspended in 1ml of sterile water. It was subsequently moved to an Eppendorf tube that was first

weighed on the scale. The cells were covered with another lid with a small hole in the middle; after which the cells were frozen at -80^{o}C for 48 hours. They were then lyophilized, for 72 hours. The lid with a hole in the middle was removed after this process, the dried pellets were covered with the original lid from the tube; the tube was weighed on the scale again.

2.7.6 Fluorescence Microscopy

After staining the cells with Nile red or after tagging them with a GFP marker the cells were visualized under a microscope (Axiovert 200M; Zeiss) equipped with an Exfo X-site 120 excitation light source, band-pass filters (Zeiss, Inc. and Chroma), an α Plan-Fluar 100x/1.45 NA or plan-Apochromat 63x1.4 NA objective lens (Zeiss) and a digital camera (orca ER; Hamamatsu Phototonics). The cells were imaged using velocity software. There were three channels which are brightfield, green channel, and red channel. Then the images were collected and merged into one file via ImageJ and photoshop, where the cell boundaries were coloured in blue.

Chapter 3:

Gene editing and development of new tools in *D. hansenii*

3.1 Introduction:

Although *D. hansenii* is increasingly being researched for biotechnology, the number of reports on genetically modifying this yeast are few and tools are limited. We set out to generate new tools to efficiently modify the genome of *D. hansenii* with the ultimate goal of increasing lipid accumulation as a proof-of-concept study. To make *D. hansenii* accumulate more fatty acids some genes were knocked out of the genome by homologous recombination (HR). Homologous recombination (HR) is the exchange between two DNA sequences in the region of aligned homology (Kuzminov, 2011).

A limited number of reports describe the use of HR in modifying the genome in *D. hansenii* (Minhas, Biswas and Mondal, 2009; Yaguchi, Rives and Blenner, 2017; Navarrete, Estrada and Martínez, 2022). This method is based on a plasmid which was used for HR, with a designed marker and two flanked regions of the targeted gene. Prista et al., (2016) report that gene disruption is difficult in *D. hansenii* because of the low efficiency of HR in this yeast; that is why we used a 1kb upstream flank before the open reading frame (ORF), and a 1kb downstream flank size after the ORF of the targeted gene see Figure 11.

We created new dominant selectable markers for *D. hansenii*. As *D. hansenii* is one of the CTG clade yeast, which reads the CTG (leucine) codon as serine, the CTG codons were modified in our heterologous selection cassettes in a way that they were translated to leucine instead of serine, by changing the CUG codon for serine to CTG codon for leucine in the snap gene file. The next objective was to improve the method of genome modification using HR in *D. hansenii* by using different flank sizes. This flank size analysis allowed us to develop a PCR-mediated gene deletion

method for *D. hansenii*, previously described for *S. cerevisiae* (Baudin *et al.*, 1993). We optimized various parameters that affect transformation and gene deletion efficiency. Ten different isolates of *D. hansenii* were used to explore the PCR-mediated gene deletion method, to identify strains that are readily amenable to genetic modification, a requirement for metabolic engineering. Combined we developed a robust method for genome modification in *D. hansenii*. In addition, tools were developed to specifically target cassettes for the expression of heterologous proteins to a 'safe' locus in the genome.

3.2 Tools for genomic editing and *ARG1* gene deletion:

We first set up a genome modification system by generating a gene deletion cassette for the *ARG1* gene. The *ARG1* gene encodes Arginosuccinate synthase which is required for arginine biosynthesis. As a consequence, an *ARG1* gene deletion mutant will become an arginine auxotroph and can be easily identified as it cannot grow on arginine deficient media.

First, new dominant selectable markers were designed that work in *D. hansenii,* using the *D. hansenii* strain NCYC 102*.* The first cassette contained the open reading frame (ORF) for the hygromycin phosphotransferase from *E. coli*, which phosphorylates hygromycin B and thereby inactivates this antibiotic (Smulian *et al.*, 2007). Expression was under the control of the *TEF1* promoter and *TEF1* terminator from *Scheffersomyces stipitis*; *S. stipitis* is closely related to *D. hansenii* and these regulatory sequences were considered likely to be active in *D. hansenii* but different enough to inhibit homologous recombination in the *TEF1* locus of *D. hansenii* and is, therefore, equivalent to the use of the *TEF1* promoter and *TEF1* terminator from *Ashby gossyppii* in genome modification in *S. cerevisiae* (Steiner and Philippsen, 1994).

Hegemann et al., (2014) reports that the gene deletion cassette needs to consist absolutely of heterologous DNA with the intention to prevent HR with sequences everywhere within the yeast genome. Additionally, loxP sites were included before the promoter and after the terminator. This cassette can be removed from the genome upon expression of Cre-recombinase, making it a recyclable selectable marker. This was done in case multiple gene deletions were needed, so the same marker can be used recurrently; otherwise, different selectable markers would be needed each time a deletion was carried out in the same strain (Figure 11). The incorporation of LoxP sites was based on the removable selectable markers used in previous work in *S. cerevisiae* and *Schizosaccharomyces pombe* (Hegemann *et al.*, 2014).

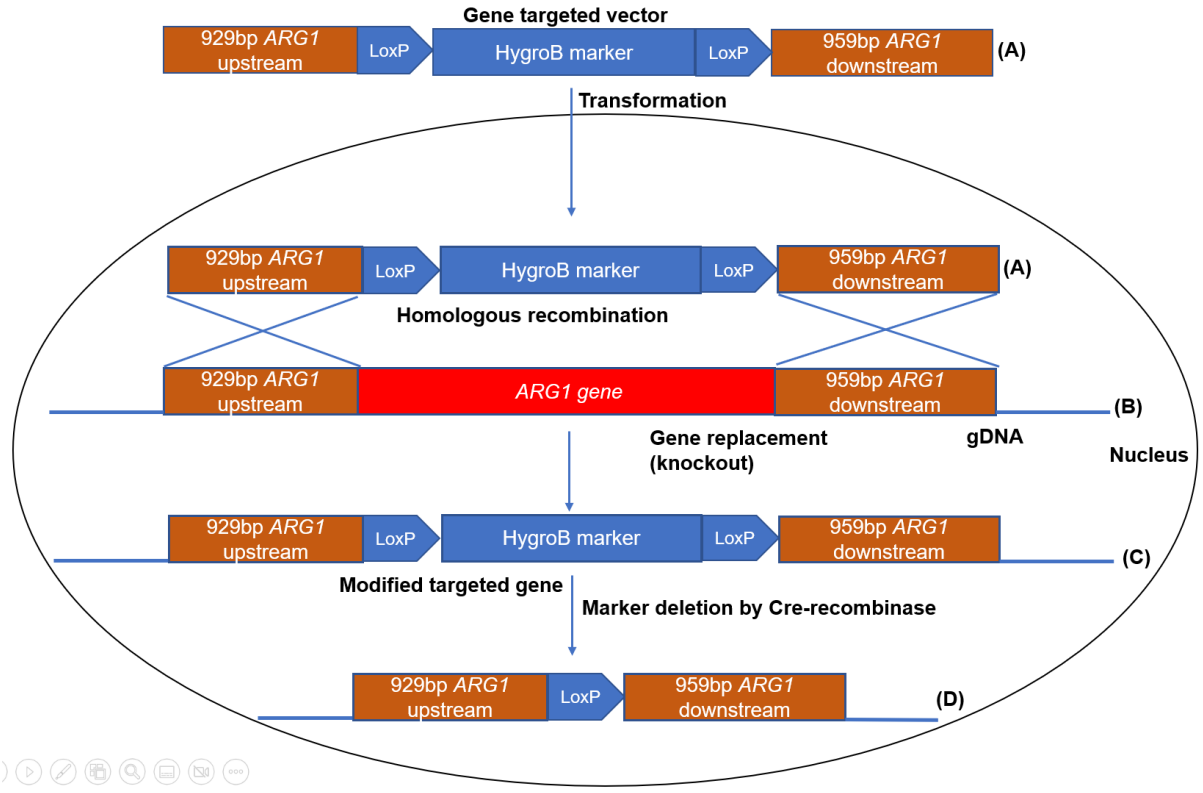

Figure 11 The process of gene replacement through homologous recombination in D. hansenii; and the Cre-recombinase reaction at the end. The insert of the gene targeting vector is amplified by PCR resulting in product A. This is introduced into the cells through electroporation. The 1kb homology arm allows for homologous recombination with the chromosome (B) thereby replacing the ARG1 with the HygroB marker (C). If another gene needed to be removed using the HygroB marker the Cre-recombinase removes the HygroB marker and leaves one LoxP site (D).

A similar cassette was created using the ORF for bacterial aminoglycoside phosphotransferase (kan^r), which gives resistance for instance in bacteria to kanamycin and in eukaryotes to geneticin (G418). Expression of KanR was designed to be controlled through the *ACT1* promoter and the *ACT1* terminator from *S. stipitis*. These cassettes were designed by Selva Turkolmez in the Hettema lab and were subsequently ordered to be synthesised by Genscript. The cassettes were synthesized and cloned into the pUC19 MCS.

The *ARG1* ORF was identified by blasting the sequence of *S. cerevisiae ARG1* gene to *D. hansenii*, then get the Uniprot code, after that KEGG code was used; this protein code shows all the hallmarks of *ARG1* gene Figure 12. After that the sequence was copied to SnapGene; primers were designed on SnapGene at the beginning of the 1kb upstream and the beginning of the *ARG1* gene for the upstream flank then at the end of gene and end of 1kb downstream for the downstream flank (Figure 13). The primers were designed with the appropriate restriction enzymes for each flank. Then the DNA isolated from *D. hansenii* was PCR amplified with the primers.

```
S.c     MSKGKVCLAYSGGLDTSVILAWLLDQGYEVVAFMANVGQEEDFDAAKEKALKIGACKFVC   60
D.h     MSKGKVCLAYSGGLDTSVILAWLLEEGYEVIAYLANIGQEEDFEEAERKALAIGATKFVV   60
S.s     MSKGKVCLAYSGGLDTSVILAWLLEEGYEVIAFLANIGQEEDFEAAEKKALAIGATKFVV   60
        *************************::****:*::**:******: *:.*** *** ***

S.c     VDCREDFVKDILFPAVQVNAVYEDVYLLGTSLARPVIAKAQIDVAKQEGCFAVSHGCTGK   120
D.h     VDVRKEFVEQVCFPAIQTNAIYENVYLLGTSLARPVIAQAHIKVAEENGCFAVSHGCTGK   120
S.s     VDVRKEFVESVCFPAIQANAIYENVYLLGTSLARPVIAQAQIKVAEENGCFAVSHGCTGK   120
        ** *::**:.: ***:*.**:**:***************:*:*.**:::************

S.c     GNDQIRFELSFYALKPDVKCITPWRMPEFFERFAGRKDLLDYAAQKGIPVAQTKAKPWST   180
D.h     GNDQVRFELAFYALKPDVTVIAPWRDPDFFNRFAGRKDLLEYAGSKNIPVAQTKAKPWST   180
S.s     GNDQVRFELSFYALKPDVVVIAPWRDPAFFNRFAGRNDLLEYAASKNIPVAQTKAKPWST   180
        ****:****:********  *:*** * **:*****:***:**..*.**************

S.c     DENQAHISYEAGILEDPDTTPPKDMWKLIVDPMDAPDQPQDLTIDFERGLPVKLTYTDNK   240
D.h     DENLAHISFEAGILEDPDTTPPKDMWKLTVDPLDAPDTPEDFSVYFEKGIPKKLILDGGK   240
S.s     DENLAHISFEAGILENPDTTPPKDMWKLTVDPTDAPDTPEDFTVVFEKGLPVKLILDGGK   240
        *** ****:******:************ *** **** *:*::: **:*:* **   ..*

S.c     TSKEVSVTKPLDVFLAASNLARANGVGRIDIVEDRYINLKSRGCYEQAPLTVLRKAHVDL   300
D.h     ----KVITEPVELFTEANALARRNGVGRIDIVENRFIGIKSRGCYETPGLTILRSAHIDL   296
S.s     ----KVITESVELFLEANALARRNGVGRIDIVENRFIGIKSRGCYETPGLTILRSTHIDL   296
             :*: :::*  *. *** **********:*:*.:*******   **:**.:*:**

S.c     EGLTLDKEVRQLRDSFVTPNYSRLIYNGSYFTPECEYIRSMIQPSQNSVNGTVRVRLYKG   360
D.h     EGLTLDREVRAIRDQFVTTTYSKLLYNGMYFTPECEYVRTMIDPSQKTVNGVVRARAYKG   356
S.s     EGLTLDREVRAIRDQFVSVTYSKLLYNGMYFTPECEYVRSMIPPSQITVNGQVRARAYKG   356
        ******:*** :**.**: .**:*:*** ********:*:** *** :*** **.* ***

S.c     NVIILGRSTKTEKLYDPTESSMDELTGFLPTDTTGFIAIQAIRIKKYGESKKTKGEELTL   420
D.h     SLSILGRSSDTEKLYDETESSMDELTGFSPEDTSGFIAVQSIRIKKYGEAVREKGNTLSL   416
S.s     SLTILGRSSETEKLYDETESSMDELTGFSPEDTSGFIAVQSIRIKKYGEAAREKGQTLNL   416
        .: *****:.****** *********** * **:****:*:*********: : **: *.*
```

Figure 12 protein alignment code for ARG1 gene in S. cerevisiae, D. hansenii, S. stipitis.

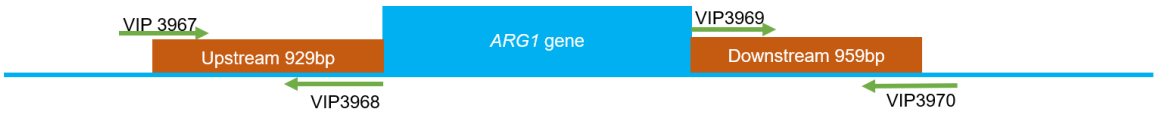

Figure 13 Chromosomal organization of ARG1 and primers used in the construction of the ARG1 gene deletion cassette. Green arrows are primers, numbers represent individual primer identification codes.

After that, the pUC19 plasmid was cut by *EcoRI* and *BamHI* restriction enzymes to insert the upstream *ARG1* flank; and by *SalI* and *SphI* restriction enzymes to insert the downstream of *ARG1* flank, with the kanamycin marker. Since the initial kanamycin cassette failed to result in robust selection of G418, the HygroB marker cassette was also flanked by the1kb upstream and 1kb downstream genomic regions of the *ARG1* gene. This was achieved through digesting the pUC19 plasmid

with kanamycin marker and *ARG1* upstream and downstream flanked regions with *BamHI* and *SalI* restriction enzymes to insert the Hygro B marker Figure 11 and 14.

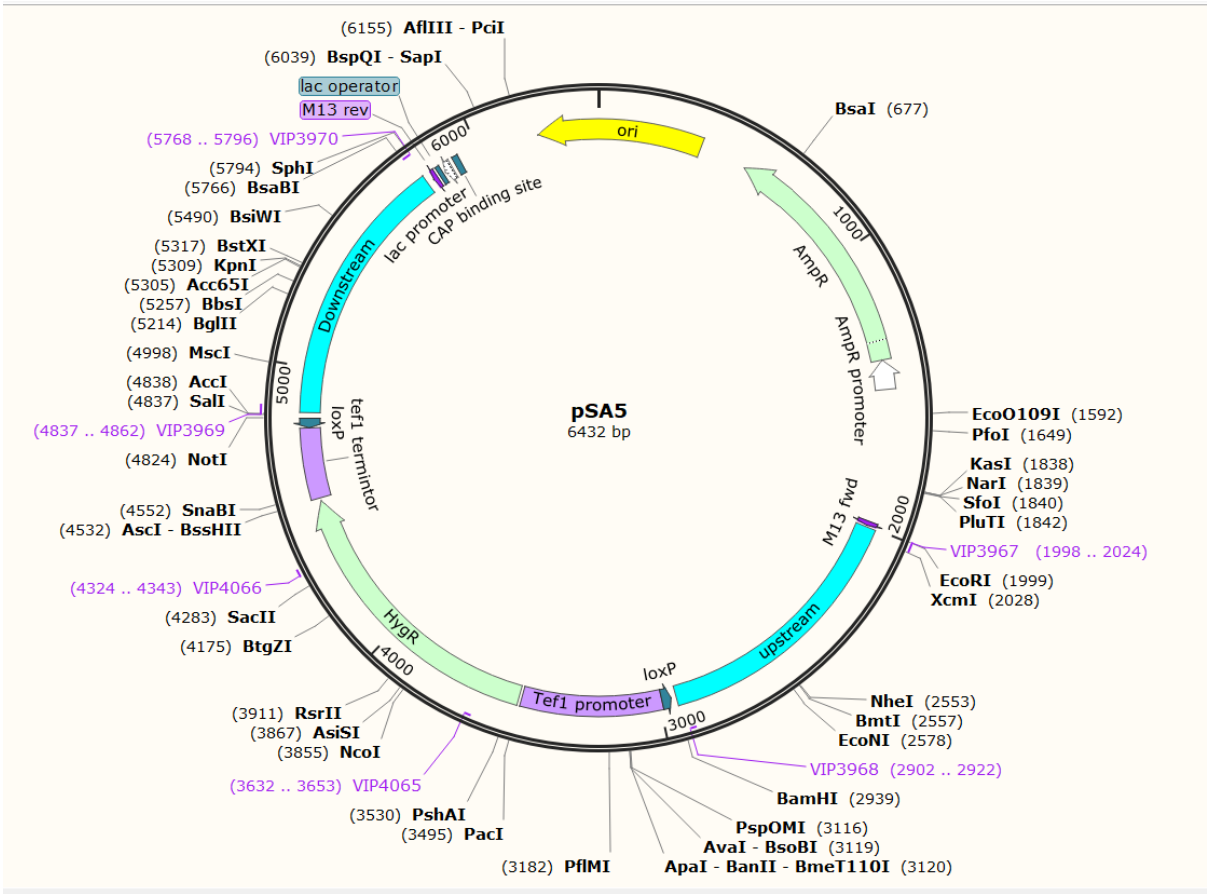

Figure 14 Schematic representation of the ARG1 gene deletion cassette. The pUC19 plasmid with HygroB cassette and the ARG1 upstream and ARG1 downstream regions, after inserting the HygroB cassette in the plasmid, under the control of S. stipites TEF1 promoter and terminator and with the LoxP sites.

Then the whole knockout cassette, which consists of the flanking regions and the selectable marker, was amplified by PCR to generate a linearized DNA fragment. The fragment (300ng) was subsequently, without further treatment, transformed into *D. hansenii* cells using electroporation conditions as described in Materials and Methods section (2.4.3). After electroporation, the cells were recovered before being plated out on YM deb medium containing 50 µg/ml Hygromycin B and incubated for 3-4 days. Colonies were restreaked on YM deb medium with 80 µg/ml Hygromycin B to get pure colonies. Then, the colonies were tested by PCR and growth on arginine (-) media.

Four transformants were obtained, however, all the transformants grew on arginine (-) media. The transformants did contain properly targeted deletion of the *ARG1* gene as revealed by PCR (Figure 15). However, when the same total DNA of WT and two *ARG1* KO transformants were checked for the presence or absence of the *ARG1* ORF, it was found to be present in the *arg1Δ* mutants. From this, it was concluded that the strain NCYC102 has at least 2 copies of the *ARG1* gene (Figure 16). The diagrams before the PCR show where the primers for the PCR start and end to check the presence or absence of the *ARG1* gene.

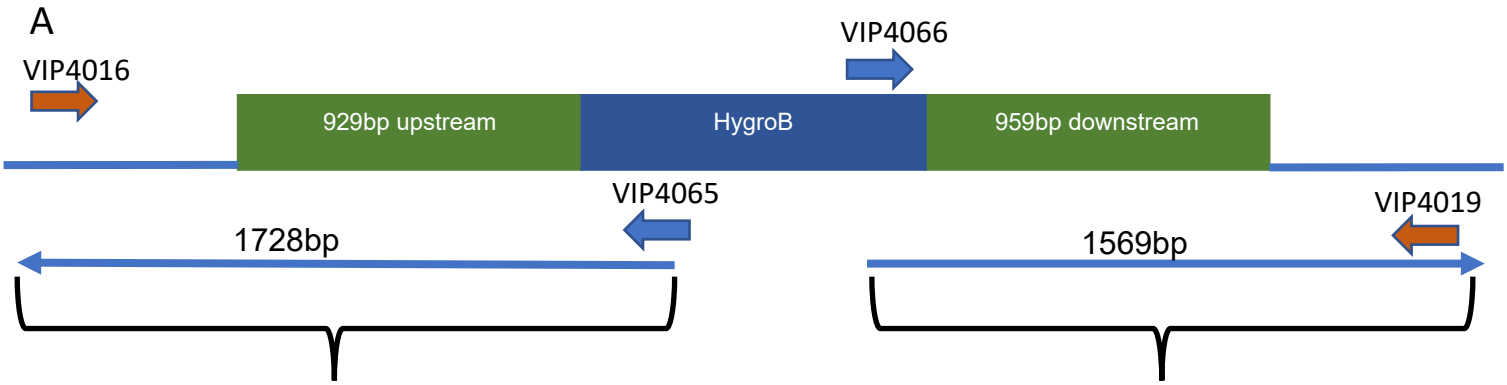

VIP4016 &VIP4065 primers are used to check the upstream chromosomal region upon deletion of *ARG1* gene

(Only KO cells give this band)

VIP4066 &VIP4019 primers are used to check the downstream chromosomal region upon deletion of *ARG1* gene

(Only KO cells give this band)

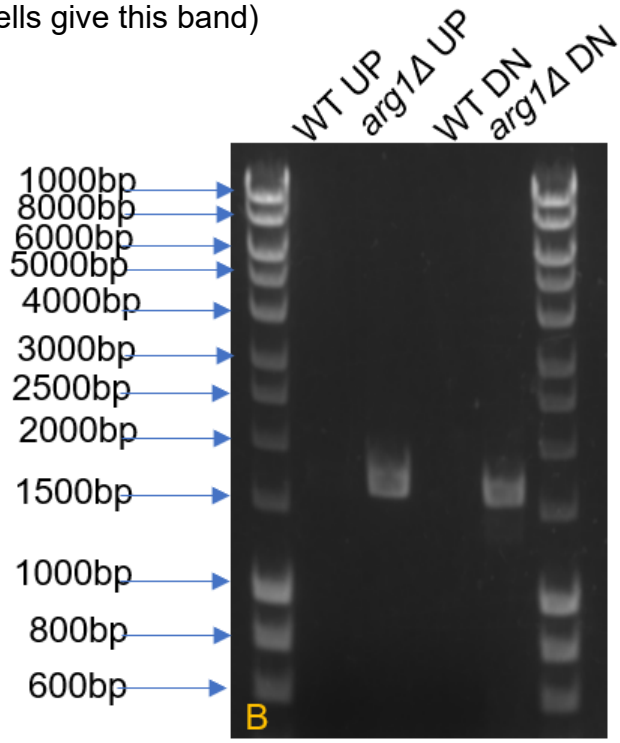

Figure 15 PCR analysis of ARG1 gene deletion mutants. A) Schematic representation of the chromosomal ARG1 region after gene deletion. Coloured arrows indicate primers used in PCR analysis. B) 1% agarose gel analysis of PCR products for the upstream (UP) and downstream (DN) region in WT and arg1Δ cells in the strain NCYC 102.

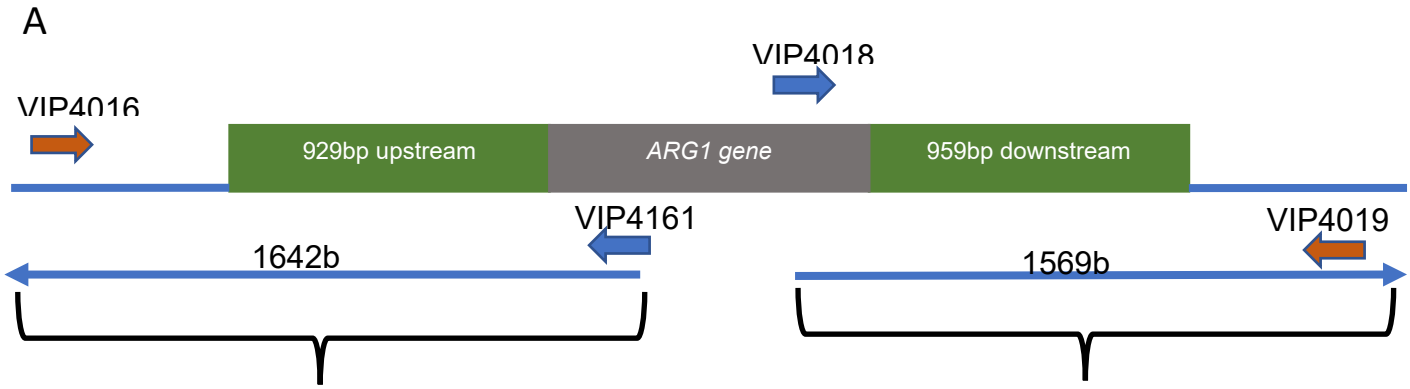

VIP4016 &VIP4161 primers are used to check the upstream second copy of the chromosomal region of *ARG1* gene

(Only WT cells give this band)

VIP4018 & VIP4019 primers are used to check the downstream second copy of the chromosomal region of *ARG1* gene

(Only WT cells give this band)

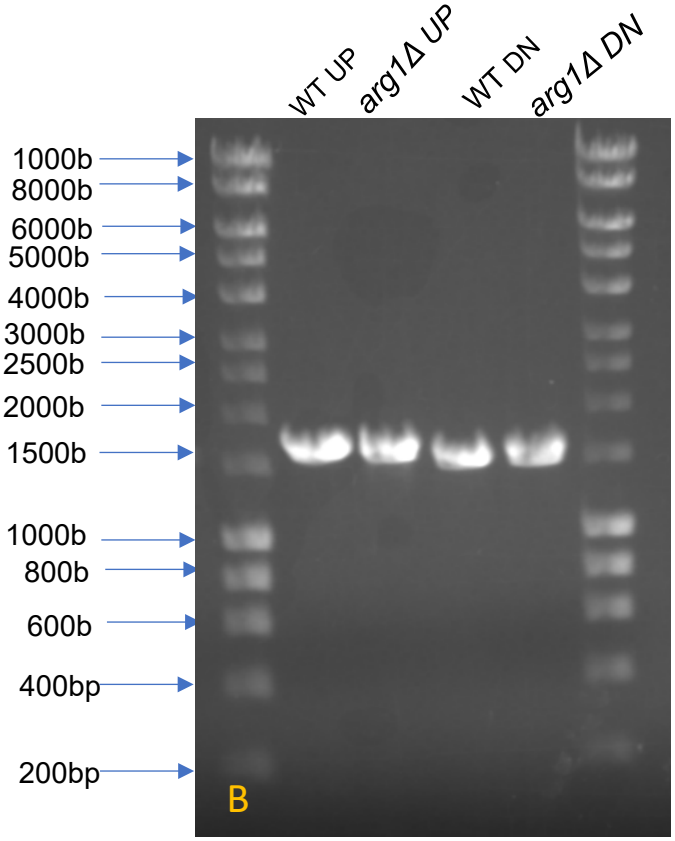

Figure 16 PCR analysis for the presence of an intact copy of the ARG1 gene. A) Schematic representation of the chromosomal ARG1 ORF Coloured arrows indicate primers used in PCR analysis. B) 1% agarose gel analysis of PCR products for the upstream (UP) and downstream (DN) region in WT and arg1Δ cells in the strain NCYC102.

3.3 Using two different strains:

Most of the *D. hansenii* isolates are considered to be haploid, containing six chromosomes but further studies have shown genome size heterogeneity and increase in chromosome number with some strains being described to be diploid or aneuploid. Additional sequence duplications can be observed attributed to multiple alleles on the same chromosome produced by sequence duplication and subsequent translocation can generate multiple alleles of different sizes (Petersen and Jespersen, 2004). Chromosome number fluctuations have also been reported in many other yeast species (Petersen and Jespersen, 2004; Jacques, Mallet and Casaregola, 2009; Jacques *et al.*, 2010). The size of the genome differs from one *D. hansenii* strain to another; this explains why the NCYC102 had two copies of *ARG1* gene while NCYC 3981 and NCYC 3363 had only one copy of *ARG1* gene.

Subsequently, two different *D. hansenii* isolates were used, one collected in a lagoon in Greenwich Island, Antarctica and one found originally in soy sauce, in the Netherlands (NCYC 3981 and NCYC 3363, respectively), and were used to transform the *ARG1* knockout cassette. Twenty-two transformants were obtained, fifteen from NCYC 3363 and seven from NCYC 3981, and the total DNA was isolated from 5 transformants and PCR checked for the insertion of the Hygromycin B cassette into the *ARG1* locus. In parallel, five transformants from each of the strains were grown in arginine (-) media, and none of the transformants grew in contrast to the WT (Figure 17 B&C). That meant the *ARG1* gene was deleted successfully in the NCYC 3981 and NCYC 3363 strains, and that both strains only had a single copy of the *ARG1* gene. The PCR shows the successful KO of the *ARG1* gene in both strains (Figure 17D). The 3 different strains (NCYC102, NCYC 3363, and NCYC 3981) WT and KO were grown on YM deb media and arginine (-)

media, the difference in growth is that the NCYC 3363 and NCYC 3981 strains have one single gene, so they are unable to grow on arginine (-) media while the NCYC102 have 2 copies of the *ARG1* gene they can grow on arginine (-) media (Figures 17&18).

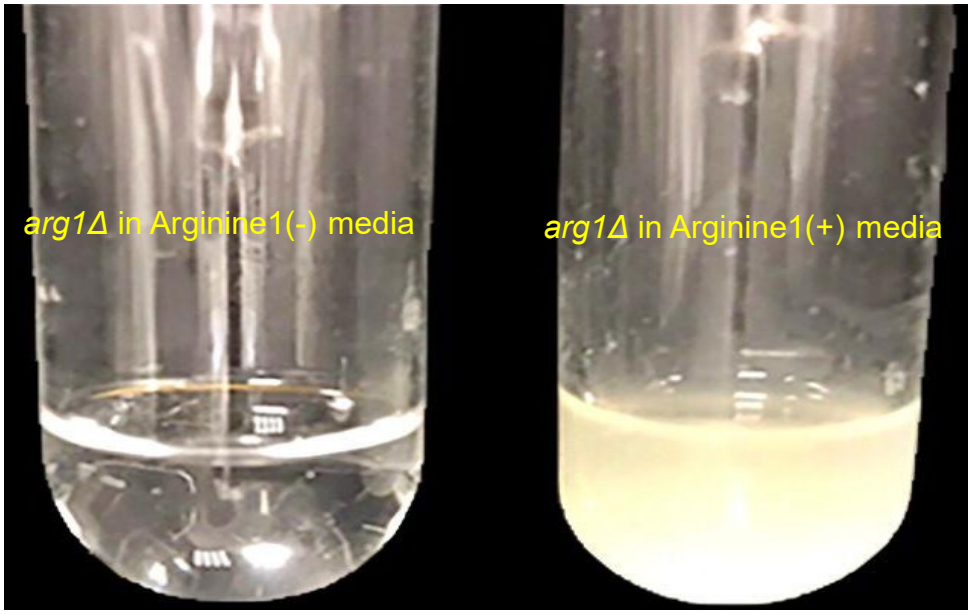

Figure 17 Growth test of arg1Δ cells on selective liquid media with arginine and without arginine. The NCYC 3363 strain with the arg1Δ was able to grow on the media with arginine and it did not grow on the media without arginine. The same result was obtained in the NCYC 3981 strain. That meant there is only one single copy of ARG1 gene in both strains.

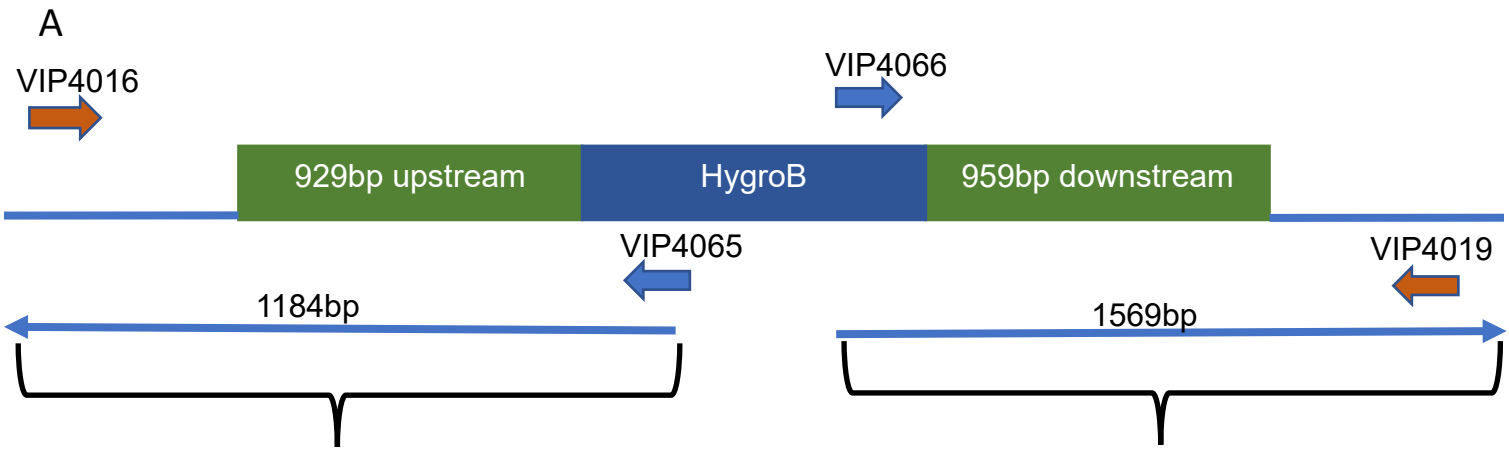

VIP4016 &VIP4065 primers are used to check the upstream chromosomal region upon deletion of *ARG1* gene (Only KO cells give this band)

VIP4066 &VIP4019 primers are used to check the downstream chromosomal region upon deletion of *ARG1* gene (Only KO cells give this band)

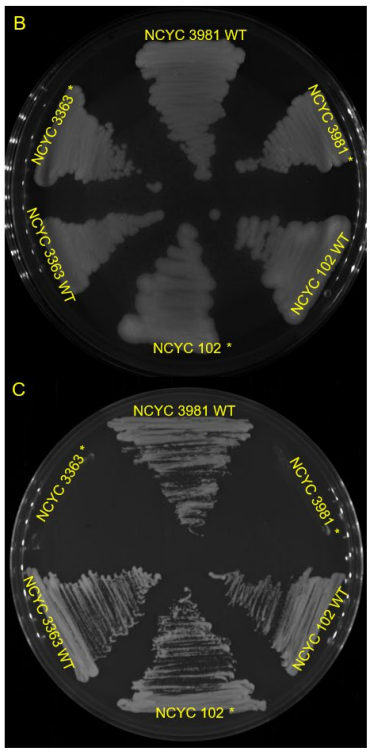

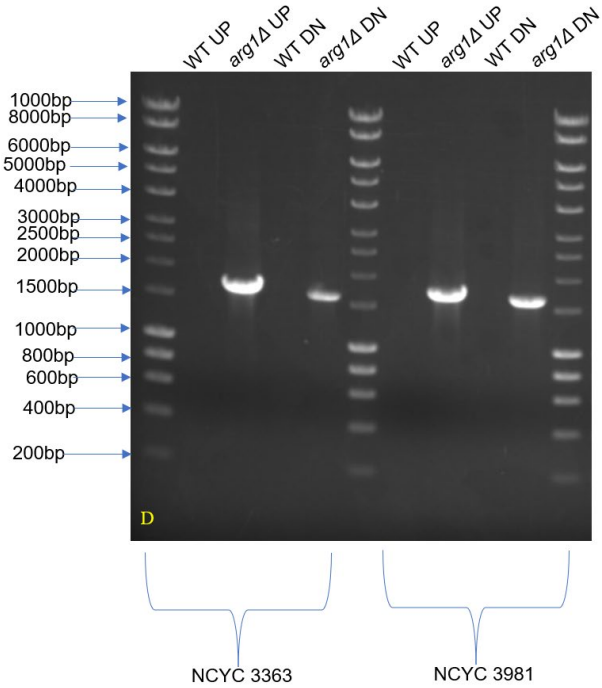

*Figure 18 PCR analysis of ARG1 gene deletion, and the growth of different D. hansenii strains on YM deb media and arginine (-) media. A) Schematic representation of the chromosomal ARG1 region after gene deletion. Coloured arrows indicate primers used in the PCR analysis. B&C) The growth of WT and arg1Δ in 3 different strains backgrounds (NCYC 102, NCYC 3363, and NCYC 3981) on YM deb media (B) and on Arginine (-) media (C); the * shows the arg1Δ in each strain. D) 1% agarose gel analysis of PCR products for the upstream (UP) and downstream (DN) region in WT and arg1Δ cells in both strains NCYC 3363 and NCYC 3981 background.*

3.4 Reducing the flank region:

It was decided to start reducing the flanks by PCR to check the efficiency of homologous recombination at what optimal flank size it would work. Different flank sizes were utilized, such as 750bp, 500bp, 200bp, 150bp, 100bp, 63bp, and 50bp (Figure 19). Primers were designed to achieve the size of the flanks. Subsequently, the PCRs were performed, and reactions were precipitated, and DNA concentration was determined. Next, the various isolates of *D. hansenii* were transformed using electroporation explained in the Materials and Methods. After electroporation, the cells were recovered in 1ml YM deb medium with 0.1M sorbitol for 4 hours at 25^{o}C with shaking at 120rpm before being plated out on YM deb medium containing 50 µg/ml Hygromycin B and incubated for 3-4 days. Colonies were restreaked on YM deb medium with 80 µg/ml Hygromycin B to get pure colonies. Then, the colonies were tested by PCR, and growing them on arginine (-) media. Table 10 below shows the results of the different transformations in NCYC 3363; while table 11 shows the transformation for NCYC 3981 for 1kb and 50bp flanks. The initial approach resulted in a large gene deletion, including ORF and 549bp upstream and 103bp downstream regions. So, reducing the flanks was done by reducing the flanks away from the *ARG1* gene only the last 50bp in the table was done exactly 50bp away from the *ARG1* ORF and results in deletion of the ORF only. Figure 20 shows the *ARG1* gene in chromosome B in *D. hansenii* and the genes surrounding it. The *ARG1* gene is labelled in green, to show that deleting the *ARG1* gene did not interfere with other genes. Even though we had a mistake we were able to prove that the 50bp flank method worked in *D. hansenii* see Figure 21.

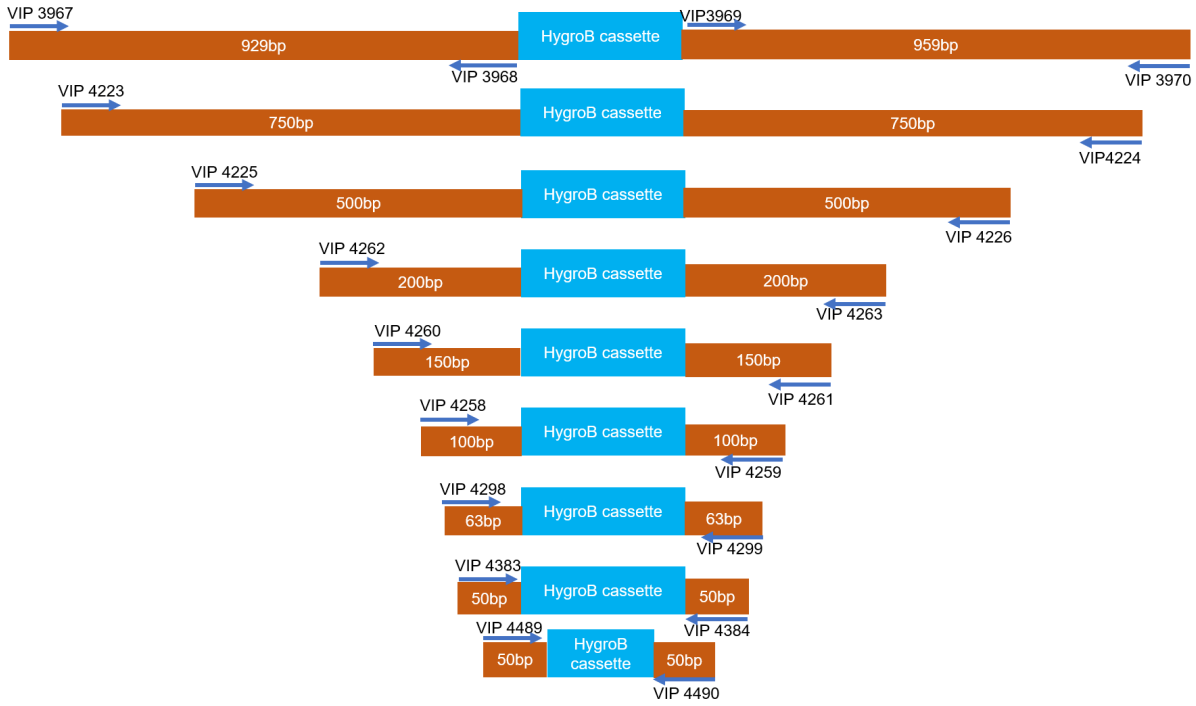

Figure 19 the length of the flanks upstream and downstream away from the HygroB cassette. The HygroB cassette includes HygroB marker, TEF1 promoter and TEF1 terminator, and the loxP sites, from 1kb flank size to 50bp flank size aligned with their primers in the NCYC 3363 strain.

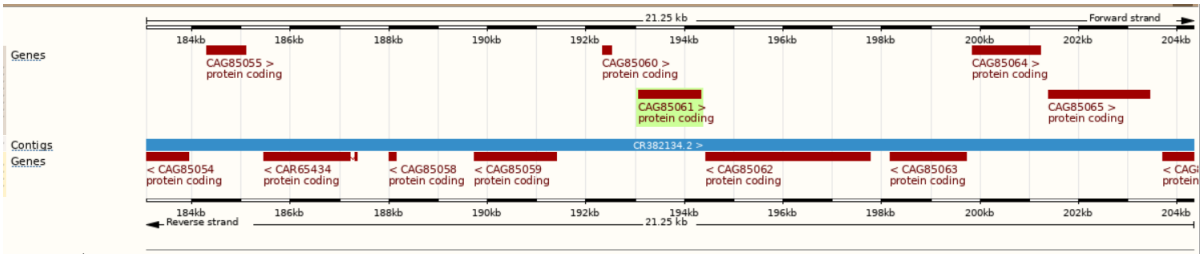

Figure 20 The ARG1 gene in the chromosome B of D. hansenii and the genes around it. This is to show that deleting the ARG1 gene did not interfere with the other genes near it. The ARG1 is labelled in green (Ensembl Fungi Debaryomyces hansenii CBS767, 2022).

Size of flank	Number of colonies	DNA mass	Percentage of colonies with successful knockout	Yeast strain
1000bp	17 colonies	300 ng	94%	NCYC 3363
750bp	1 colony	300 ng	100%	NCYC 3363
500bp	440 colonies	500 ng	90%	NCYC 3363
200bp	16 colonies	1084 ng	100%	NCYC 3363

150bp	5 colonies	1099 ng	100%	NCYC 3363
100bp	9 colonies	1184 ng	88%	NCYC 3363
63bp	10 colonies	800 ng	70%	NCYC 3363
50bp	131 colonies	500ng	80%	NCYC 3363
50bp away ORF	13 colonies	500ng	100%	NCYC 3363

Table 10 The table shows the different transformation analysis in NCYC 3363 strain, showing the different flank size away from the ARG1 gene, the amount of DNA used in the transformation, and the percentage of colonies with successful knockouts.

Flank size	**Number of colonies**	**DNA mass**	**Percentage of colonies with successful knockout**	**Yeast strain**
1000bp	5 colonies	300ng	100%	NCYC 3981
50bp	47 colonies	500ng	80%	NCYC 3981

Table 11 the transformation in NCYC 3981 strain.

Figure 21 shows the PCR of the successful knockout of the *ARG1* gene with only 50bp in NCYC 3363 and NCYC 3981 strains compared with the WT. In addition, different amounts of DNA mass were tested to record the optimal concentration to use in each transformation. 2µg, 1µg, 075µg, and 0.5µg of the precipitated DNA were used with the 63bp flank (Table 12). It was decided to use 0.5µg as the optimal concentration of the precipitated DNA because it gave more colonies. To increase the concentration of DNA some DNA was precipitated and some were purified with a PCR purification kit described in Materials and Methods section (2.6.4) then it was transformed to NCYC 3363 strain via electroporation explained in Materials and

Methods section (2.4.3) (Table 13). The precipitated DNA gave more colonies which is why it was decided to precipitate the DNA. To confirm that the 50bp flank method worked in *D. hansenii* the transformation was done on 10 different strains of *D. hansenii*.

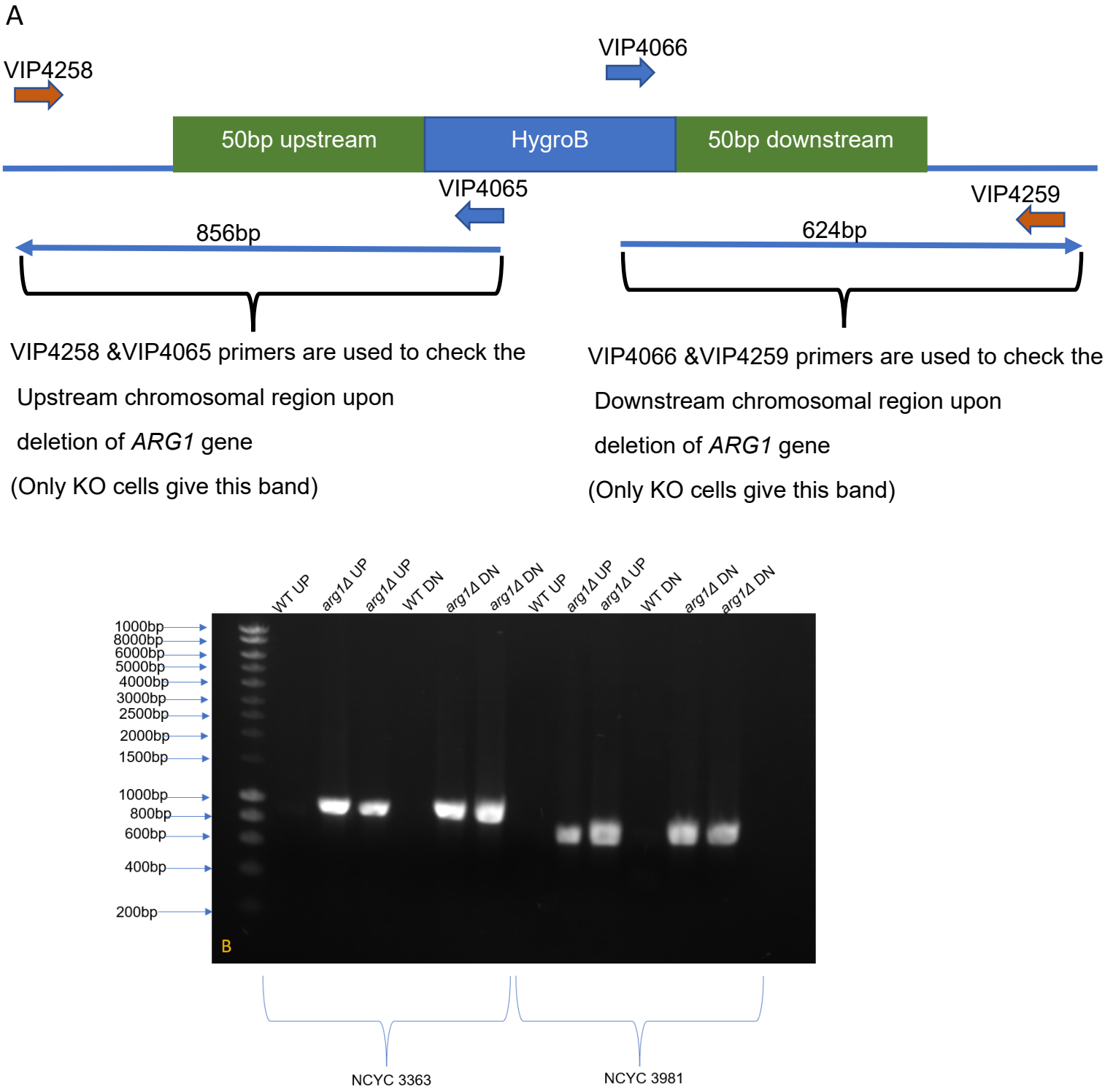

Figure 21 PCR analysis of ARG1 gene deletion mutants with 50bp flank. A) Schematic representation of the chromosomal ARG1 region after gene deletion. Coloured arrows indicate primers used in PCR analysis. B) 1% agarose gel analysis of PCR products for the upstream (UP) and downstream (DN) region in WT and arg1Δ with 50bp only in both strains NCYC 3363 and NCYC 3981 backgrounds.

Flank size	DNA mass	Number of colonies	Percentage of colonies with successful KO	Yeast strain
63bp	2µg	No colonies		NCYC 3363
63bp	1µg	26 colonies	50%	NCYC 3363
63bp	0.75µg	15 colonies	33%	NCYC 3363
63bp	0.625µg	43 colonies	74%	NCYC 3363
63bp	0.5µg	77 colonies	41.5%	NCYC 3363
63bp	0.444µg	15 colonies	53%	NCYC 3363

Table 12 the different concentrations of DNA used in the NCYC 3363 strain with 63bp flanks.

Size of Flank	DNA mass	Precipitated number of colonies	Percentage of Successful KO in precipitated DNA	Purified number of colonies	Percentage of Successful KO in purified DNA	Yeast strain
50bp	0.5µg	131 colonies	80%	20 colonies	85%	NCYC 3363

Table 13 the difference between the precipitated and purified DNA to increase its concentration.

3.5 Different strains of *D. hansenii*

The 50bp flank method was tested on 10 different strains of *D. hansenii* alongside the 500bp flank to delete the *ARG1* gene. The 10 different strains were CBS 13215, CBS 767, CBS 7848, CBS 13202, CBS 1102, CBS 5139, CBS 5307, CBS 13195, CBS 1142, CBS 1099. The sources of strains are different: Zooplankton, Carlsberg laboratories, Takuan Japanese salted pickle, Southern Ocean seawater 497M, beef-pork sausage, skin of man, stomach of fish, Southern Ocean seawater 4509M, sake-moto, and cheese respectively. A HygroB marker was used, flanked by 50bp upstream and 50bp downstream away from the *ARG1* ORF; and 500bp upstream and 500bp downstream away from the *ARG1* ORF. Then 500ng PCR product, after precipitation, was introduced into *D. hansenii* by electroporation. The cells were recovered before being plated out on a YM deb medium containing 50 µg/ml Hygromycin B and incubated for 3-4 days. Colonies were re-streaked on the YM deb medium with 80 µg/ml Hygromycin B to obtain pure colonies. The colonies were then tested by PCR and grown on an arginine (-) media. Each strain gave a different number of colonies as shown in Table 14, and 15. Following this, the colonies were re-streaked at 80µg/ml HygroB in the YM deb plates to obtain pure colonies. The NCYC 3363 strain was used as a control; unfortunately, all 10 strains had 2 copies of the *ARG1* gene. Table 14 shows the results of the transformation for the 10 strains of *D. hansenii* with the 50bp flank size while Table 15 shows the 500bp flank size. Figures 22 show the PCRs that were performed to check if the transformation was correct and Figure 23 shows if there was another copy of the *ARG1* gene. All colonies of the 10 different strains transformants grew on the arginine (-) media. The diagram before the PCR shows where the primers anneal for each PCR. To confirm that a 50bp flank size could be used to delete other genes; the transformation for *PEX3* gene was achieved with only 50bp: the results were 22 colonies in the NCYC

3363 strain, of which 72% had successful knockouts. This will be further discussed in Chapter 5. Also, Tarad Abalkhail another student in the Hettema lab was able to knock out *ADE2* gene which encodes for P-ribosyl-amino-imidazole-carboxylase which catalyzes the sixth step in purine biosynthesis (Gedvilaite and Sasnauskas, 1994) with only 50bp flank PCR in NCYC 3363 strain. We were able to conclude that the 50bp PCR method does work in *D. hansenii*. All of the strains we obtained from Central Bureau of Schimmelcultures (CBS) and one out of the 3 strains from NCYC had an extra copy of *ARG1* gene. All strains were able to be transformed and targeted gene deletions were obtained, although with different frequencies.

Strains	**DNA mass**	**Flank size**	**Results**	**Arg1(-)**	**PCR Check**
CBS 13215	500ng	50bp	220 colonies	21 all grew	Has a 2nd copy
CBS 767	500ng	50bp	41 colonies	All grew	Has a 2nd copy
CBS 7848	500ng	50bp	2 colonies	All grew	Has a 2nd copy
CBS 13202	500ng	50bp	240 colonies	16 all grew	Has a 2nd copy
CBS 1102	500ng	50bp	300 colonies	18 all grew	Has a 2nd copy

CBS 5139	500ng	50bp	380 colonies	16 all grew	Has a 2nd copy
CBS 5307	500ng	50bp	none	0	
CBS 13195	500ng	50bp	90 colonies	21 all grew	Has a 2nd copy
CBS 1142	500ng	50bp	280 colonies	15 all grew	Has a 2nd copy
CBS 1099	500ng	50bp	none	0	
NCYC 3363 as (+) control	500ng	50bp	18 colonies	11 only 6 had the KO	1 single copy

Table 14 the transformation of 50bp in the 10 strains of D. hansenii while the NCYC 3363 was used as a control.

Strains	**DNA mass**	**Flank size**	**Results**	**Arg1(-)**	**PCR check**
CBS 13215	500ng	500bp	120 colonies	14 all grew	Has a 2nd copy
CBS 767	500ng	500bp	none	0	
CBS 7848	500ng	500bp	2 colonies	All grew	Has a 2nd copy
CBS 13202	500ng	500bp	92 colonies	11 all grew	Has a 2nd copy

CBS 1102	500ng	500bp	140 colonies	11 all grew	Has a 2nd copy
CBS 5139	500ng	500bp	280 colonies	15 all grew	Has a 2nd copy
CBS 5307	500ng	500bp	2 colonies	All grew	Has a 2nd copy
CBS 13195	500ng	500bp	22 colonies	17 all grew	Has a 2nd copy
CBS 1142	500ng	500bp	160 colonies	17 all grew	Has a 2nd copy
CBS 1099	500ng	500bp	32 colonies	20 all grew	Has a 2nd copy
NCYC 3363 as (+) control	500ng	500bp	4 colonies	2 had KO	1 single copy

Table 15 the transformation of 500bp in the 10 strains of D. hansenii while the NCYC 3363 was used as a control.

A

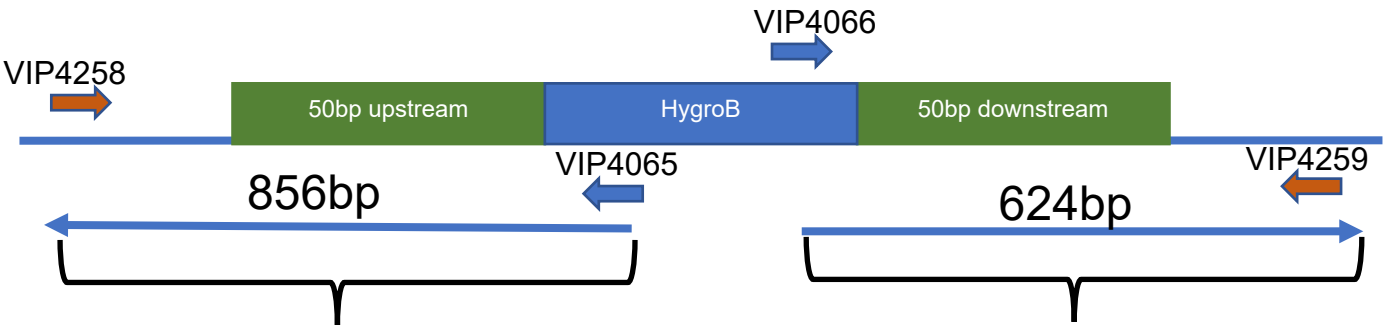

VIP4258 &VIP4065 primers are used to check the Upstream chromosomal region upon deletion of *ARG1* gene (Only KO cells give this band)

VIP4066 &VIP4259 primers are used to check the Downstream chromosomal region upon deletion of *ARG1* gene (Only KO cells give this band)

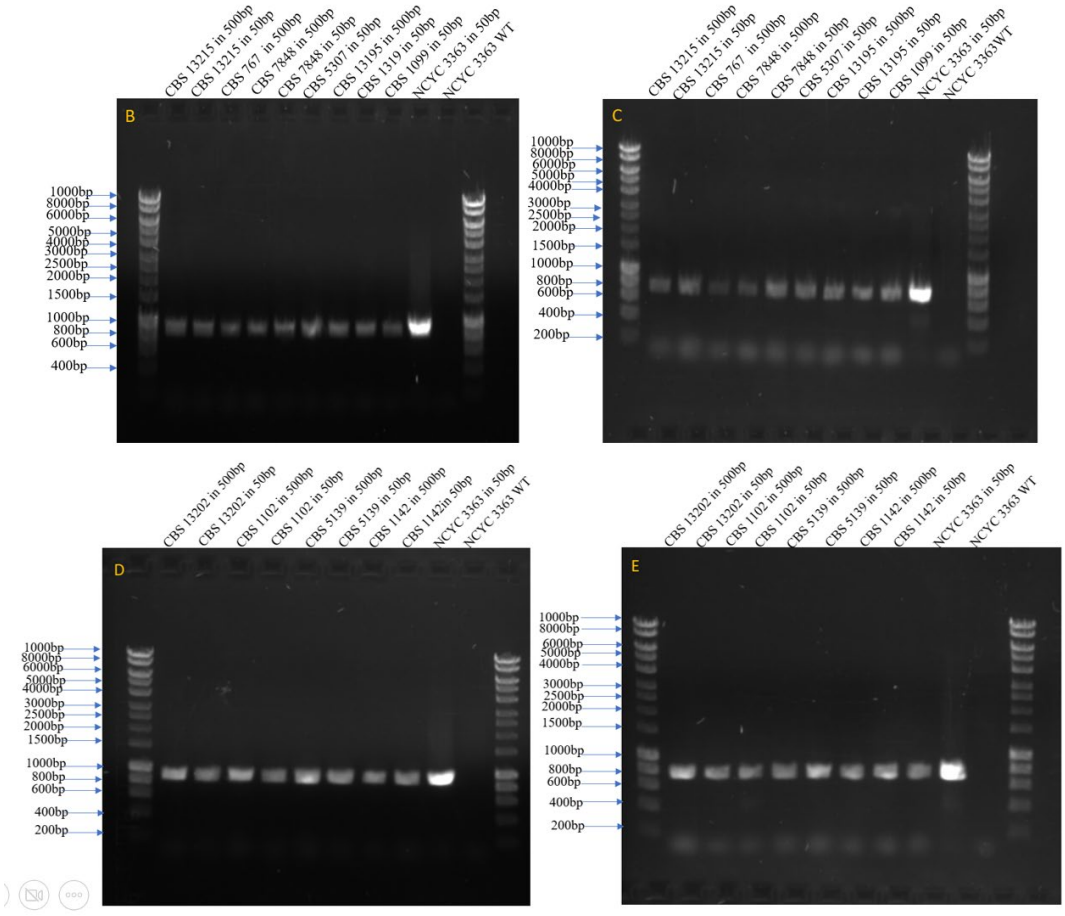

Figure 22 PCR analysis of ARG1 gene deletion mutants generated with 50bp and 500bp homology flank. A) Schematic representation of the chromosomal ARG1 region after gene deletion. Coloured arrows indicate primers used in PCR analysis. B) 1% agarose gel analysis of PCR products for the upstream region in arg1Δ cells in CBS 13215, CBS 767, CBS7848, CBS5307, CBS13195, and CBS 1099 background. C) 1% agarose gel analysis of PCR products for the downstream region in arg1Δ cells in CBS 13215, CBS 767, CBS7848, CBS5307, CBS13195, and CBS 1099 background. The WT of NCYC 3363 strain used as a control. D) 1% agarose gel analysis of PCR products for the upstream region in arg1Δ cells in CBS 13202, CBS 1102, CBS 5139, and CBS 1142 background. E) 1% agarose gel analysis of PCR products for the downstream region in arg1Δ cells in CBS 13202, CBS 1102, CBS 5139, and CBS 1142, background. The WT of NCYC 3363 strain used as a control.

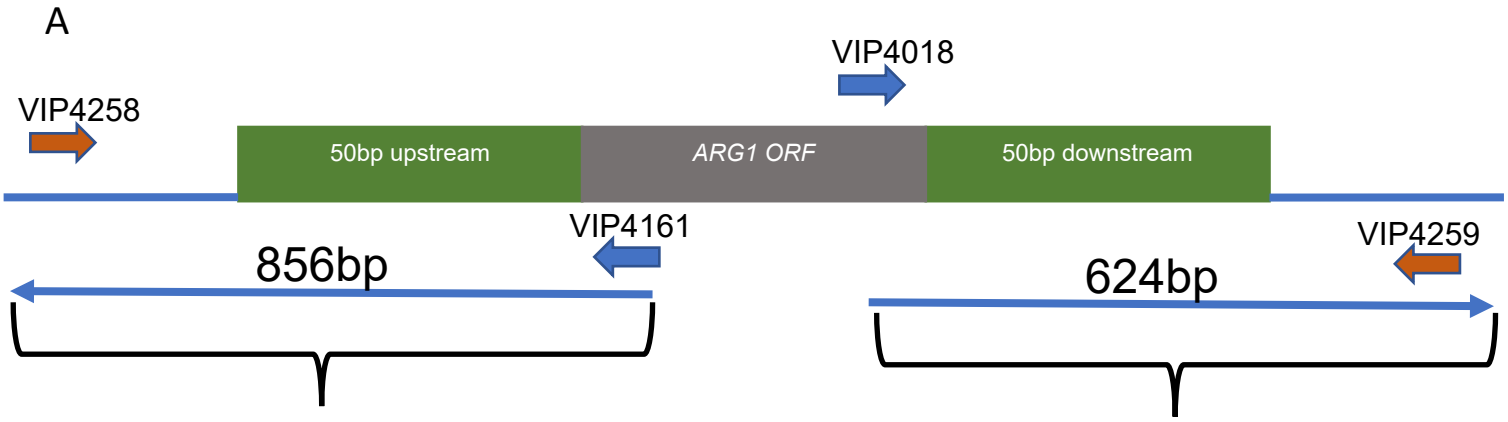

VIP4258 &VIP4161 primers are used to check the upstream second copy of *ARG1*

(Only WT cells give this band)

VIP4018 &VIP4259 primers are used to check the downstream second copy of *ARG1*

(Only WT cells give this band)

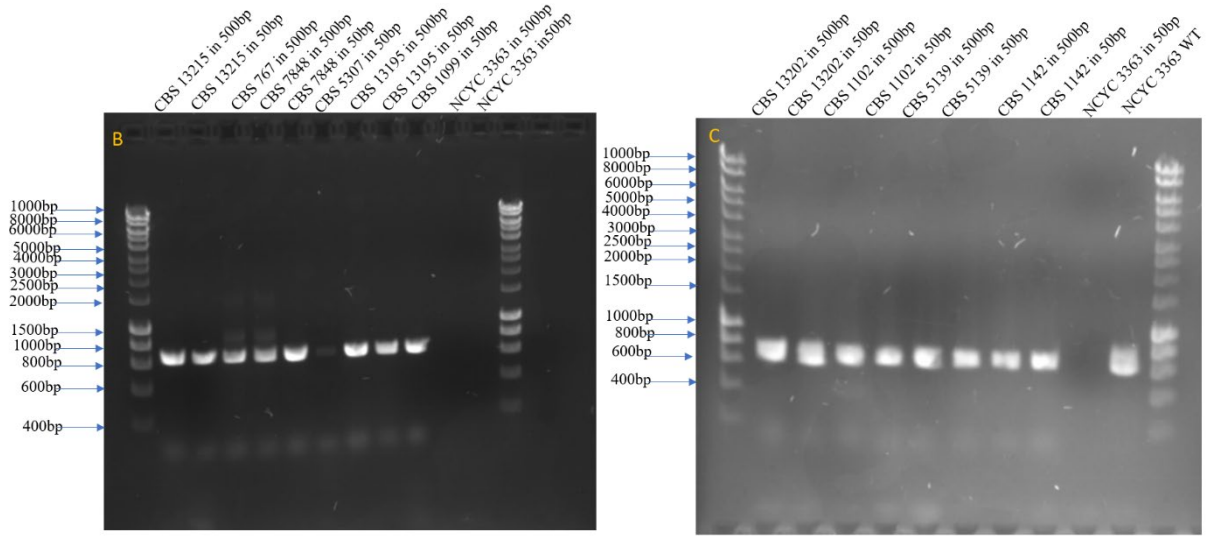

Figure 23 PCR analysis of second copy of ARG1 gene mutants with 50bp and 500bp flank. A) Schematic representation of the chromosomal ARG1 ORF. Coloured arrows indicate primers used in PCR analysis. B) 1% agarose gel analysis of PCR products for the upstream region in arg1Δ cells in CBS 13215, CBS 767, CBS 7848, CBS 5307, CBS 13195, and CBS 1099 background. C) 1% agarose gel analysis of PCR products for the upstream region in arg1Δ cells in CBS 13202, CBS 1102, CBS 5139, and CBS 1142, background. The WT of NCYC 3363 strain used as a control.

3.6 Discussion:

In summary, Hygromycin B and Kanamycin cassettes were generated as genetic tools to work with *D. hansenii.* The cassette contained the ORF for a kinase that phosphorylates hygromycin B and thereby inactivates this antibiotic. A similar cassette was created using the ORF for bacterial aminoglycoside phosphotransferase (kan^r), which gives resistance in eukaryotes to geneticin (G418); these cassettes were cloned in the pUC19 MCS.

The *ARG1* gene was successfully deleted using the HygroB marker in the NCYC102 strain, unfortunately, it had two copies of the *ARG1* gene while the NCYC 3981 and NCYC 3363 strains had only one single copy. The first attempt at the gene disruption of *ARG1* was with a 1kb flanked region from the *ARG1* gene, then the flanks were shortened using 750bp, 500bp, 200bp, 150bp, 100bp, 63bp, 50bp and 50bp flanking the ORF only.

The main reason for reducing the flanks was that in the *S. cerevisiae* and *S. pombe* gene disruption can be achieved with short flanks such as 30-50bp in *S .cerevisiae* and 80-100bp for *S. pombe* (Hegemann *et al.*, 2014), this was done by PCRing the selectable marker flanked by 50bp upstream and downstream away from the gene ORF, then transforming that to the yeast (Baudin *et al.*, 1993; Kaur, Ingavale and Bachhawat, 1996). It was desirable to see if the same could be achieved in *D. hansenii.* Previously, to generate a knockout in *D. hansenii* several steps are required. First, the DNA was isolated from *D. hansenii*. Then a PCR was performed to amplify the region of interest using primers, designed in the Snap Gene program, to anneal both the start and the end of the region of interest. First one side of the flank (upstream) was inserted into the plasmid, the PCR product was then purified to

obtain pure DNA. The plasmids were transformed to *E. coli*, and then mini prepped. After that, a restriction digest was performed to cut the plasmid and DNA; gel extraction, ligation, and *E. coli* transformation were then achieved. To check the insert was correct a mini prep and restriction digest was completed. The sequences were sent for sequencing, as per the previous section 2.6.8. To insert the other side of the flank or downstream restriction digest, a gel extraction, and ligation were performed on the plasmid. Then *E. coli* transformation, colony PCR, miniprep and another restriction digest were completed to check the insert was correct, and this was proven to be the case. Following this, the samples were sequenced (section 2.6.8). Finally, the plasmids were cut to linear DNA by PCR and then transformed to *D. hansenii* Figure 24. Then a replica plate technique was used for the *D. hansenii* colonies to check the knockout of the gene. The cells were then grown on selective media plates with high antibiotics to get pure colonies. This method was difficult to achieve and took a long time to complete, however, now it is simple to get a gene deletion in *D. hansenii* with the new 50bp flank method just PCR and then transform to *D. hansenii*.

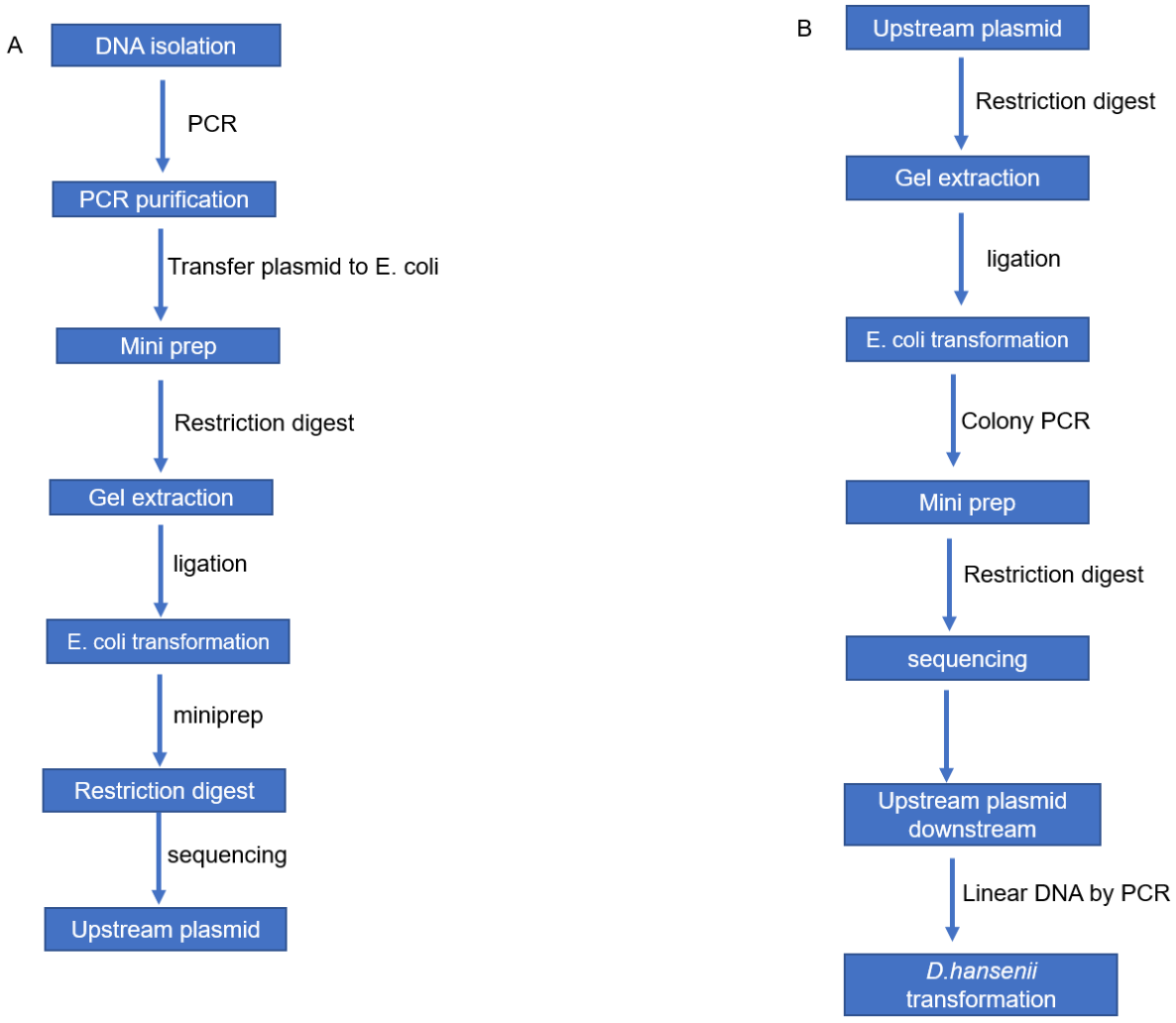

Figure 24 Flowchart showing the steps required for the generation of the gene deletion cassette and the selection and checking of the knockout before transforming to D. hansenii A) shows the steps for the upstream flank region of ARG1 cassette, B) shows the steps for adding the downstream flank region of arg1Δ to the plasmid.

To verify the knockout procedure with 50bp flank method is widely applicable in *D. hansenii,* as when we tried it in 13 different strains of *D. hansenii*, we obtained knock outs in all strains although, with different efficiencies. Many (10 out of 13) strains had however a second copy of *ARG1* gene.

The key factor for the knockout to work is the concentration of the DNA, the PCR product had to be precipitated to gain a higher concentration of the DNA: precipitating the DNA also improved the efficiency of the knockout. We are the first group to find that using the PCR amplification with 50bp flanks is effective in the *D.*

hansenii. This method provides a quick and effective strategy for genome modification and opens the way to improve strains through metabolic engineering for biotechnology.

Chapter4:

Physiological characteristics affecting the growth of a variety of *D. hansenii* isolates

4.1 Introduction:

In order to develop a robust *D. hansenii* strain for Biotechnology, we investigated 13 isolates for their ability to grow under a range of salt concentrations and temperatures. From this study, it became clear that the strains vary in the different parameters and careful selection may be required if *D. hansenii* is to be used for metabolic engineering and biotechnology. Since little is known about *D. hansenii*, it was decided to investigate and learn about the growth requirements of this yeast: two factors that are of interest for biotechnology were tested in different *D. hansenii* strains to see their effect on the growth.

The first one was salt tolerance; *D. hansenii* can grow at 4M NaCl while *S. cerevisiae* can grow at 1.7M NaCl (Larsson et al., 1990; Minhas et al., 2009). The main target for salt resistance in *D. hansenii* is the *HAL2* gene, which encodes lithium and sodium-sensitive phosphatase that hydrolyses 3-phosphoadenosine-5-phosphate (pAp). Yeast salt toxicity is due to the inhibition of Hal2 and the accumulation of pAp, which inhibits sulfate assimilation and RNA processing (Gil-Mascarell *et al.*, 1999; Prista *et al.*, 2005). Furthermore, the salt tolerance was tested on different mutants such as *pex3Δ*, and *fox2Δ*, these mutants have a proper block to β-oxidation of fatty acid, to see if the salt tolerance is related to peroxisomes because in *S. cerevisiae* peroxisomal fatty acid β-oxidation are shown to be required in high salt resistance (Manzanares-Estreder *et al.*, 2017).

The second factor was the temperature; different temperatures were tested such as 20ºC, 25ºC, and 30ºC. Studying the factors that influence *D. hansenii* cell growth is important because it helps to understand this yeast in order to provide the optimal environment for it to grow. One of the advantages of *D. hansenii* is that it can grow on a wide variety of carbon sources such as glucose, galactose, glycerol and oleate this was tested on the WT, *pex3Δ*, and *fox2Δ* mutants. Growth curves were conducted as a phenotype for the *pex3Δ* knockout explained in Chapter 5 since they do not grow on oleate as sole carbon source.

4.2 The *FOX2* gene:

The *FOX2* gene encodes the multifunctional protein in yeast that catalyses the second and third step in peroxisomal beta-oxidation as shown in Figure 25 (Hiltunen *et al.*, 1992). The gene was knocked out in two strains (NCYC 3363 and NCYC 102) by Selva Turkolmez in the Hettema lab, using a HygroB marker under the control of *TEF1* promoter and *TEF1* terminator from *Scheffersomyces stipitis. FOX2* turned out to be single copy in NCYC 3363 whereas in NCYC 102 there was a second copy of the gene. As expected, the NCYC 3363 *fox2Δ* mutant shows a growth deficiency on the oleate as it cannot utilise fatty acids because the fatty acid β-oxidation pathway is blocked. The mutants used in this chapter are *fox2Δ* and *pex3Δ*, which are further analysed and described in Chapter 5.

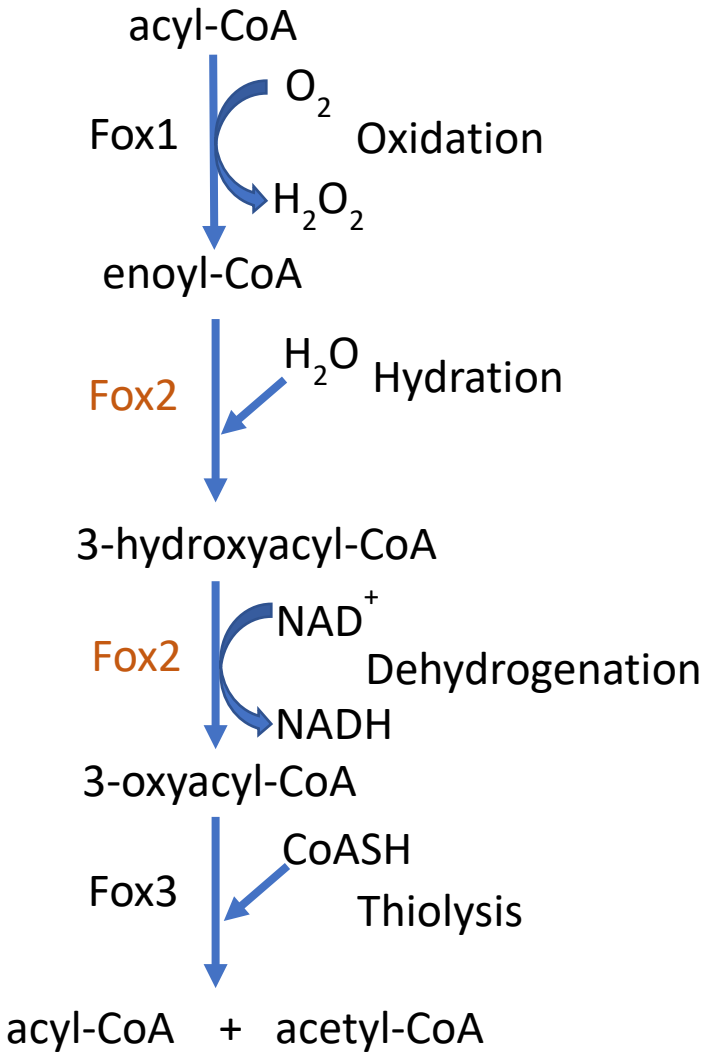

Figure 25 fatty acid β-oxidation in yeast. This pathway occurs in peroxisomes, showing the Fox2 protein mechanism (Visser et al., 2007). Fox1 is an acyl-CoA oxidase.

4.3 Salt tolerance:

D. hansenii is a halophilic yeast which can grow in a media containing various salt concentrations (Guerrero *et al.*, 2005). A number of scholars have observed that sodium protects *D. hansenii* from oxidative stress and additional abiotic stresses

such as excessive pH and high temperature (Almagro *et al.*, 2000; Papouskova and Sychrova, 2007; Navarrete *et al.*, 2009, 2022). This lineament gives the yeast the opportunity to be used in food fermentation in the industry because it can tolerate high-stress levels. In discussing salt tolerance in yeast, Thomé,(2007) explains that the cells create and store glycerol under hyperosmolarity conditions. The *DhGPD1* is involved in the osmotically regulated synthesis of glycerol (Thomé, 2007). Thomé,(2007) points out that *DhGPD1*, *DhENA1*, *DhENA2*, and *DhGDH1* are the genes controlling the salt resistance in *D. hansenii*. *DhGPD1* encodes for glycerol-3-phosphate dehydrogenase. *DhGPD1* localizes to peroxisomes (Selva Turkolmez) suggesting that peroxisomes may also play a role in salt tolerance in *D. hansenii*. *DhENA1* and *DhENA2* encode Na^+ ATPases which are mainly influenced by the ionic environment of the cell and function in the outflow of sodium. *DhGDH1* encodes for $NAPD^+$ dependent glutamate dehydrogenase (Thomé, 2007). Another, different feature about *D. hansenii* is that the sodium stimulates potassium transport at pH=4.5 while in *S. cerevisiae* the sodium inhibits the potassium uptake (Almagro *et al.*, 2000). Different concentrations of salt (NaCl) were tested: 0M, 1M, 2M, 2.5M, 3M, and 4M respectively on different strains of *D. hansenii*, and *S. cerevisiae*, the strain used for this experiment was NCYC 3363.

Salt tolerance was investigated with different concentrations of glucose to test if the salt stress adaptation in *D. hansenii* requires a peroxisomal function as has been reported for *S. cerevisiae* (Manzanares-Estreder *et al.*, 2017). The experiment was carried out several times with different amount of glucose such as 2%, 1%, 0.5%, and 0.1% and on different media YM deb and YPD. This was done via the spot assay procedure explained in the Materials and Methods. First, the cells were grown overnight in YM deb media, then inoculated to a fresh YM deb till the OD_{600} reached

0.1, then the cells were moved to the 96-well microtiter plate for the spot assay method. The cells were then replica plated on YM deb or YPD media with different amounts of NaCl and glucose. Then they were incubated at 25^{o}C for 3-4 days for *D. hansenii*, while for *S. cerevisiae* the cells were incubated at 30^{o}C for 3-4 days.

D. hansenii WT and *pex3Δ* were able to grow with the different amounts of glucose in the YM deb media at 0M, 1M, 2M, 2.5M, 3M NaCl. From Figure 26 we can see that there was no difference between the WT and *pex3Δ* in growth; however, at 4M NaCl, there was no growth at all. In contrast, in the 0.5% glucose YM deb media at 2M, 2.5M, and 3M NaCl the *pex3Δ* mutant and the WT barely showed signs of growth; while in the 0.5% glucose YPD at both 2.5M and 3M NaCl the cells hardly grew. Moreover, in the YPD media at 0.1% glucose and at 3M NaCl the cells struggled to grow.

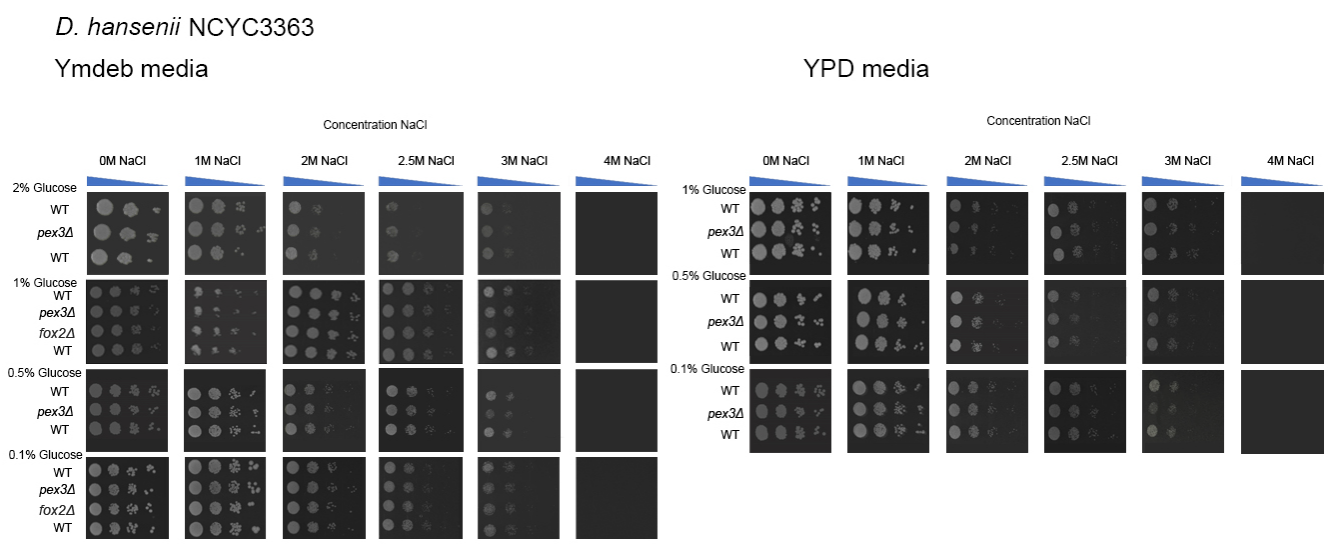

Figure 26 Sensitivity of D. hansenii growth to NaCl concentrations on various glucose containing YM deb media or YPD media. The amounts of glucose were 2%, 1%,0.5%, and 0.1%. Cells were dropped onto the plate as serial dilutions and incubated for 3-4 days at 25ºC. Blue triangles indicate decreasing cell density from left to right.

On other hand, in *S. cerevisiae* the cells were able to grow at 0M, and 1M NaCl only, and the different amounts of glucose as shown in Figure 27. Additionally, there was no difference in growth between the WT and *pex3Δ* cells, across all the different NaCl and glucose amounts. However, at 0.5% glucose and 1M NaCl and 3% ethanol, the cells partially grew. Since there is no difference between the WT and the *pex3Δ* growth across all the different media and different glucose levels the results confirm that the salt tolerance is not related to the peroxisomes in *D. hansenii*. This also indicates that *D. hansenii* is different from *S. cerevisiae* in responding to salt stress.

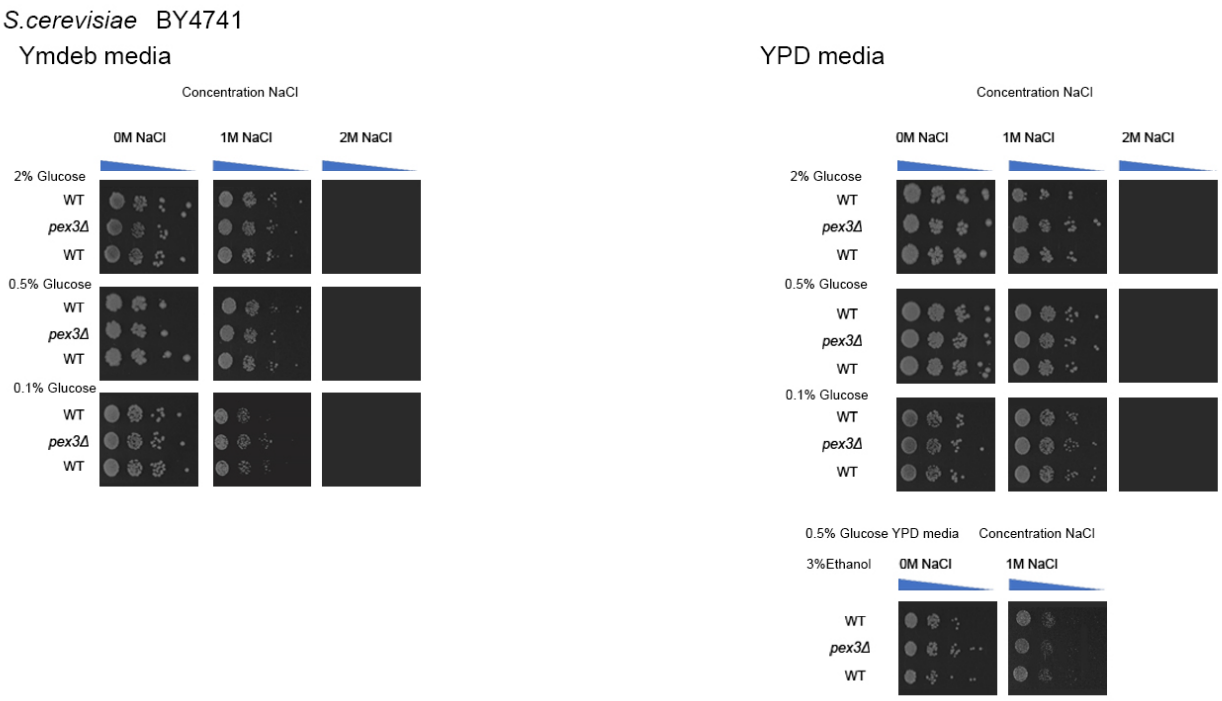

Figure 27 Sensitivity of S. cerevisiae growth to NaCl concentrations on various glucose containing YM deb media or YPD media. The amounts of glucose were 2%, 1%,0.5%, and 0.1%. Cells were dropped onto the plate as serial dilutions and incubated for 3-4 days at 30°C. Blue triangles indicate decreasing cell density from left to right.

First, salt tolerance was tested on the NCYC 3363 strain of *D. hansenii.* Then we set out to test 10 isolates; Because the salt tolerance is of interest to biotechnology it was decided to test it in10 different strains of *D. hansenii*: CBS 13215, CBS 767, CBS 7848, CBS 13202, CBS 1102, CBS 5139, CBS 5307, CBS 13195, CBS 1142, CBS 1099. The sources of strains are different: Zooplankton, Carlsberg laboratories, Takuan Japanese salted pickle, Southern Ocean seawater 497M, beef-pork sausage, skin of man, stomach of fish, Southern Ocean seawater 4509M, sake-moto, and cheese respectively. The cells were grown at 0M, 1M, 2M, 2.5M, 3M, and 4M NaCl for 3-4days at 25°C; this was repeated three times. The cells were grown the same way described earlier for the NCYC 3363. The highest amount of salt the cells can grow at was 2.5M NaCl; at 3M some strains were not able to grow: CBS 13215, CBS 767, CBS 13202, and CBS 1102; while at 4M NaCl all 10 strains were

not able to grow at all. Since the strains are from different sources this explains the difference in growth between the isolates. The media used to grow the cells was a YM deb agar plate media with 0.1% glucose. Figure 28 shows the results of the 10 different strains growing on different amounts of salt.

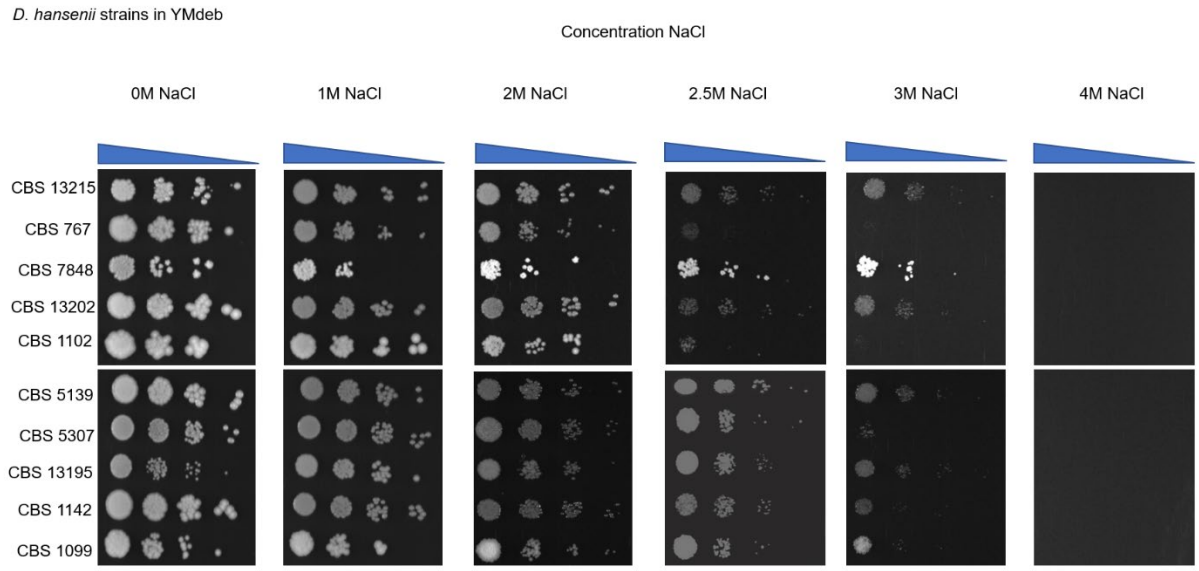

Figure 28 Sensitivity of the growth of D. hansenii different strains to NaCl concentrations on 0.1% glucose in YM deb media. The 10 different strains are CBS 13215, CBS 767, CBS 7848, CBS 13202, CBS 1102, CBS 5139, CBS 5307, CBS 13195, CBS 1142, CBS 1099 Cells were dropped onto the plate as serial dilutions and incubated for 3-4 days at 25ºC. Blue triangles indicate decreasing cell density from left to right.

4.4 Temperature:

Navarrete,and Martínez (2020) support the notion that *D. hansenii* can grow in a wide range of temperatures from 20ºC to 35ºC, but our initial results disagree with that because the strains NCYC102, NCYC 3363, and NCYC 3981 cells were not able to grow at 30ºC. *D. hansenii* cells were grown at different temperatures such as 20ºC, 25ºC, and 30ºC in the YM deb media. First, the cells were grown overnight in the YM deb, then they were inoculated to a fresh YM deb till the OD_{600} reached 0.1. After that, 200µl of cells were moved to the 96-well microtiter plate to do the spot assay explained in the Materials and Methods section. The cells were than incubated

at the required temperature for 3-4 days. This procedure was repeated three times to obtain the optimal temperature for *D. hansenii* cell growth, this was found to be 25ºC. Figure 29 below shows the growth of different strains of *D. hansenii* at 3 different temperatures; the strains are NCYC 102, NCYC 3363, and NCYC 3981. At 30ºC only the NCYC 102 showed growth in the first column, while at 20ºC, and 25ºC the cells grew properly. Since the temperature is one of the factors of interest in biotechnology, it was decided to test it at all 10 universal isolates of *D. hansenii:* CBS 13215, CBS 767, CBS 7848, CBS 13202, CBS 1102, CBS 5139, CBS 5307, CBS 13195, CBS 1142, CBS 1099, were grown at different temperatures such as 20ºC, 25ºC, and 30ºC, in the same way, described earlier. Figure 29 shows the 10 different strains of *D. hansenii* grown at 20ºC, 25ºC, and 30ºC. The cells were grown in triplicate for each different temperature. From the results, the optimal temperature for *D. hansenii* to grow at is 25ºC; because at 30ºC the strains CBS 13215, CBS 767, CBS 13195, and CBS 1099 showed no growth. Also, at 20ºC the strain CBS 5307 struggles to grow, while at 25ºC degree all the strains grow easily. Clearly, different strains have different temperature requirements for optimal growth. Knowing the optimal temperature for the yeast is crucial because the cells can successfully grow at the required media while at low and high temperatures the cells did not grow.

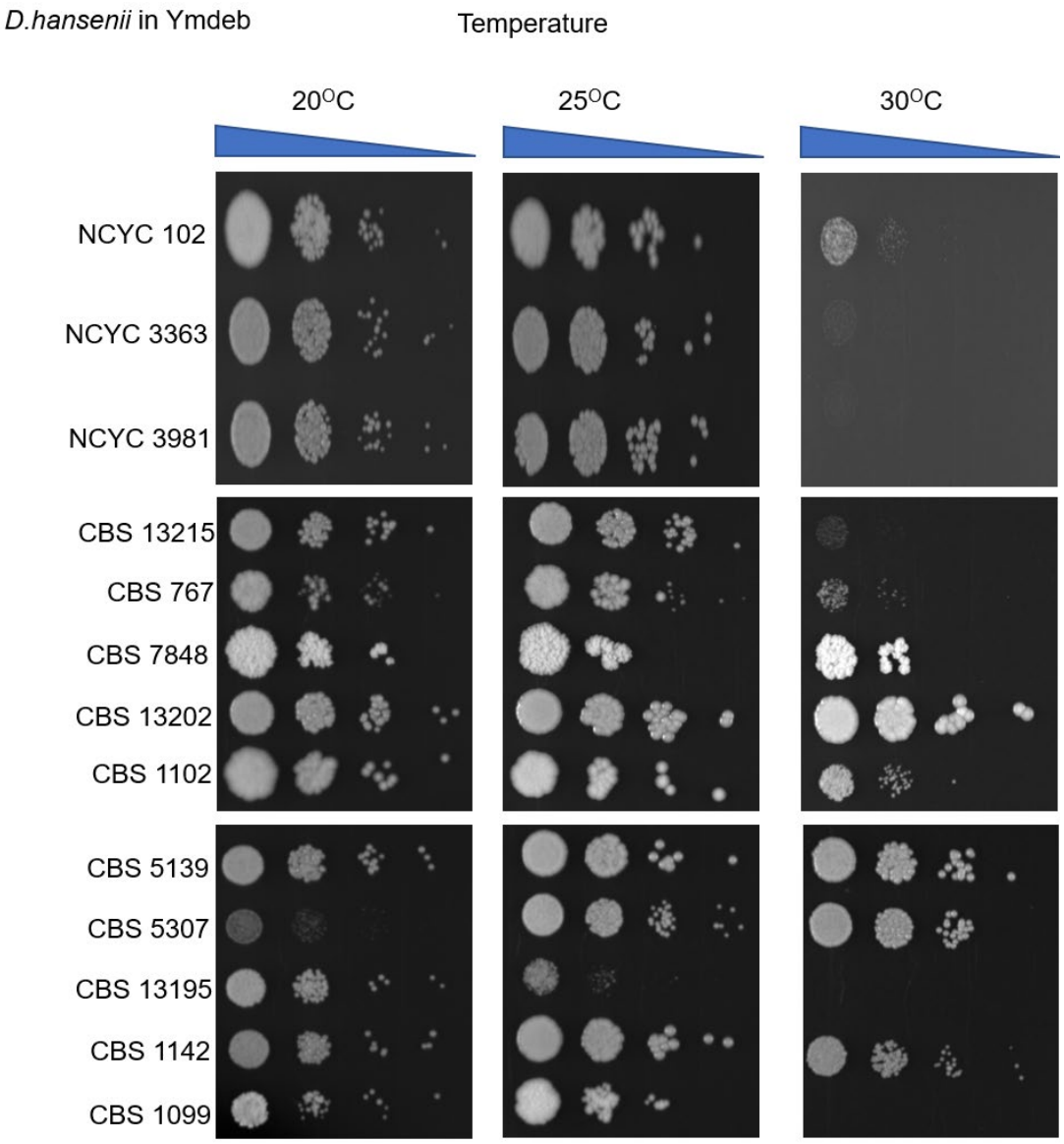

Figure 29 Sensitivity of D.hansenii strains to different temperatures on YM deb media. Cells were dropped onto the plate as serial dilutions and incubated for 3-4 days at the required temperatures (20°C, 25°C, and 30°C). Blue triangles indicate decreasing cell density from left to right.

4.5 Different carbon source:

The growth of *D. hansenii* was compared to the growth of different yeast strains species including *S. cerevisiae, S. cerevisiae pex3Δ, Hansenula polymorpha, Kluyveromyces lactis, Y. lipolytica, Pichia pastoris, and Cryptococcus curvatus*. *D. hansenii* showed growth on all different media while other yeasts such as *S. cerevisiae* had difficulty growing on both oleate and glycerol media as shown in Figure 30.

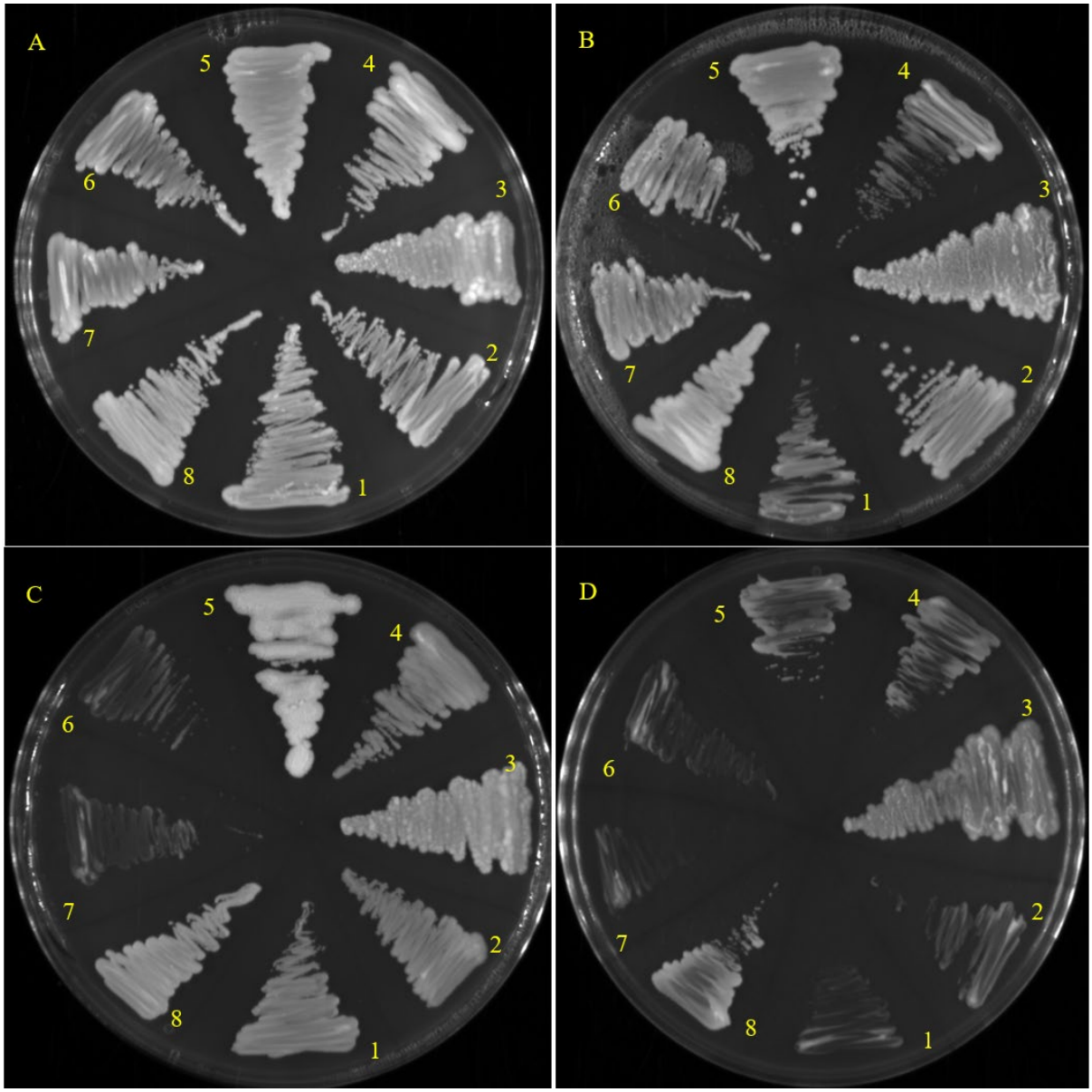

Figure 30 Comparison of D. hansenii growth with other yeasts on different carbon source. The carbon sources are A) glucose, B) galactose, C) glycerol, D) oleate. The different yeasts are 1. H. polymorph; 2. K. lactis; 3. Y. lipolytica; 4. P. pastoris; 5. C. curvatus; 6. S. cerevisiae; 7. S.cerevisiae pex3Δ; 8 D. hansenii.

Similarly, different mutants of *D. hansenii* were grown on different carbon sources such glucose, galactose, glycerol and oleate, as in Figure 31. While the cells were able to use glucose, galactose, and glycerol as a carbon source, the *pex3Δ* and *fox2Δ* mutant cells were not able to use oleate as a carbon source, since fatty acid β-oxidation is blocked in both *pex3Δ* and *fox2Δ* mutants. In Figure 31 the cells in *pex3*Δ show a small and slowly growth while the *fox2Δ* mutant shows no growth at all, because in both mutants the β-oxidation pathway, the fatty acid breakdown, is

obstructed. In the literature on *D. hansenii,* there seems to be general agreement that *D. hansenii* can utilize a wide range of sugars commonly found in lignocellulosic biomass (Navarrete, Estrada and Martínez, 2022). This has made it possible to extrapolate to other strains of the same species (Dyerberg, Navarrete and Martínez, 2022). This explains the results where *D. hansenii* had the ability to grow on different carbon sources, even the mutants constructed had the same ability. Thus it apperas that *D. hansenii* has good potential to be used in Biotechnology.

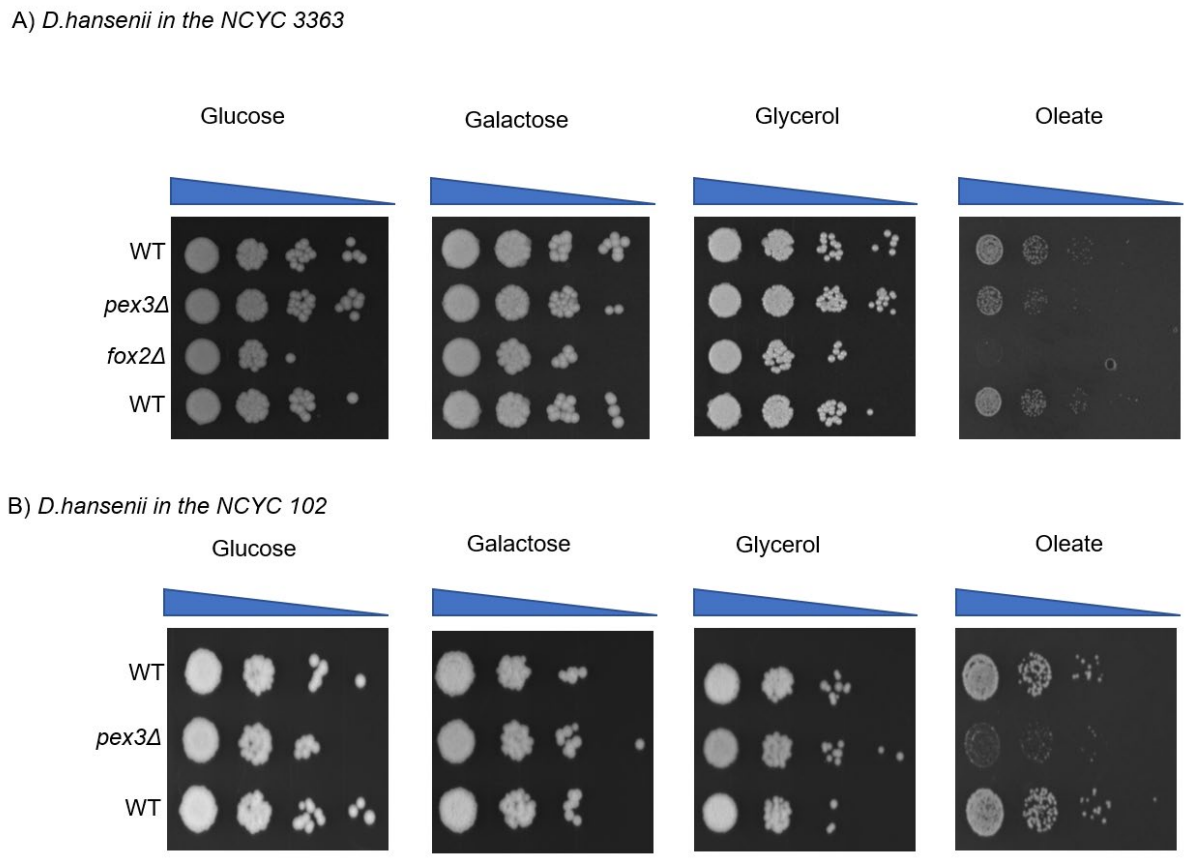

Figure 31 Growth of D. hansenii strains NCYC 3363 and NCYC 102 on different carbon sources. The different carbon sources are glucose, galactose, glycerol, and oleate. The cells were WT, pex3Δ, and fox2Δ mutants. Cells were dropped onto the plate as serial dilutions and incubated for 3-4days at 25ºC. Blue triangles indicate decreasing cell density from left to right.

4.6 Growth curves

Growth curves of cell grown on different carbon source containing media were determined. The carbon sources used were glucose, galactose, glycerol, and oleate. The growth curves for glucose, galactose, and glycerol were similar in terms of their WT and in the case of the *pex3Δ* knockout because both *D. hansenii* WT and the *pex3Δ* knockout can grow on sugars even without peroxisomes (Figures 32, 33, 34). On the other hand, *pex3Δ* knockout cells grew very slowly on the oleate because the β-oxidation was blocked. In the growth curve on the oleate, the difference was very clear between the WT and the *pex3*Δ knockout because the WT could break the oleate down easily while the *pex3Δ* knockout could not (Figure 39). In the same way, *S. cerevisiae pex3Δ* mutant grows very slowly on oleate media while the WT can use oleate easily (Al-Saryi *et al.*, 2017). The OD_{600} was measured every half an hour for glucose, galactose, and glycerol media for the duration of 6 hours at 25^{o}C, shaking at 200rpm. For growth on the oleate medium (Figures 39,40, and 41) YM2 glucose (Figure 35) and YM2 glycerol (Figure 36), measurements were taken every 3 days, one reading in the morning and one reading in the afternoon. Growth curves were recorded in the NCYC 102 strain, because it had only one single copy of *PEX3, and* it was the first strain we investigated. Eight curves were the results of the WT and *pex3Δ* cells on different carbon sources. A problem occurred at the beginning of the oleate growth curve this problem will be discussed before the oleate curves below.

1)The first curve was performed on glucose as the carbon source, the WT and *pex3Δ* mutant curves overlap because both cells can grow on glucose Figure 32.

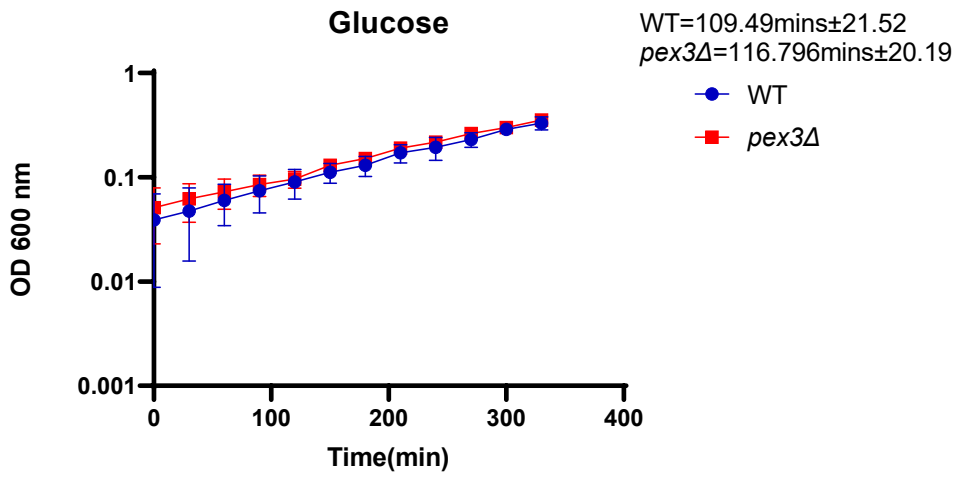

Figure 32 the WT, pex3Δ D. hansenii NCYC 102 cells growing on YM deb media with glucose as a carbon source, with the doubling time and standard deviation of these, for the WT=109.49min±21.52, and pex3Δ= 116.796mins±20.19. This was done triplicate.

2)The second curve used galactose as the carbon source, the WT and *pex3Δ* mutant curves overlap because both cells can grow on galactose Figure 33.

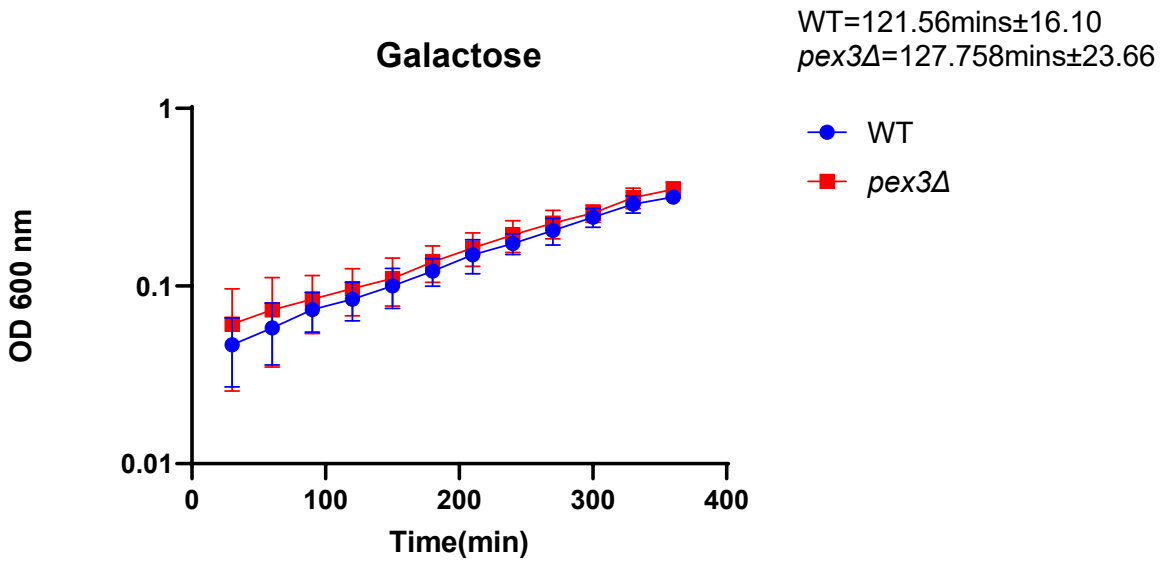

Figure 33 the WT, pex3Δ of D. hansenii NCYC 102 cells growing on YM deb media with galactose as a carbon source, with the doubling time and standard deviation of these, for WT= 121.56mins±16.10, and pex3Δ= 127.758mins±23.66. This was done triplicate.

3)The third curve was with glycerol as the carbon source, the WT and *pex3Δ* mutant curves overlap because both cells can grow on glycerol Figure 34.

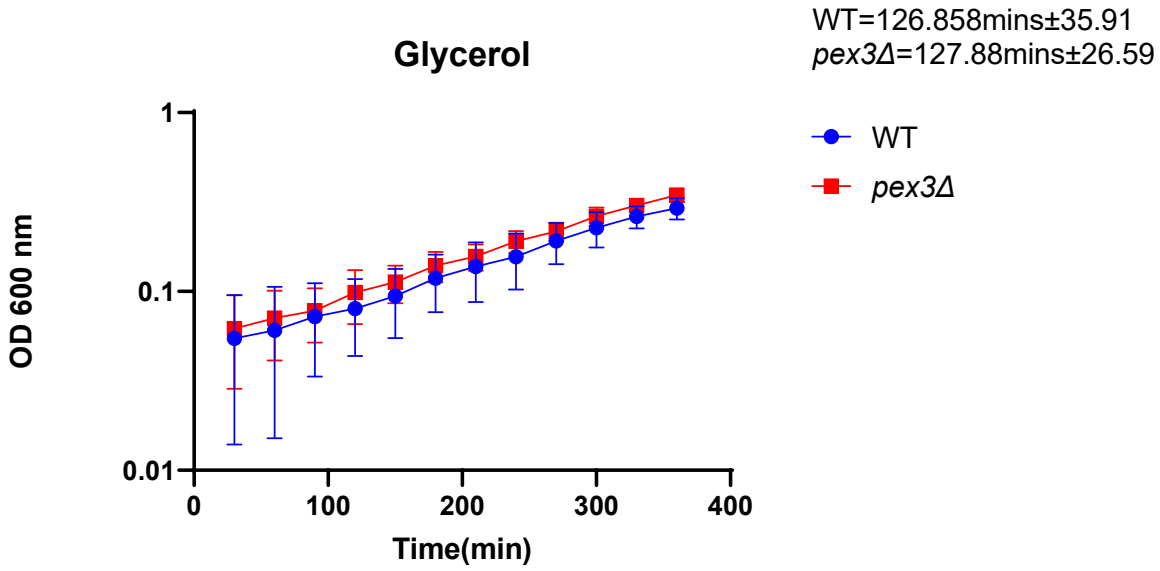

Figure 34 the WT, pex3Δ of D. hansenii NCYC 102 cells growing on YM deb media with glycerol as a carbon source, with the doubling time and standard deviation of these, for WT= 126.858mins±35.91, and pex3Δ=127.88mins±26.59. This was done triplicate.

4)The fourth curve utilized YM2 glucose, the curves overlap because the cells are able to utilize glucose Figure 35.

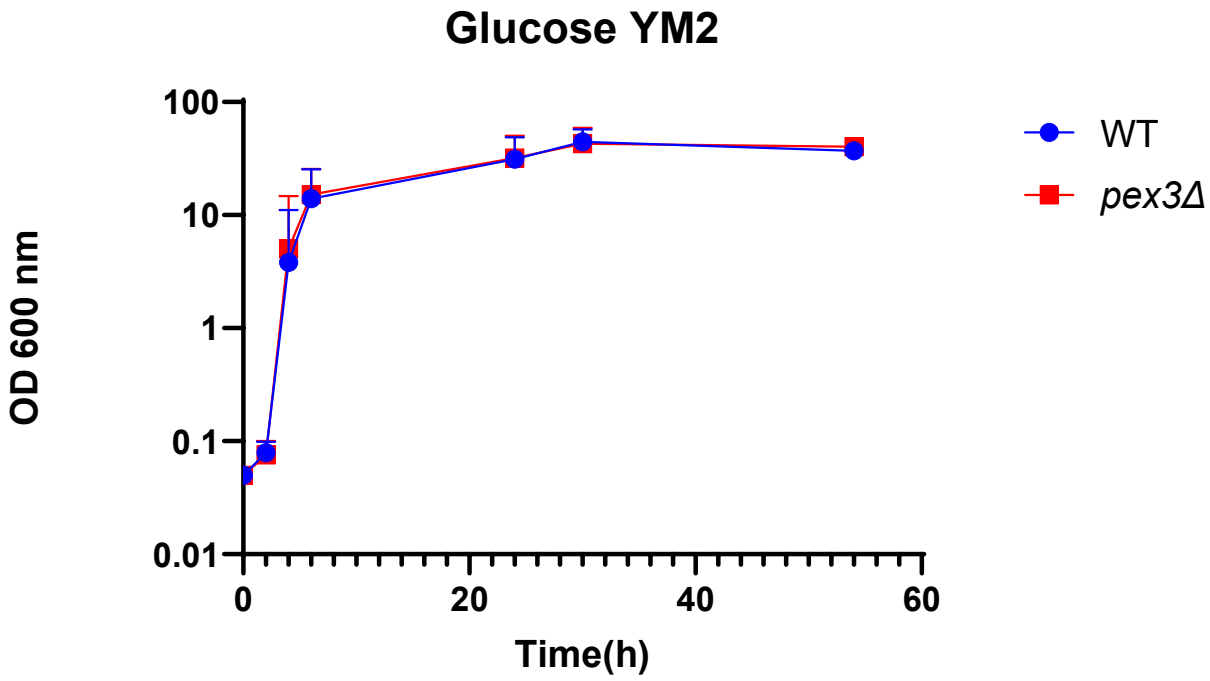

Figure 35 the WT and pex3Δ D. hansenii NCYC 102 cells using glucose as a carbon source on YM2 media. Both cells can grow on glucose as a carbon source in YM2 media. As shown in the figure the curves overlap with each other so there is no difference in growth. This was done triplicate.

5)The fifth curve was carried out on YM2 glycerol, the curves overlap because the cells are able to utilize glycerol Figure 36.

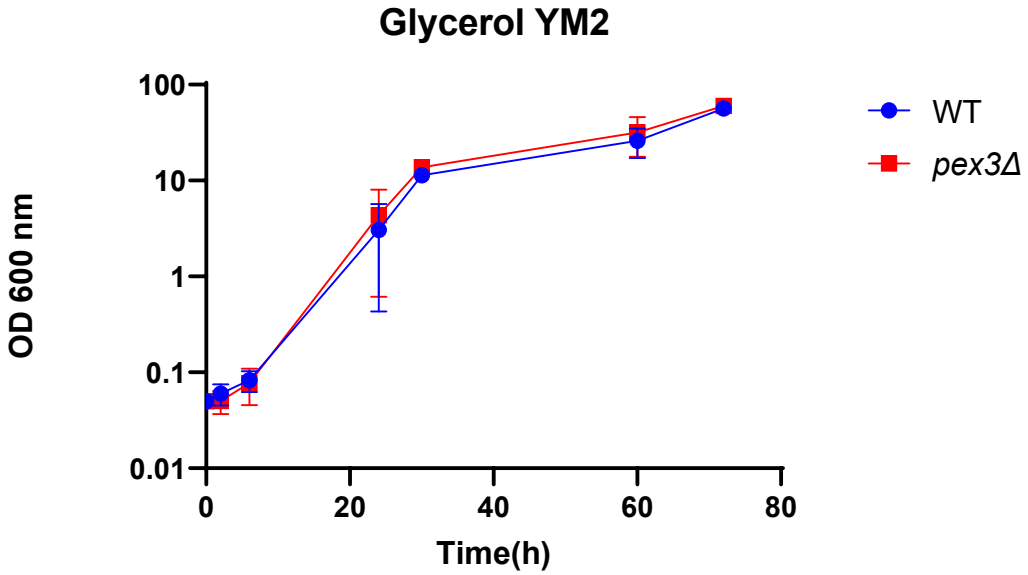

Figure 36 the WT and pex3Δ D. hansenii NCYC 102 cells using glycerol as a carbon source on YM2 media. Both cells can grow on glycerol as a carbon source in YM2 media. As shown in the figure the curves overlap each ether so there is no difference in growth. This was done triplicate.

4.7 Choosing the correct media for the oleate

A problem was found at the beginning of the oleate growth curve. The WT and *pex3Δ* knockout (to be explained in Chapter 5) both grew on the oleate media, which was not expected. As a result, different oleate media were tested. Malt extract was eliminated from the media because the cells were able to use it as a carbon source see Figure 37. All the media used for testing the oleate were dissolved in Millipore water to a final volume of 50ml, mixed with a magnetic follower and then autoclaved. In addition, 500µl (100x) of leucine (0.3g leucine in 100ml H_2O), 500µl (100x) of uracil (0.2g uracil in 100ml H_2O), and 500µl (100x) tryptophan (0.2g tryptophan in 100ml H_2O) were added to the fourth and fifth media only. The first media was used in this study for the oleate growth curves (Table 16). Figure 38 shows the growth curves for the WT *D. hansenii* on the different oleate media.

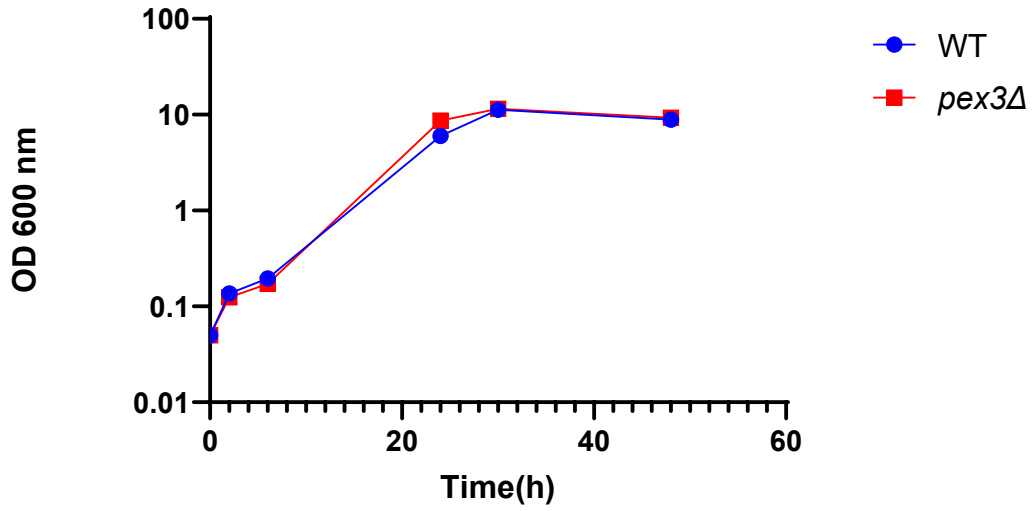

Figure 37 the WT and the pex3Δ growing on YM deb media with malt extract as a carbon source. D. hansenii NCYC 102 was able to use Malt extract as a carbon source.

name	Components for 50ml media
Media #1	0.06ml oleate + 0.1ml Tween 40, 0.05g yeast extract, 0.25g peptone, 5ml 500mM KPI (potassium phosphate buffer) buffer pH=6.
Media #2	0.05g yeast extract, 5ml of 500mM KPI buffer pH=6, and 0.25g peptone.
Media #3	0.1ml Tween 40, 0.05g yeast extract, 5ml of 500mM KPI buffer pH=6, and 0.25g peptone.
Media #4	0.06ml oleate, 0.1ml Tween 40, 5ml 500mM KPI buffer pH=6, 0.5g casamino acids, 0.25g ammonium sulphate, 0.085g yeast nitrogen base.
Media #5	5ml of 500 mM KPI buffer pH=6, 0.5g casamino acids, 0.25g ammonium sulphate, and 0.085g yeast nitrogen base.

Table 16The different media used for the oleate growth curves.

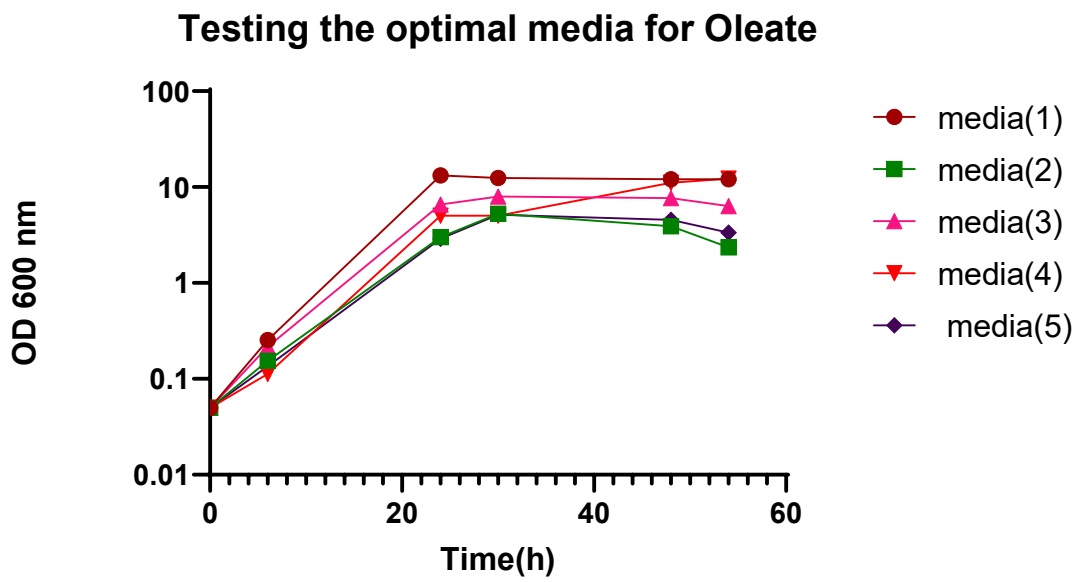

Figure 38 the growth curves done on 5 different media to choose the best medium for the oleate growth curve. The different media are media#1, media#2, media#3, media#4, and media#5. This was done on the WT D. hansenii NCYC 102 cells.

6)The sixth curve saw oleate used as a carbon source, the WT cells can utilize oleate easily while the *pex3Δ* mutant struggle to grow on oleate Figure 39.

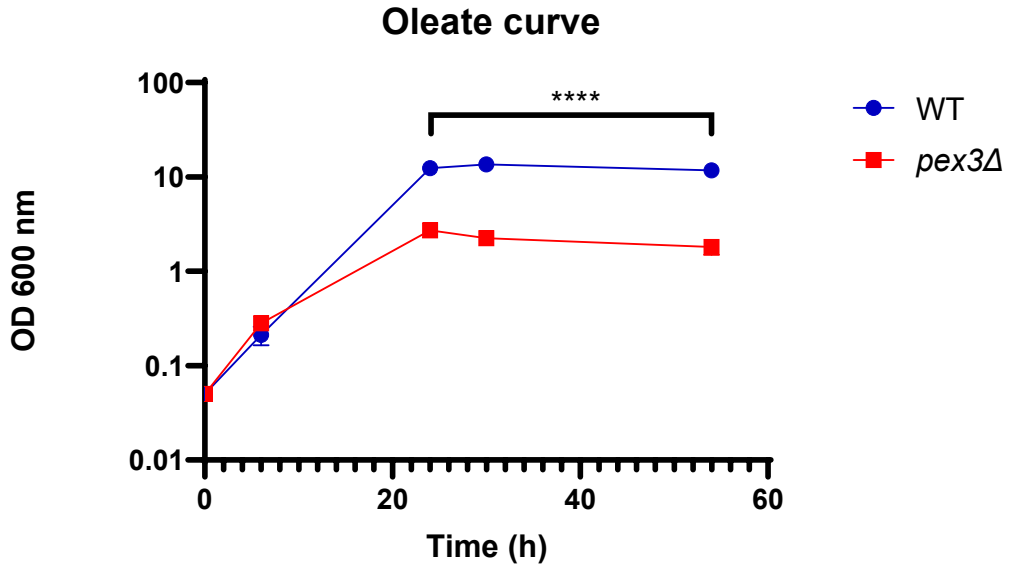

*Figure 39 the difference between the pex3Δ and the WT D. hansenii NCYC 102 cells on oleate media. The WT can easily grow on oleate while pex3Δ cells have a reduction in β-oxidation so they cannot breakdown the oleate efficiently. This caused the pex3Δ cells to grow slowly on oleate. The **** shows there is a significantly difference between the two curves t-test was done with P value 0.0001. This was done triplicate.*

7) D. hansenii WT and *pex3Δ* knockout cells were grown on the oleate at different starting points and readings were taken after 16 hours and 19 hours. For this curve the cells were inoculated at 6:00 pm in the evening; the *pex3Δ* knockout also grew very slowly while the WT showed a different growth pattern shown in curve 7 in Figure 40.

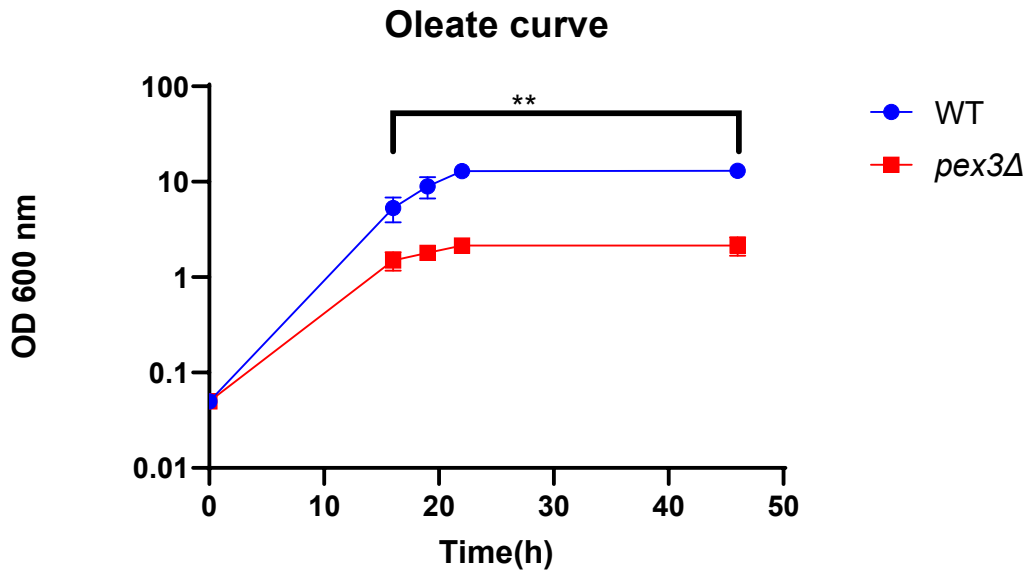

*Figure 40 D. hansenii NCYC 102 cells growing at different starting points to get a reading after 16 and 19 hours on oleate media. The ** shows the t-test and there is a significantly difference with P value=0.0046. This was done triplicate.*

8)The eighth growth curve, used the cells that were inoculated from the previous oleate growth curve and moved to a new oleate media. This was to show that the *pex3Δ* knockout would still not grow on oleate, as shown in Figure 41.

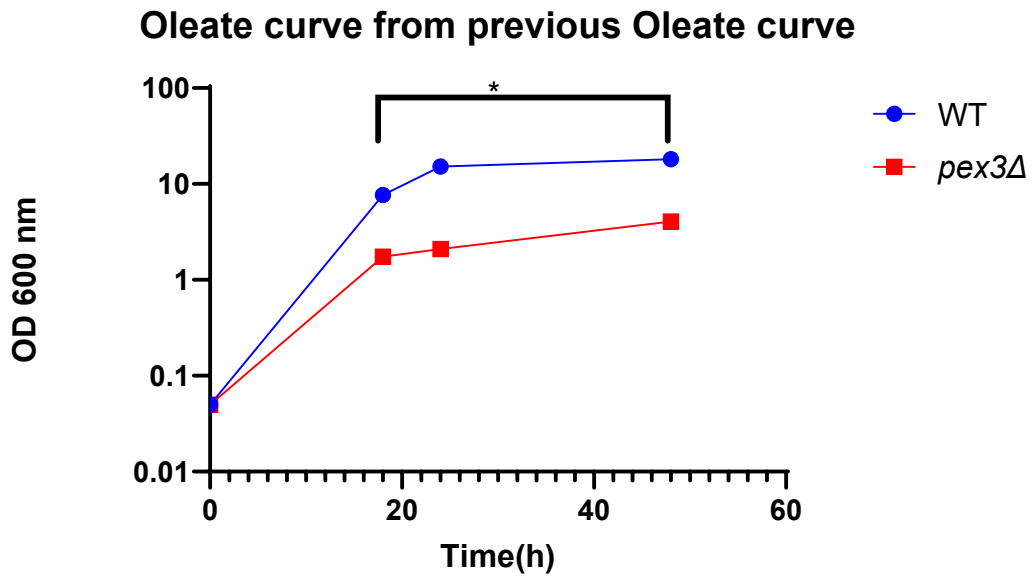

*Figure 41 pex3Δ and WT of D. hansenii NCYC 102 cells growing on oleate media which were inoculated from the previous oleate growth curve. The * shows the t-test was done there is a significantly different with P value 0. 0258. This was done triplicate.*

The growth curves show how the WT cells and the *pex3Δ* cells react on different carbon sources. In the glucose, galactose, and glycerol both cells show no difference in growth where the curves overlap. However, in the oleate media there is a significant difference between the WT and *pex3Δ* cells mutant with P value=0.0001. This proves that the β-oxidation pathway is blocked because the cells were not able to grow on the oleate. This will make the cells obtain more lipid: further information about lipid accumulation will follow in Chapter5.

4.8 Discussion:

It is generally accepted knowledge that *D. hansenii* can grow at 4M NaCl (Larsson *et al.*, 1990; Minhas, Biswas and Mondal, 2009; Navarrete, C.,and Martínez, 2020), but these results were different because the highest concentration of salt the cells

can grow on was 3M NaCl, there was no growth at 4M NaCl in all the strains we tested in the lab. This is probably due to the fact that it has been found growing in cheese, and soy sauces; so it appears it can tolerate salt up to 4M NaCl. Manzanares-Estreder et al. (2017) found evidence that under sugar limitation in *S. cerevisiae,* the salt stress adaptation requires a peroxisomal function; this is because the stress-activated protein kinase *HOG1* is essential for genes involved in the fatty acid β-oxidation which controls the growth on glucose and oleate. Our results contradict this paper because here the mutants (*pex3Δ*and *fox2Δ*) cells grew in the different salt concentrations under low amounts of glucose. Since the *pex3Δ* and *fox2Δ* mutants were able to grow in high amount of salt, and there was no difference in growth between the WT and the mutants we can conclude that the *D. hansenii* salt stress adaption does not require a peroxisomal function even though the *DhGPD1* is localized to peroxisomes (Selva Turkolmez) which suggest that peroxisomes may play a role in salt tolerance in *D. hansenii* but apparently it did not. Although *D. hansenii* reacts differently to salt tolerance than *S. cerevisiae*. Also, our results in *S. cerevisiae* contradict (Manzanares-Estreder *et al.*, 2017): there was no difference in growth between the WT and *pex3Δ*; even when the same conditions as described in the paper were used, we were unable to reproduce the data in the paper. The *pex3Δ* mutant in *D. hansenii* and *S. cerevisiae* was able to grow like the WT on all different media used with different amount of glucose and salt. This experiment was conducted several times: the same result was obtained in all experiments. Salt tolerance is a crucial feature in *D. hansenii* because it indicates that the yeast is strong and can tolerate different stress conditions used in industry. So, it is a promising yeast to use in biotechnology.

The temperature was tested as one of the factors that affects *D. hansenii* growth it was tested on different strains of *D. hansenii*; this was done to get a better understanding of yeast environment. Studying the factors affecting the growth of *D. hansenii* is important because it gives a clear view about the yeast and it's metabolism. Navarrete, C.,and Martínez (2020) acknowledge the fact that *D. hansenii can grow* in a wide range of temperatures from 20^{o}C to 35^{o}C*,* and the results demonstrate that they were not able to grow at 30^{o}C for the strains tested in the lab. The optimal temperature for *D. hansenii* was 25^{o}C, but there was a clear variation between different strains and the top temperature tolerated.

Then, the growth of *D. hansenii* on different carbon sources was tested and compared to a variety of other yeasts. It clearly showed that *D. hansenii* has the ability to grow robustly on all different carbon sources tested, frequently better than *S. cerevisiae*. Moreover, the mutants *pex3Δ* and *fox2Δ* were able to grow on all different carbon sources: glucose, galactose, and glycerol. However, they initially grew slowly on media with the fatty acid as main carbon source before growth ceased. The initial growth is on components in the media other than oleate that can support low level of growth. This is one of the features of *D. hansenii* that it can utilize a large variety of carbon sources such as maltose, lactose, arabinose, sucrose, and xylose (Dyerberg, Navarrete and Martínez, 2022) and grow in the presence of specific inhibitors such as vanillin and methanol makes it an excellent option for work in industrial bioprocesses for both lignocellulosic and non-lignocellulosic biomass materials (Navarrete, Estrada and Martínez, 2022).

Finally, growth curves were conducted as a phenotype of the *pex3Δ* explained in Chapter 5. The WT and *pex3Δ* were able to grow on glucose, galactose, and glycerol as a carbon source because the curves overlap each other, and the *pex3Δ*

can utilize the sugars without peroxisomes. On the other hand, on oleate the *pex3Δ* grows very slowly, the t-test was conducted and calculated the P value=0.0001, which demonstrates that there is a significant difference between the WT curve and the *pex3Δ* curve. In this chapter our results gave an overview about *D. hansenii, and* how it reacts to variety of salt concentrations, and different temperatures. Also, it has the ability to grow on different carbon sources. Also, at the end growth curves were shown to prove the *pex3Δ* (Chapter 5) was correct. Since little was known about this yeast it was important to study in detail the factors affecting the growth of *D. hansenii*.

Chapter5:

Lipid accumulation in the *D. hansenii* strains NCYC 102 and NCYC 3363

5.1 Introduction:

Debaryomyces hansenii is an oleaginous yeast that is able to accumulate more than 20% of its biomass as natural lipids (Jiru and Abate, 2014). The main lipids that are stored in the cells are triglycerides (TAG), which comprise 3 fatty acids and glycerol. TAG plays a role in energy storage and protection (Fakas, 2017). The glycerol backbone of the TAGs is synthesized from glycerol-3-phosphate (G3P) (see Figure 41). G3P can be synthesized through the phosphorylation of glycerol by glycerol kinase (*GUT1*) or through the reduction of dihydroxyacetone phosphate (DHAP) by G3P dehydrogenase (GPD1). The GPD1 reaction is reversible by another G3P dehydrogenase encoded by *GUT2* (Beopoulos *et al.*, 2008). NADH is oxidized back into NAD+ in the cytoplasm by reducing DHAP into G3P. In the mitochondria, G3P is oxidized back to DHAP by *GUT2* which is the glycerol-3-phosphate dehydrogenase using FAD to $FADH_2$, and $FADH_2$ is oxidized to ubiquinone(Q); this is called the G3P shuttle (Larsson *et al.*, 1998) (Figure 42). By knocking out the *GUT2* gene, G3P is not oxidized to DHAP; this increases the G3P levels which will increase the lipid accumulation (Thierry and Jean-Marc, 2011). The *GUT2* gene encodes Glycerol-3-phosphate dehydrogenase. Cells without the *GUT2* gene cannot grow on glycerol as sole carbon source (Beopoulos *et al.*, 2008). The lipids are stored in unique organelles called lipid bodies (LB) (Thierry and Jean-Marc, 2011). The lipid bodies are stained with Nile red upon excitation between 450 and 500 nm, Nile red will emit yellow fluorescence peaking at 485 nm under the microscope (Greenspan, Mayer and Fowler, 1985). Accumulation of lipids is caused by restrictions of nutrients such

as nitrogen, phosphate or sulphate (Yaguchi, Rives and Blenner, 2017). The restriction of nitrogen is easy to control and has a significant impact on lipid accumulation (Thierry and Jean-Marc, 2011). The cells were grown in a medium with low nitrogen; because the cells need nitrogen in the synthesis of proteins and nucleic acids and lowering the amount of nitrogen channels the carbon towards lipid synthesis and accumulation of TAG in oleaginous microorganisms (Thierry and Jean-Marc, 2011). One of the aims of this study is to test if *D. hansenii* accumulates more lipids if fatty acid breakdown is blocked. Since Fatty acid β-oxidation the anabolic pathways of fatty acid degradation is restricted to peroxisomes in yeast, the *PEX3* gene was knocked out from the *D. hansenii* genome as this evolutionarily conserved gene is essential for peroxisome formation. Also, a double knockout of the *pex3/gut2Δ* strain was generated to check if it accumulates more lipid. Subsequently, the mutants were grown under various growth conditions to induce and optimise TAG accumulation. The lipid content of the yeast was determined when the cells had been incubated in Nile red.

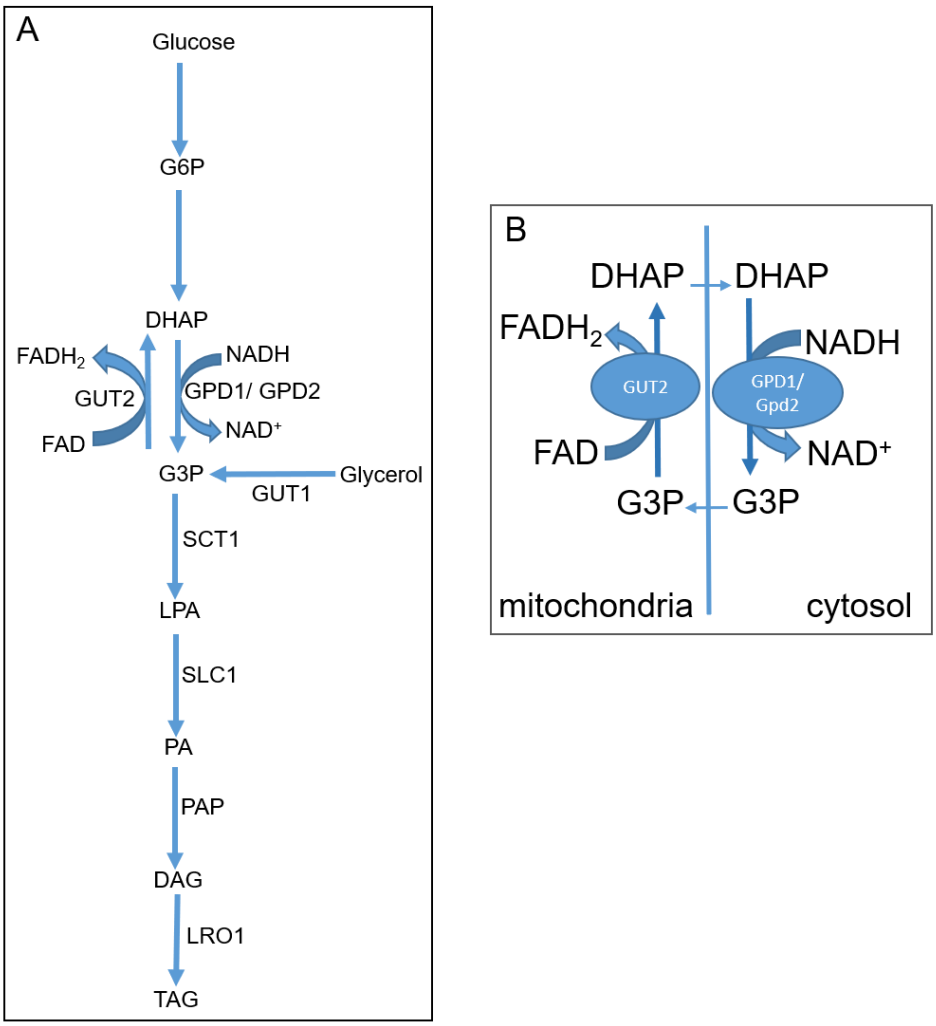

Figure 42 the synthesis of TAG and the functions of GUT1, GUT2, GPD1, and GPD2.A) First, the glucose is phosphorylated to glucose-6-phosphate by hexokinase using ATP. Glucose-6-phosphate is isomerized to fructose-6-phosphate by phosphoglucoisomerase. Fructose-6-phosphate is catalyzed by phosphofructokinase-1 to produce fructose-1,6-bisphosphate. The aldolase enzyme catalyzes the fructose-1,6-bisphosphate to glyceraldehyde-3-phosphate and dihydroxyacetone phosphate (DHAP) (Miesfeld and McEvoy, 2017). The DHAP is phosphorylated to glycerol-3-phosphate (G3P) by G3P dehydrogenase. G3P is acylated to lysophosphatidic acid (LPA) by G3P acyltransferase (SCT1), and then further acylated to phosphatidic acid (PA) by LPA acyltransferase (SLC1). This is followed by dephosphorylation of PA with PA phosphohydrolase (pAp) which releases diacylglycerol (DAG). In the final step, DAG is acylated by phospholipid DAG acyltransferase (LRO1 containing the glycerophospholipids as an acyl donor) to produce the TAG (Thierry and Jean-Marc, 2011). B) the G3P shuttle, the function of Gut2 using FAD to $FADH_2$, and GPD1, GPD2, NADH is oxidized back to NAD.

5.2 PEX3 gene deletion:

Pex3 is responsible for peroxisome membrane biogenesis, peroxisome segregation and peroxisome degradation (Hettema *et al.*, 2000; Fang *et al.*, 2004; Munck *et al.*, 2009; Motley, Nuttall and Hettema, 2012; Yamashita *et al.*, 2014). *PEX3* was knocked out to block peroxisome formation, which is expected to result in a block of β-oxidation of fatty acid in yeasts. The cells will not be able to break down the fatty acids efficiently, so more fatty acids are expected to accumulate and be available for TAG production. A potential candidate for *PEX3* ORF was identified by blasting the sequence of *S. cerevisiae PEX3* gene to *D. hansenii*, then get the Uniprot code, after that KEGG code was used; this protein code shows all the hallmarks of the *PEX3* gene as shown in Figure 43.

```
S.c     MAPNQRSRSLLQRHRGKVLISLTGIAALFTTGSVVVFFVKRWLYKQQLRITEQHFIKEQI   60
D.h     MPIFSSLNSFLRRHKKKLIVTATLTFSAY---FLVNQFIIKKLKNFQNSLRQELFVKEQI   57
S.s     MAIFSSLASFFNRHKRKIFITSTLTVSIY---FLFNHFVIKKFRDYQNALRQELIFKQQI   57
        *   .   *::.**: *:::: *   : :    :.  *: : : . *  : :: :.*:**

S.c     KRRFEQTQEDSLYTIYELLPVWRMVLNENDLNLDSIVTQLKDQKNQ---LTRA-------   110
D.h     KRRFVQTQNDCYLTILALLPVLTQPIIN-HLPIELITQALKLKKTNSNPTPQE-----IS   111
S.s     KQRFIQTQQDCYYTLLALLPVLTTPVID-YLPVELITHVLRLKKNNPNGQTAAGSVTGGS   116
        *:** ***:*.  *:  ****    : :  * :: *.  *: :*.:

S.c     ----------------KSSESRESSPLKSKAELWNELELKSLIKLVTVTYTVSSLILLTR   154
D.h     DSLLTTDNLTM-HQNTNDSSDLSHYMSLSKTELWKLLKIKTLTRTLTLMYSISGLLLLTR   170
S.s     NSELTTDNLNLLDTNNNPQSKMTVYMNKSKVELWALLKIKTITRTLTLIYSISGLLLITR   176
                      : ...       **.***  *::*:: : :*: *::*.*:*:**

S.c     LQLNILTRNEYLDSAIKLTMQQENCNKLQNRFYNWVTSWWSDPEDKADDAMVMAAKKSKK   214
D.h     LQLNILARRSYLESAIILAGGKVN---------------------------------DT   196
S.s     LQLNILARRSYLESAISMAGVKSTNN-------------------------------DI   204
        ******:*..**:*** ::  : .                                   .

S.c     EGQEVYINEQAFLSLSWWILNKGWLSYNEIITNQIEIEFDGIHPRDTLTLEEFSSRLTNI   274
D.h     ETSQDYFIEQSYLSLSWWLLNKGWLKISDLVEKVVTEKFNTINARTELSINKFDDLLCEM   256
S.s     NPHDNYLIEQSYLSLSWWLLNKGWVNLNSIIEPLVIKKFESITPKSELSIEQFDLILHDI   264
        :  : *: **::******:*****:. ..::   :  :*: *  :  *::::*.  * ::

S.c     FRNTNSQ--------IFQQNNNNLTSILLPKDSSGQEFLLSQTLDADALTS---------   317
D.h     VNELSTNHNQEILNAVFPISYDNLIESLLNTN---PELIKELDIEDSIMLKLINETTYLV   313
S.s     VNDISINHKQTILANLFPLNYDDLVETLFSTN---PDLLVQLEISDSNLNKLINETNSIM   321
        ..: . :        :*  . ::* . *: .:    ::: .  :. . : .

S.c     FHSNTLVFNQLVNELTQCIESTATSIVLESLINESFHFIMNKVGIKTIAKKKPGQEDQQQ   377
D.h     SNE--AFGDILINMVDSCKSTLIENLLL----------SLDPENAYTNQEKVIDISNIKQ   361
S.s     LDSQSGFFDLFNSVVSNMLNTLANNLSL----------SMNNGNDIAAE--SFLSNANKT   369
         ..   . : : . : .  .:   .: *           ::  .  :        .  :

S.c     YQMAVFAMSMKDCCQE-------MLQT------TAGSSHSGSVNEYLATLDSVQPLDDLS   424
D.h     FKLANLLAQLSIQCGVLCDNNNLMNDT---------FSNELSGNIYMNNLNEIESLDEFS   412
S.s     FKLASFLAQLSVQNFILSDNDNLKLEDQVNEEDDIEGNNDLTGNVYINNLY-LEELDDFS   428
        :::* :  .:.              :           .:. : * *: .*  :: **::*

S.c     ASVYSNFGVSSSFSFKP      441
D.h     ASIYSNFE---------      420
S.s     AGIYSNFE---------      436
        *.:****
```

Figure 43 the protein sequence (code) alignment for the PEX3 gene in S. cerevisiae (S. c), D. hansenii (D. h), and S. stipites (S. s).

Having identified a candidate *PEX3* gene, a gene deletion construct was generated. The construct was made in the plasmid pBluescriptSK (+) containing nourseothricin resistance marker (SAT1) under the control of *Candida albicans ACT1* promoter and *Candida albicans URA3* terminator flanked by 927bp upstream and 948bp downstream away from *PEX3* ORF (Figure 44). The SAT1 selectable marker cassette was originally developed for use in *C. albicans* and is a CTG codon adapted for use in CTG clade yeasts (Reuß *et al.*, 2004). As *D. hansenii* belongs to the CTG clade yeasts, we decided to use it for the disruption of the *PEX3* gene.

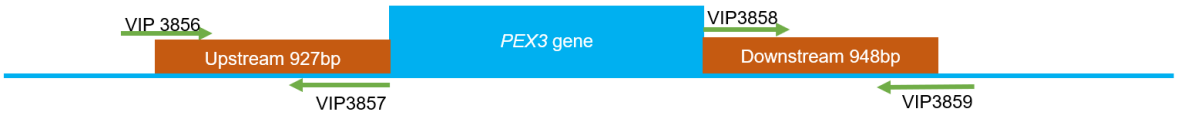

Figure 44 Chromosomal organization of PEX3 and primers used in the construction of the PEX3 gene deletion cassette. Green arrows are primers, numbers represent individual primer identification codes.

The plasmid pBluescriptSK (+) SAT1 was generated by Dr Zeena Alwan, a student in Hettema Lab and Gilmour Lab and used for the generation of the *GUT2* gene disruption cassette. After that, the sequence was copied to SnapGene to amplify the 927bp upstream region of the *PEX3* gene and 948bp downstream region (Figure 44). These PCR products were used as homology arms for gene deletion through homologous recombination (HR).

In order to generate a *PEX3* gene deletion construct, both flanks including the required restriction sites were created through PCR on total DNA from *D. hansenii* NCYC 102 strain. Then it was digested with the appropriate enzymes *KpnI* and *EcoRI* for the insertion of the 927bp upstream *PEX3* flank region. Then gel extraction and ligation were performed explained in Materials and Methods. Correct clones were identified and digested with *XbaI* and *SacI* to insert the 948bp downstream *PEX3* flank region Figure 45.

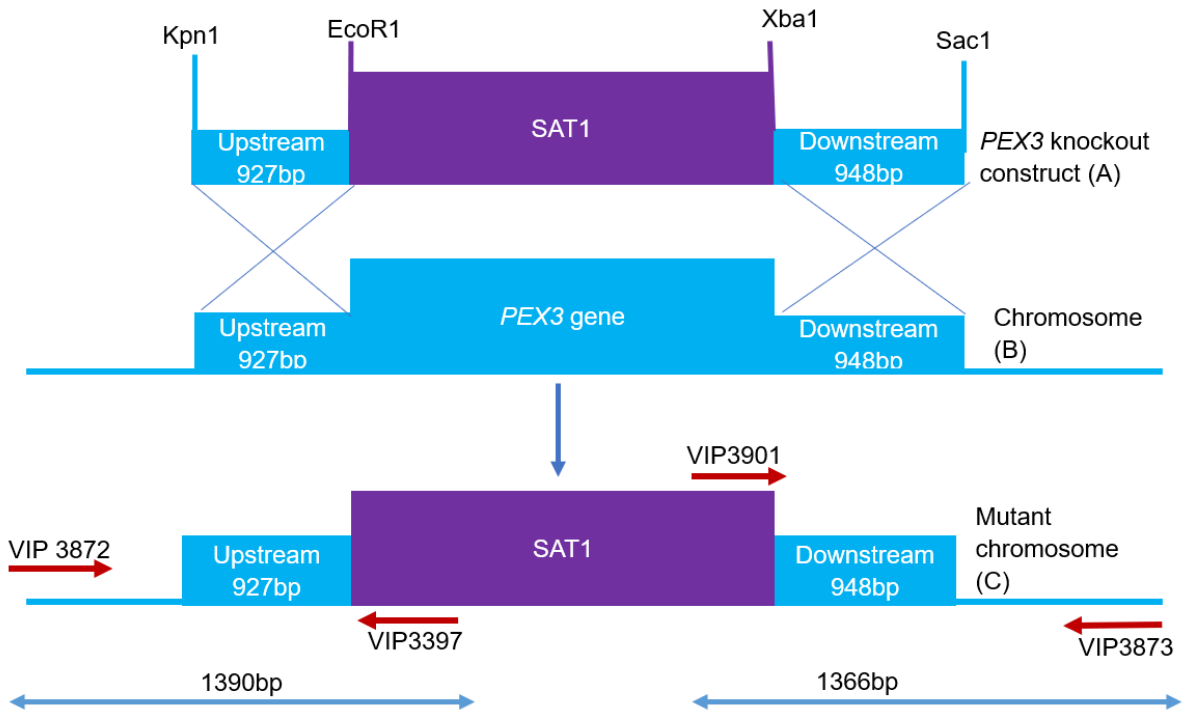

Figure 45The process of gene replacement through homologous recombination in D. hansenii. The insert of the pBluescriptSK(+)SAT1 plasmid is amplified by PCR resulting in product A. This is introduced into the cells through electroporation. The 1kb homology arm allows for homologous recombination with the chromosome (B) thereby replacing the PEX3 with the SAT1 marker (C). PEX3 was knocked out using the pBluescriptSK(+) SAT1 plasmid. The red arrows indicate the primers used in the PCR analysis while the blue arrows indicate the size of the PCR fragment.

The plasmid was then checked by DNA sequencing and was found to be correct. In order to generate a linearized DNA fragment comprising the gene deletion cassette, the whole cassette, which consists of the flanking regions and the selectable marker, was amplified by PCR. Subsequently, the PCR product (1µg), without further treatment, was transformed into *D. hansenii* cells (NCYC 102), through electroporation as described in Materials and Methods section (2.4.3). After electroporation, the cells were recovered in 1ml YM deb medium with 0.1M sorbitol for 4 hours at 25°C with shaking at 120rpm before plating out on YM deb medium containing 1.5µg/ml nourseothricin and incubated for 3-4 days in a 25°C constant temperature room.

Colonies were replica plated on YM deb medium with 5µg/ml nourseothricin to get pure colonies. Subsequently, the transformants were tested for the presence of the gene deletion cassette and this was indeed found to be present (Figure 46). When plated on an oleate medium, the *pex3Δ* cells grew very slowly on the oleate medium, a phenotype comparable with loss of peroxisome biogenesis and a defect in fatty acid utilisation (shown in Figure 46A).

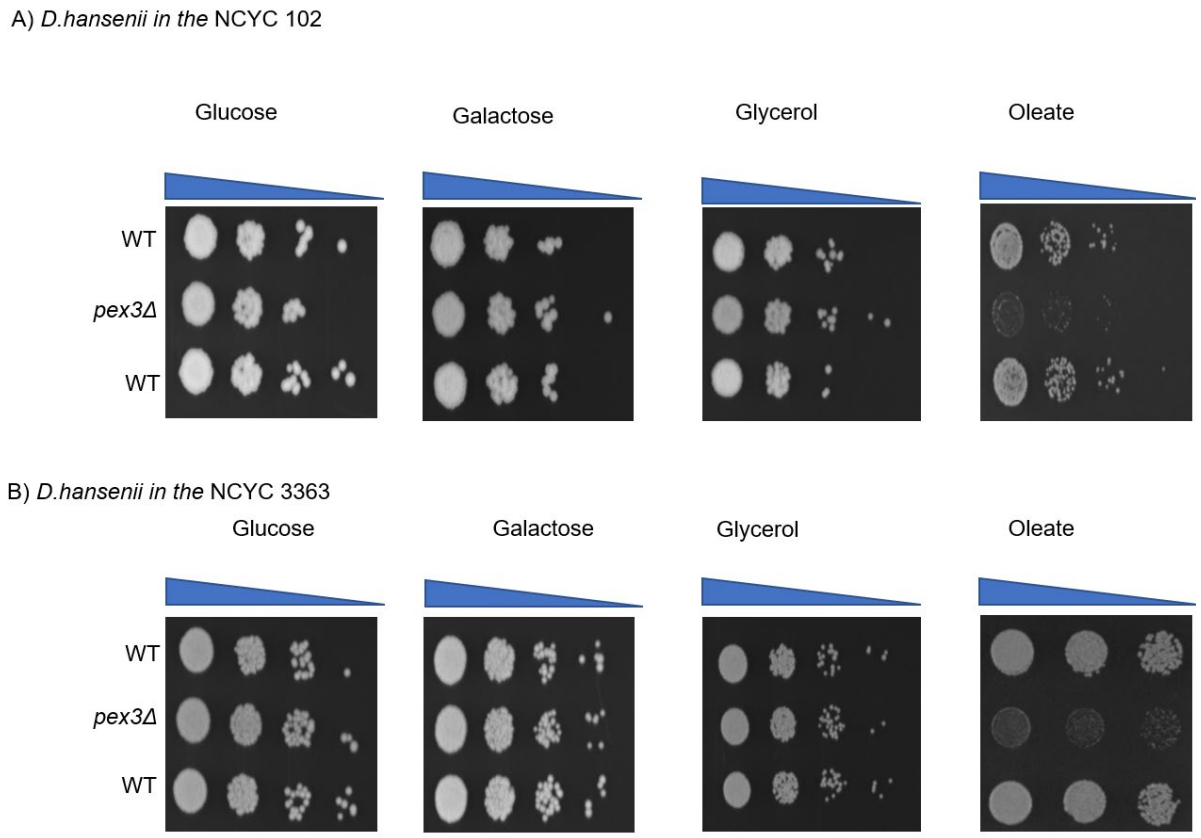

Figure 46 Growth of WT, and pex3Δ cells in two D. hansenii isolates on different carbon sources D. hansenii cells were grown in YM deb liquid culture to OD_{600}=1 and serial dilutions in water were spotted on glucose, galactose, glycerol, and oleate plates and incubated for 3 days at 25°C. A) NCYC 102 and B) NCYC 3363 strains. Both WT and pex3Δ cells grew on glucose, galactose, and glycerol. On oleate media, pex3Δ was not able to grow in both strain backgrounds. Blue triangles indicate decreasing cell density from left to right.

Although the NCYC 102 strain has one single copy of the *PEX3* gene; and also, of the *GUT2* gene, several other genes turned out to be present in multiple copies, including *ARG1* (see Chapter 3) and *ADE2* which was deleted by Tarad Abalkhail

(see Chapter 3). Selva Turkolmez in the lab found that several other genes related to fatty acid β-oxidation were also present at more than 1 copy in this strain and it was decided to focus most of our research on another strain that was identified in chapter 3 to be single copy for *ARG1*. In this strain, NCYC 3363 the *PEX3* knockout was also carried out. The PCR tests confirming that the *PEX3* ORF was deleted in *pex3Δ* cells are shown in Figure 47. The diagram shows where the primers are present for the PCR to check the absence of the *PEX3* gene. Subsequently, a PCR was carried out to check if there was still a WT *PEX3* copy present by using primers in the *PEX3* ORF. The PCR showed that in *pex3Δ* cells, no WT *PEX3* was present, and we conclude that *PEX3* is a single copy gene in NCYC 3363 (Figure 48). When *pex3Δ* cells were tested for growth on oleate media, their growth was severely affected whereas growth on glucose media, galactose media, and glycerol media was unaffected (Figure 46B).

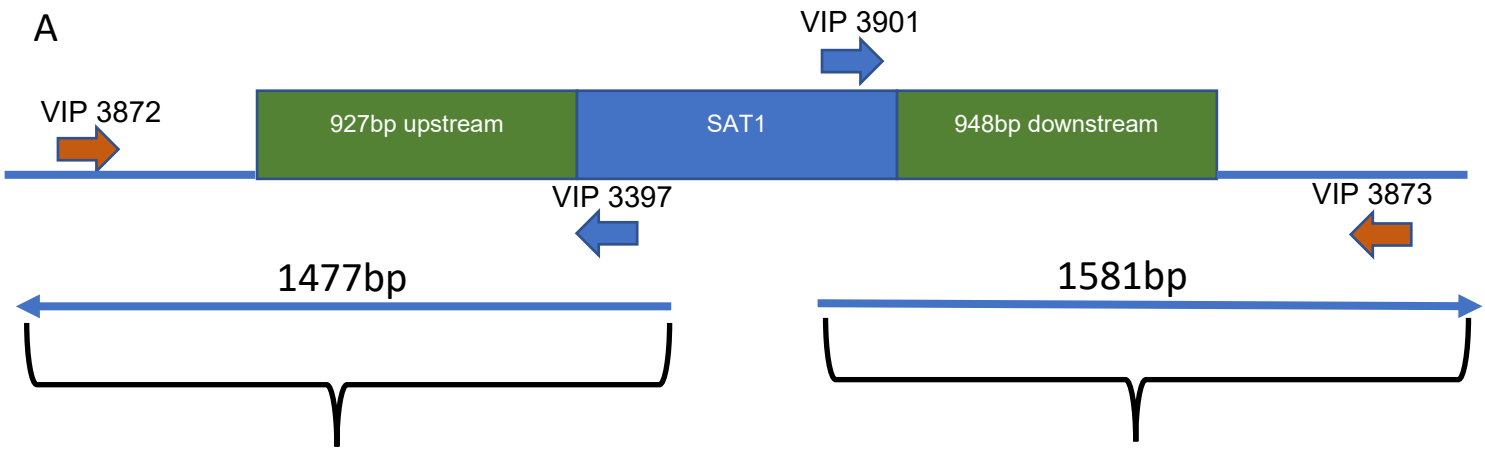

VIP3872 & VIP 3397 primers are used to check the upstream chromosomal region upon deletion of *PEX3* gene

(Only KO cells give this band)

VIP3901 &VIP3873 primers are used to check the downstream chromosomal region upon deletion of *PEX3* gene

(Only KO cells give this band)

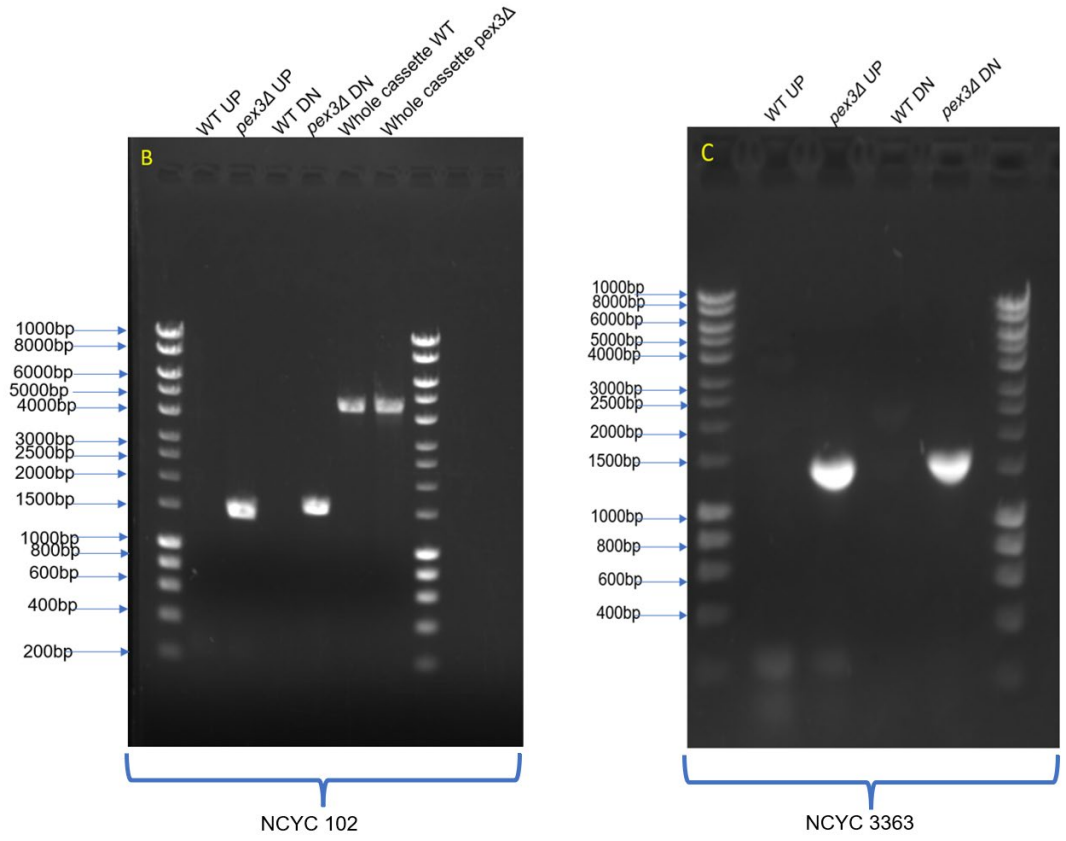

Figure 47 PCR analysis of PEX3 gene deletion mutant in D. hansenii. A) Schematic representation of the chromosomal PEX3 region after gene deletion. Coloured arrows indicate primers used in PCR analysis. B) 0.7% agarose gel analysis of PCR products for the upstream (UP) and downstream (DN) region and whole cassette in WT and pex3Δ cells in the NCYC 102 background. The primers used for whole cassette were VIP 3872 and VIP 3873 the whole cassette in pex3Δ is the same size of the genome amplified with same primers in the WT. C) 1% agarose gel analysis of PCR products for the upstream (UP) and downstream (DN) region in WT and pex3Δ cells in the NCYC 3363 background.

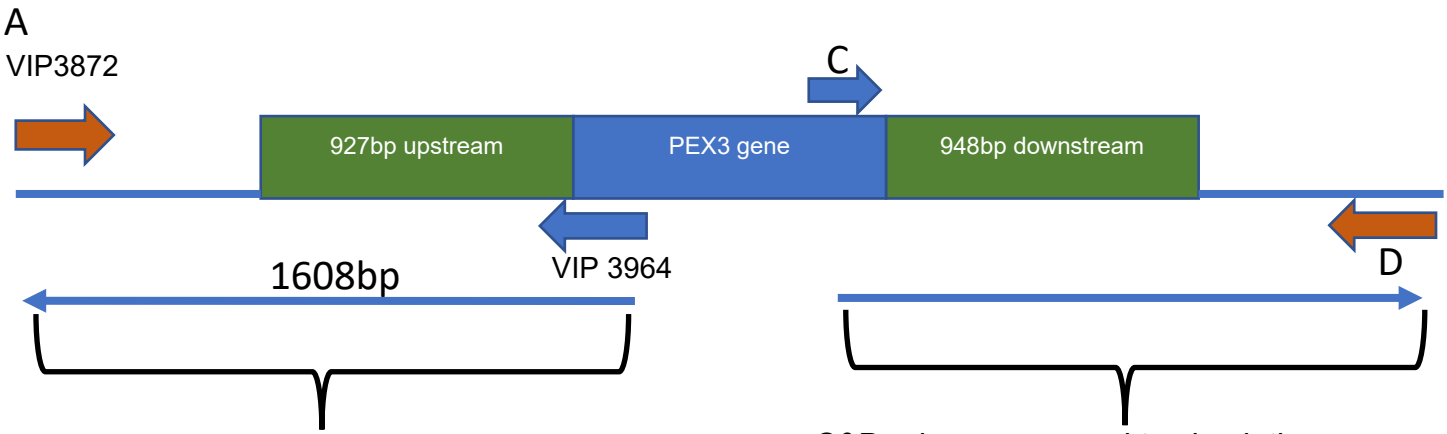

VIP3872& VIP3964 primers are used to check the upstream second copy of the chromosomal region of *PEX3* gene

(Only WT cells give this band)

C&D primers are used to check the downstream second copy of the chromosomal region of *PEX3* gene

(Only WT cells give this band)

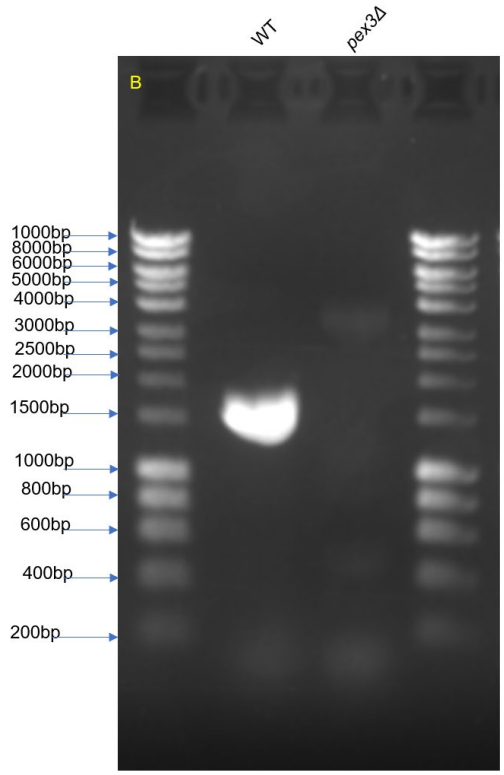

Figure 48 PCR analysis for the presence of an intact copy of the PEX3 in D. hansenii. A) Schematic representation of the chromosomal PEX3 ORF region. Coloured arrows indicate primers used in PCR analysis. B) 1% agarose gel analysis of PCR products for the upstream region in WT and pex3Δ cells in the strain NCYC 3363.

Also, In NCYC 3363 the *PEX3* gene was deleted using the 50bp PCR method developed in Chapter 3. Of 22 colonies that were obtained, 72% contained a successful knockout (table 17). Growth curves were conducted on YM2 glucose, YM2 glycerol, and oleate liquid media this was explained in Chapter 4.

Flank size	DNA mass	Number of colonies	Percentage of colonies with successful KO	strain
50bp	500ng	22 colonies	72%	NCYC 3363

Table 17 shows the 50bp flank regions for the PEX3 knockout in NCYC 3363 to prove the 50bp method is correct.

5.3 Tagging GFP-PTS1 in the *pex3Δ* cells in NCYC 102 strain background

Proteins targeted to peroxisomes depend on targeting signals embedded into their amino acid chain. Peroxisomes targeting signal type 1 is used by most peroxisomal proteins and comprises a tripeptide consisting of SKL or a derivative of this at the extreme carboxy terminus of the protein (Gould, Keller and Subramani, 1987, 1988; Gould *et al.*, 1989, 1990; Swinkels *et al.*, 1992). The PTS1 is evolutionarily conserved implying that a reporter protein with a PTS1 can be used in many different organisms. The addition of a PTS1 to the carboxy terminus of GFP is now a widely used peroxisomal marker to visualise peroxisomes in living cells. It was first introduced in *Pichia pastoris* to examine peroxisome biogenesis (Kalish *et al.*, 1996). GFP-PTS1was expressed in NCYC 102 *pex3Δ* cells and WT cells, using HygroB as a selection marker and targeted to a save landing site in the *ARG1* gene region. To do that a plasmid was constricted called pSA5 with HygroB marker, under the control

of *TEF1* promoter and *TEF1* terminator from *S. stipitis*, flanked by genomic regions of 1kb upstream and 1kb downstream from the *ARG1* gene. This plasmid was subsequently, digested with *Not1* and *Sal1* to insert the fragment consisting of the strong Dh*ACT1* promoter and GFP-PTS1, which was digested with *Not1* and *Sal1* from the plasmid pDEB21. This new integration cassette (Figure 49) was amplified by PCR to obtain a linearized construct. It was transformed to *D. hansenii* WT and *pex3Δ* cells via electroporation as described in Materials and Methods section (2.4.3) (Figure 49). Numerous transformants were obtained in both WT and *pex3Δ*. In WT cells transformed with the GFP-PTS1 construct, a punctate green, fluorescent pattern was observed in 4 colonies, whereas this was absent from the untransformed cells. As anticipated, *pex3Δ* cells do not localise GFP-PTS1 into puncta but display a diffuse cytosolic labelling, typical of *pex3Δ* mutants as they fail to import proteins into the peroxisomes or that lack peroxisomes all together. From these results I can conclude that the *PEX3* deletion in *D. hansenii* blocks peroxisomal functions as the cells fail to grow properly on a fatty acid as carbon source and a marker for peroxisome is mis localised to the cytosol (Figure 50).

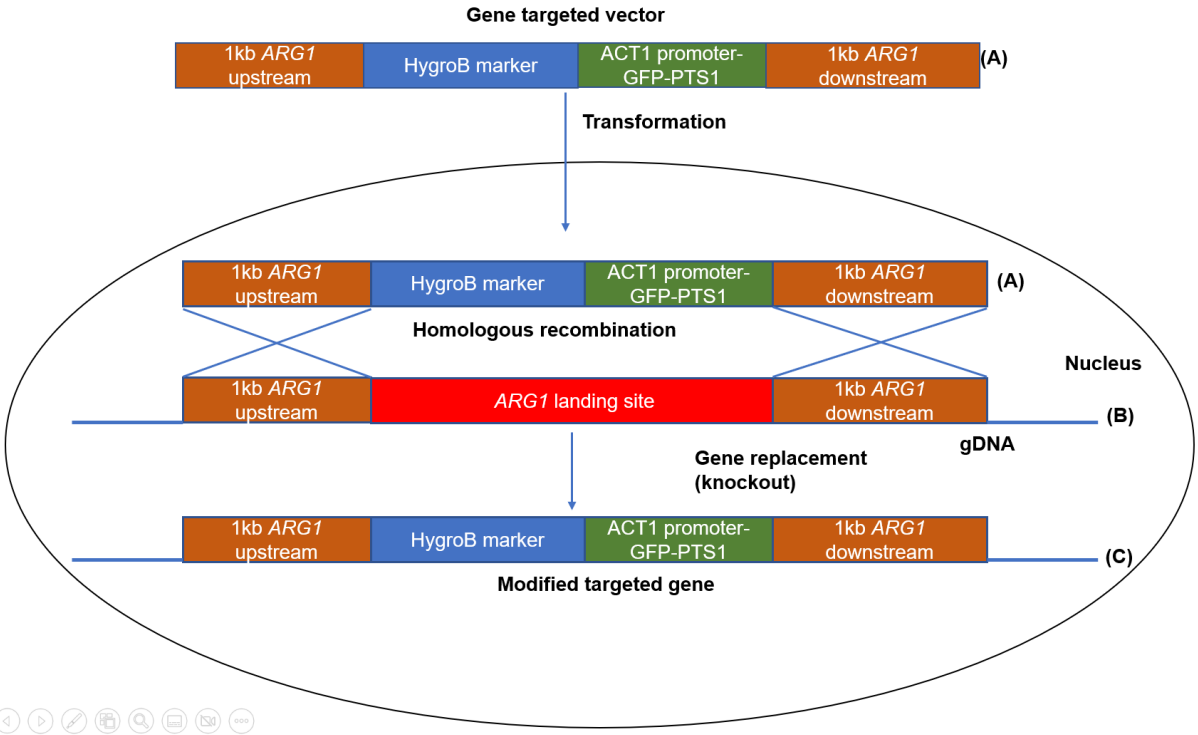

Figure 49 The process of gene replacement through homologous recombination in D. hansenii. The insert of the gene targeted vector is amplified by PCR resulting in product (A). This is introduced into the cells through electroporation. The 1kb homology arm allows for homologous recombination with the chromosome (B) thereby replacing the ARG1 with the HygroB marker (C). The ARG1 was knocked out using pUC19 plasmid in the NCYC 102 strain.

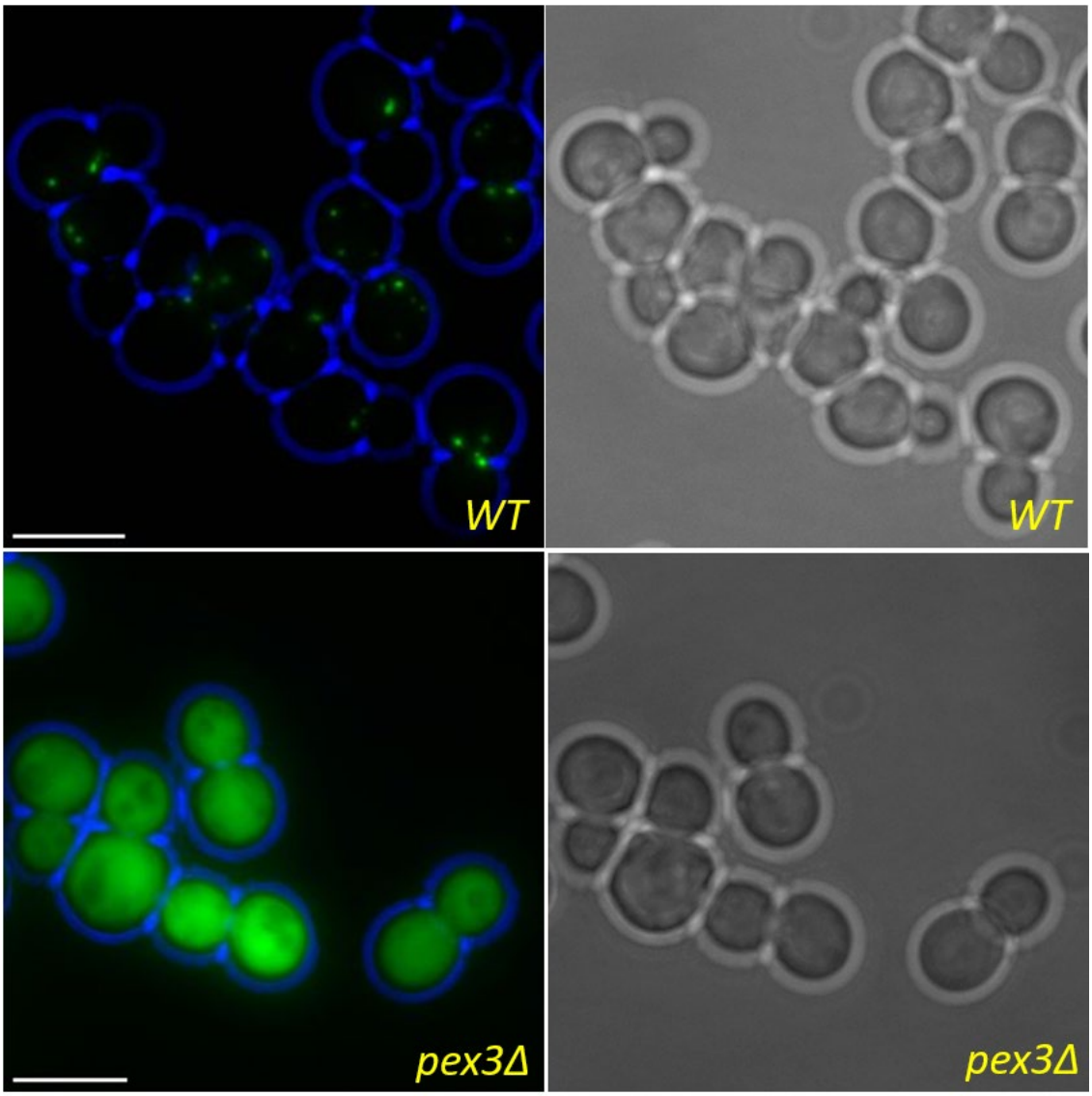

Figure 50 localization of GFP-PTS1 in the NCYC 102 strain in D. hansenii. The GFP-PTS1 was expressed in the WT and pex3Δ cells by electroporation, then the cells were incubated for 3-4 days at 25°C. Subsequently, cells were grown in liquid cultures to log phase and imaged using epifluorescence microscopy. The WT shows the peroxisomal signal in peroxisomes while the pex3Δ cells shows the signal in the cytosol indicating that the peroxisomes are deficient in the pex3Δ knockout cells. Blue colour represents the edge of cells. Bar 5μm.

5.4 Knocking out *GUT2* gene

The GUT2 gene which encodes for G3P dehydrogenase was knocked out from the *D. hansenii* genome. The NCYC102 *gut2Δ* mutant is a stock in the lab previously constructed by Dr Zeena Alwan but since we continued using the strain NCYC 3363, a *GUT2* gene deletion was constructed, using the HygroB marker for selection and

the rapid PCR amplification method which uses 50bp flanks only away from the *GUT2* gene (Figure 51). Then, the PCRed DNA was precipitated, and transformed to *D. hansenii* by electroporation conditions as described in Materials and Methods section (2.4.3). After electroporation, the cells were recovered in 1ml YM deb medium with 0.1M sorbitol for 4 hours at 25^{o}C with shaking at 120rpm before being plated out on YM deb medium containing 50 µg/ml Hygromycin B and incubated for 3-4 days. Colonies were restreaked on YM deb medium with 80 µg/ml Hygromycin B to get pure colonies. Then, the colonies were tested by PCR, and growth on glycerol. Deletion of *GUT2* results in growth defect on glycerol media as shown previously by Zeena Alwan (Esser *et al.*, 2004; Alwan, 2017). Knocking out the *GUT2* gene results in increasing the formation of G3P; shifting the pathway to form more TAG. The work of Beopoulos et al. demonstrates that the *gut2Δ* mutant showed a 3-fold increase in lipid accumulation compared to the wild-type strain in *Y. lipolytica*. Thierry and Jean-Marc claimed that *GUT2* is a FAD^{+} dependent, mitochondrial enzyme. In a similar vein, Thierry and Jean-Marc also found that deletion of *GUT2* led to an increase in lipid content reaching 30% of dry weight after 24 hours of growth in *Y. lipolytica*. PCR was done to test the knockout of *gut2Δ* in the NCYC 3363, the diagram shows the primers annealing 200bp away from *gut2Δ* upstream and 200bp away from the *gut2Δ* downstream and primers inside the HygroB cassette Figure 52. Four colonies were tested 3 colonies had the *gut2Δ* KO while 1 colony did not, the NCYC 3363 WT was used as a negative control.

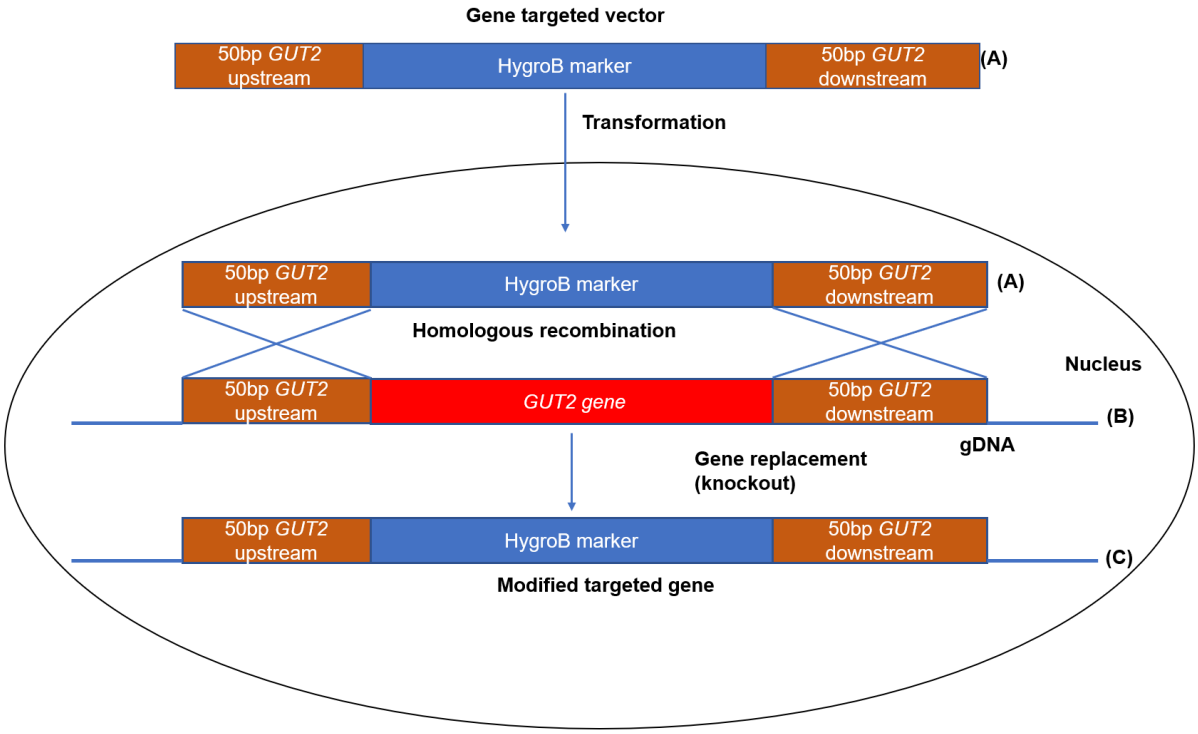

Figure 51 the process of gene replacement through homologous recombination in D. hansenii. The insert of the gene targeting vector is amplified by PCR resulting un product (A). This is introduced into the cells through electroporation. The 1kb homology arm allows for homologous recombination with the chromosome (B) thereby replacing the GUT2 with HygroB marker (C). The GUT2 gene was knocked out using pUC19 plasmid in NCYC 3363 strain.

A) deletion of *GUT2* gene

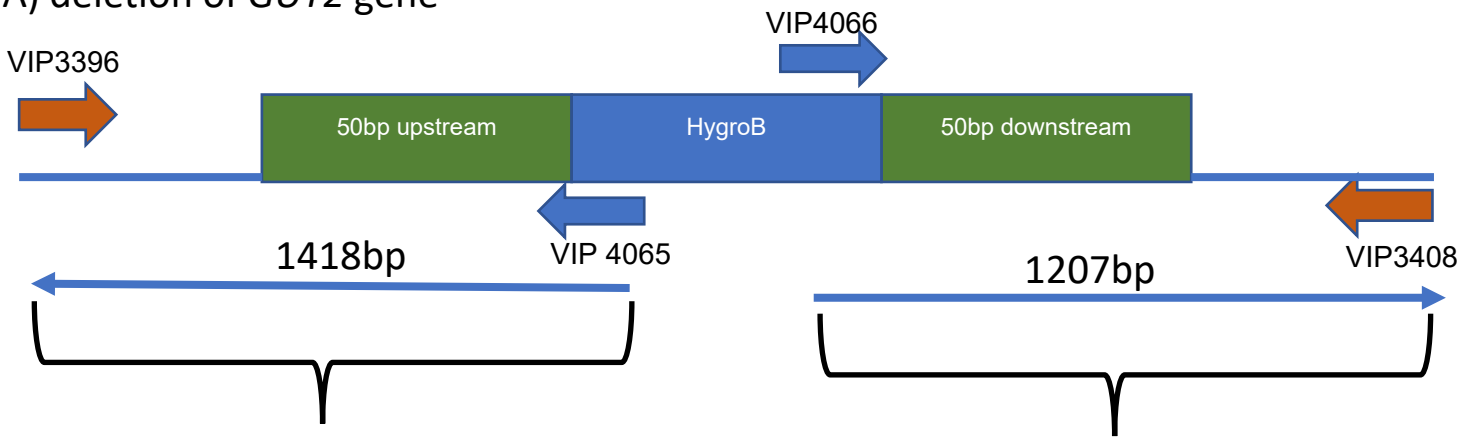

VIP3396& VIP4065 primers are used to check the upstream chromosomal region upon deletion of *PEX3* gene

(Only KO cells give this band)

VIP4066& VIP3408 primers are used to check the downstream chromosomal region upon deletion of *PEX3* gene

(Only KO cells give this band)

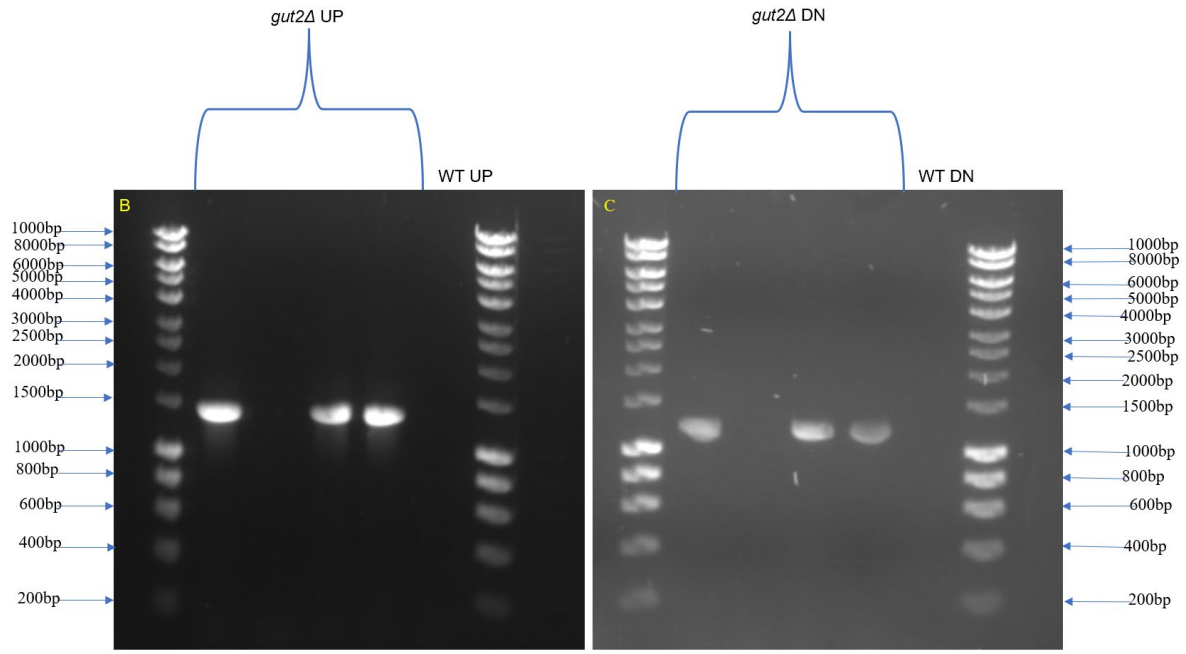

Figure 52 PCR analysis of GUT2 gene deletion mutant using 50bp flanks in D. hansenii. A) Schematic representation of the chromosomal GUT2 region after gene deletion. Coloured arrows indicate primers used in PCR analysis. B) 1% agarose gel analysis of PCR products for the upstream region in WT and gut2Δ cells in the NCYC 3363 background. C) 1% agarose gel analysis of PCR products for the downstream region in WT and gut2Δ cells in the NCYC 3363 background.

5.5 pex3/gut2Δ double Knockout:

The *pex3*/*gut2Δ* double knockout was generated by knocking out the *PEX3 gene* first with SAT1 marker under the control of *C. albicans ACT1* promoter and *C. albicans URA3* terminator flanked by1kb upstream and 1kb downstream. Followed by knocking out *GUT2* gene in the same strain with HygroB marker, using the rapid PCR amplification method with only 50bp flank. Then, the PCR product was precipitated, and transformed to *D. hansenii* by electroporation conditions as described in Materials and Methods section (2.4.3). After electroporation, the cells recovered for 4 hours, before being plated out on YM deb medium containing 50 µg/ml Hygromycin B and incubated for 3-4 days at 25^{o}C. Colonies were restreaked on YM deb medium with 80 µg/ml Hygromycin B to obtain pure colonies. The colonies were then tested by PCR, and growth on glycerol, and oleate because deletion of *pex3*/*gut2Δ* results in defect growth on oleate and glycerol as shown in Figure 53. The transformation was done in both strains NCYC 102, and NCYC 3363. It was anticipated that the double mutant accumulates more lipid, since the *pex3Δ* knockout decreases the fatty acids breakdowns while the *gut2Δ* knockout induces the G3P this will increase the formation of TAG, and the cells will accumulate more lipids. Thierry and Jean-Marc found that blocking the β-oxidation pathway with the deletion of *GUT2* gene increased the contact of TAG and free fatty acids in *Y. lipolytica*. PCR was tested to check the if the cassette was inserted in the genome, the primers used for the PCR are shown in the diagram the NCYC 3363 was used as a negative control Figure 54.

D.hansenii in the NCYC 3363

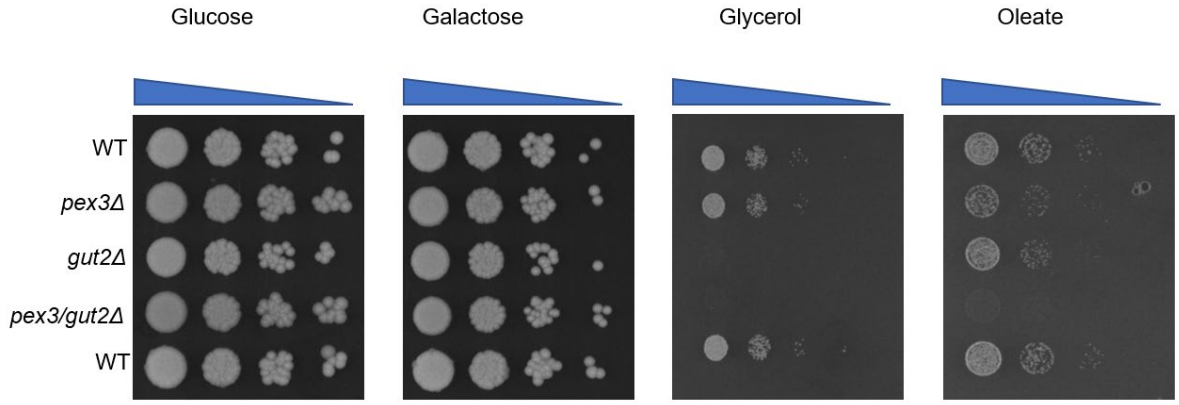

Figure 53 Growth of WT, pex3Δ, gut2Δ, and pex3Δ/gut2Δ double mutants of D. hansenii on different carbon sources. D. hansenii cells were grown in YM deb liquid culture to OD_{600}= 1 and serial dilutions in water were spotted on glucose, galactose, glycerol, and oleate plates and incubated for 3days at 25°C in NCYC 3363 strain. All the mutants grew on glucose, and galactose. The gut2Δ and pex3Δ/gut2Δ double mutants were not able to grow on glycerol; while pex3Δ and pex3Δ/gut2Δ double mutants were not able to grow on oleate. Blue triangles indicate decreasing cell density from left to right.

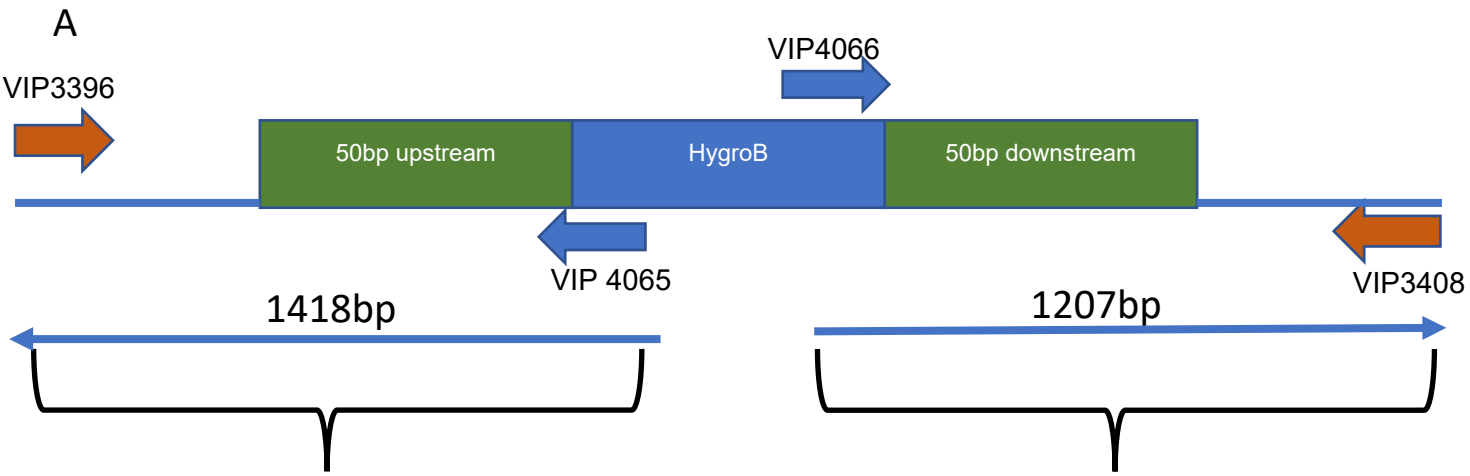

VIP3396 & VIP4065 primers are used to check the upstream chromosomal region upon deletion of *PEX3* gene
(Only KO cells give this band)

VIP4066 & VIP3408 primers are used to check the downstream chromosomal region upon deletion of *PEX3* gene
(Only KO cells give this band)

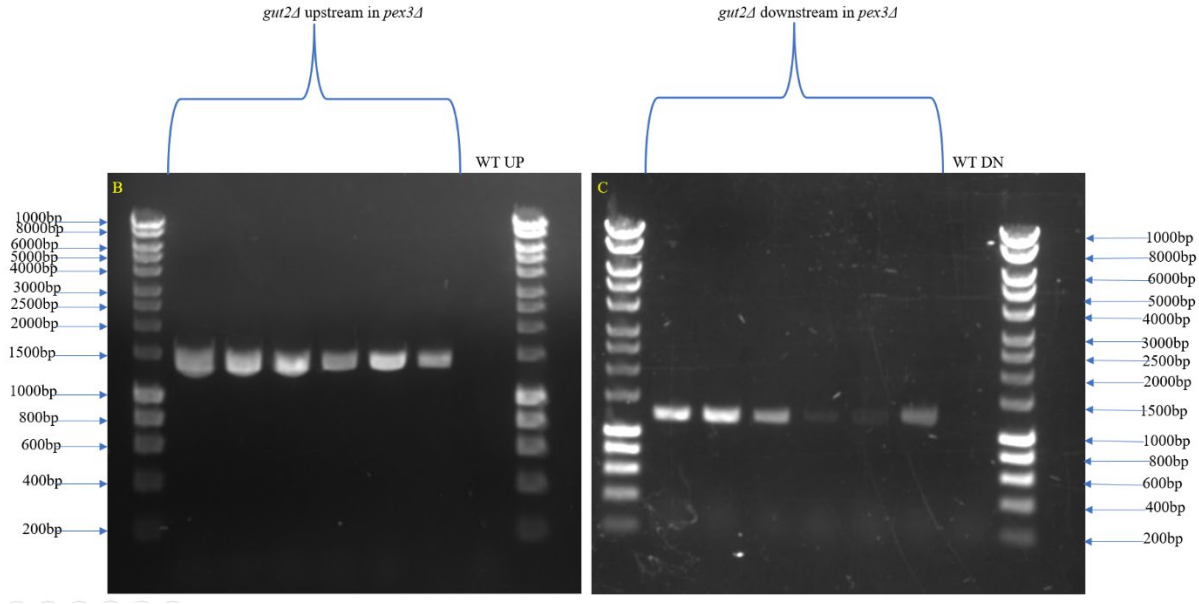

Figure 54 PCR analysis of GUT2 gene deletion mutant in pex3Δ. A) Schematic representation of the chromosomal GUT2 region after gene deletion. Coloured arrows indicate primers used in PCR analysis. B) 1% agarose gel analysis of PCR products for the upstream region in WT and gut2Δ cells in the NCYC 3363 background. C) 1% agarose gel analysis of PCR products for the downstream region in WT and gut2Δ cells in the NCYC 3363 background.

5.6 Nile Red assay

At the beginning it was decided to do an adaptation procedure for the cells from YM deb to YM1 starvation media (media with low nitrogen); this was done because the cells were not growing in the starvation media. First, the cells were grown at YM deb media for 24 hours then from that media the cells were moved to ½ YM deb media and left to grow for 24 hours then moved to ¼ YM deb media and left to grow for 24 hours then moved to ¼ YM deb with no peptone left to grow for 48 hours then moved to ¼ YM deb no peptone + no malt extract left to grow for 48 hours then the cells were transferred to the YM1 starvation media. This procedure was ineffective because the cells at the ¼ YM deb no peptone + no malt extract clumped into small clusters in the NCYC 3363 strain; and in the NCYC 102 strain the cells at YM1 starvation media gave very low amount of lipid. Table 18 shows the media components used for adaptation, and Figure 55 shows the process of adaptation.

Media name	Media components to prepare 1L
YM deb	3g Yeast extract, 3g malt extract, 5g peptone, 10g glucose.
½ YM deb	1.5g Yeast extract, 1.5g malt extract, 2.5g peptone, 10g glucose.
¼ YM deb	0.75g Yeast extract, 0.75g malt extract, 1.25g peptone, 10g glucose.
¼ YM deb no peptone	0.75g Yeast extract, 0.75g malt extract, 10g glucose.
¼ YM deb no peptone+ no malt extract	0.75g Yeast extract, 10g glucose.
YM1 starvation media	1.9g YNB, 60g glucose, 0.5g ammonium sulphate.

Table 18 shows the media used for adaptation procedure. All 7 medias were dissolved in a final volume of 1L H_2O.

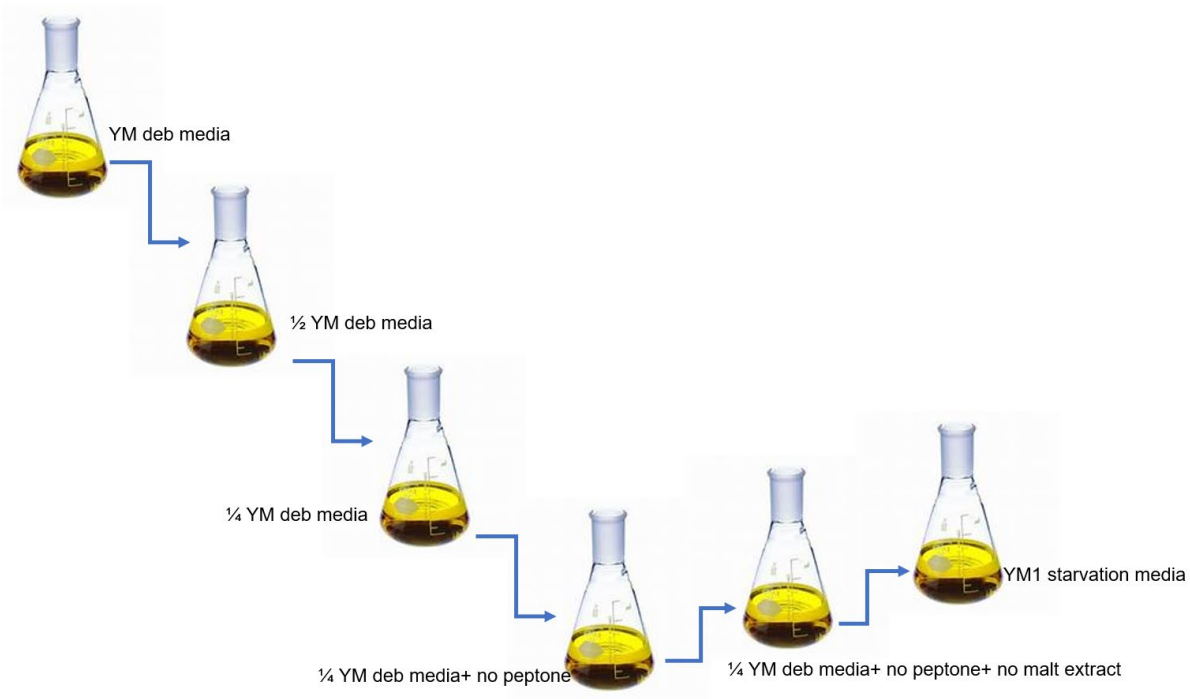

Figure 55 the process of the adaptation of different media from YM deb to YM1 starvation media. First the cells were grown on YM deb then moved to ½ YM deb. After the cells grow, they are moved to ¼ YM deb media, then moved to ¼ YM deb with no peptone. After growing the cells were moved to ¼ YM deb with no peptone and no malt extract. After growing they were moved to YM1 starvation media.

To ameliorate this situation, it was decided to grow the cells at YM deb media until they reach the stationary phase, then the cells were moved to seven different YM1 starvation media mentioned in Materials and Methods section (2.7.2). All seven media were dissolved in a final volume of 1L of H_2O. The next day the cells were harvested by centrifuging at 1610rcf for 5 minutes. After washing in 10ml water, the OD_{600} was measured and total number of OD_{600} units was calculated, and the cells were moved to 10ml H_2O with the same OD_{600} for all samples. Then they were stained with Nile Red, as described in 2.7.4. It was decided to use the starvation media number 7 because it gave a high amount of lipid in the WT and *pex3/gut2Δ* double mutant in the NCYC 102 strain.

The lipid assay was done 9 times in both the WT and mutants NCYC102 and NCYC3363 strains. All samples were grown in a low nitrogen media explained in section (2.7.2), grown for 24 and 48 hours. The amount of lipid is determined as mg Triolein equivalents per mg dry weight of yeast cells; this is because Triolein was used as standard curve see section (2.7.3). In all mutants the amount of lipids increased between 24h and 48h. The WT was compared to *pex3Δ*, *gut2Δ*, and *pex3/gut2Δ* double mutants. Figure 56 shows the difference in lipid assay for NCYC 3363 and NCYC102 strains. The NCYC 3363 chart shows that after 48 hours the WT, *pex3Δ*, and *gut2Δ* were almost similar in the amount of lipid, while the double mutant gave higher amount of lipid; as a matter of fact, the *pex3/gut2Δ* double mutant gave more lipid than the other mutants. However, in NCYC102 strain the *gut2Δ* mutant gave higher amount of lipid in at 48 hours compared to the WT and the other mutants.

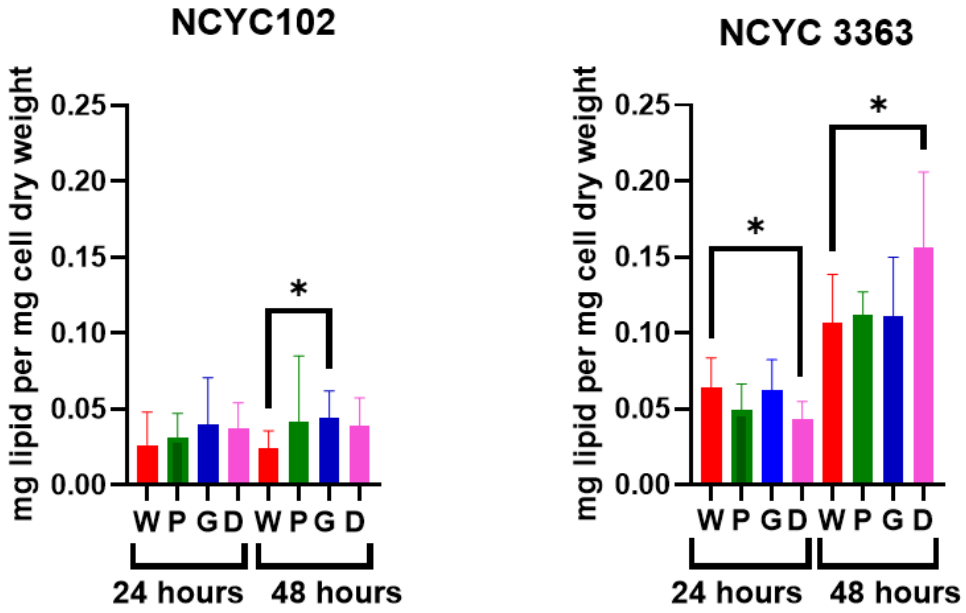

*Figure 56 charts showing the lipid accumulation done 9 times in both strains NCYC 102 & NCYC 3363 in D. hansenii. The cells were grown on YM1 starvation media for 24 hours and 48 hours. W=WT, P=pex3Δ, G=gut2Δ, and D=pex3Δ/gut2Δ double mutants. The amount of lipid is determined as mg Triolein equivalents per mg dry weight of yeast cells. * Shows a Significantly difference (t-test) between the WT and D at 24 hours P value =0.0130 and WT and D at 48 hours with P value=0.0229 for NCYC 3363 strain and between the WT and GUT2 at 48 hours for NCYC 102 with P value= 0.0101.*

Curiously, in both strains the higher the OD the cells gave after starvation the higher amount of lipid concentration was gained. The NCYC3363 strain OD was higher than the NCYC102; that might be the reason why NCYC 3363 gave a higher amount of lipid. Figures (57, 58, 59, 60, 61, and 62) show the relationship between the OD and the lipid concentration in NCYC 102, and NCYC 3363 strains respectively, at 24, and 48 hours. Since, the NCYC 102 has two copies of *FOX2* gene (explained in chapter 4) maybe this alters the reaction to breakdown the fatty acids via β-oxidation, so it does not accumulate lipids instead it breaks them down.

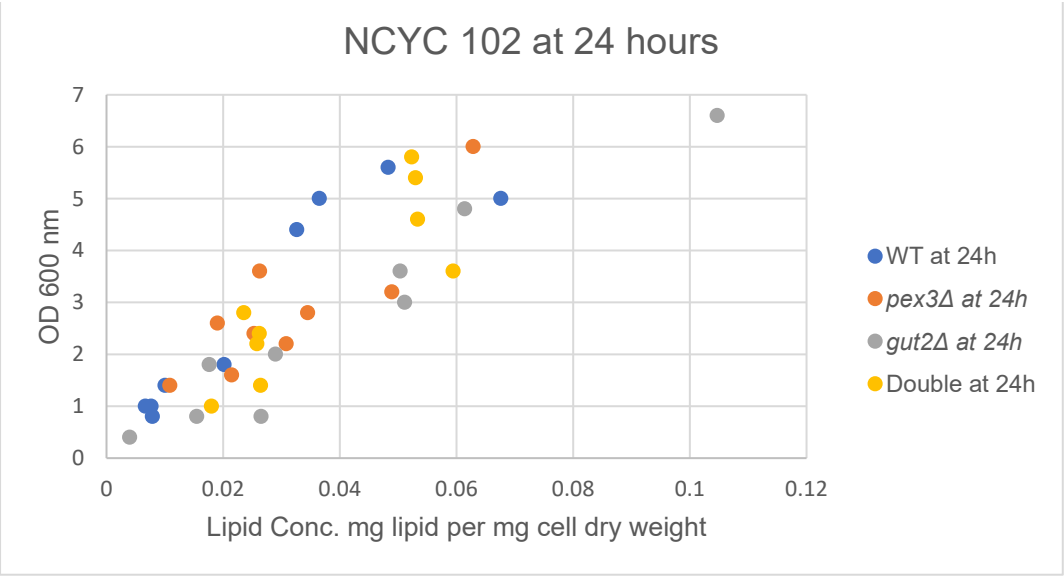

Figure 57 the relationship between the OD and the lipid concentration in the NCYC 102 strain at 24 hours for the WT, pex3Δ, gut2Δ, pex3Δ/gut2Δ cells. The lipid concentration is determined as mg Triolein equivalents per mg dry weight of yeast cells; this is because Triolein was used as standard curve.

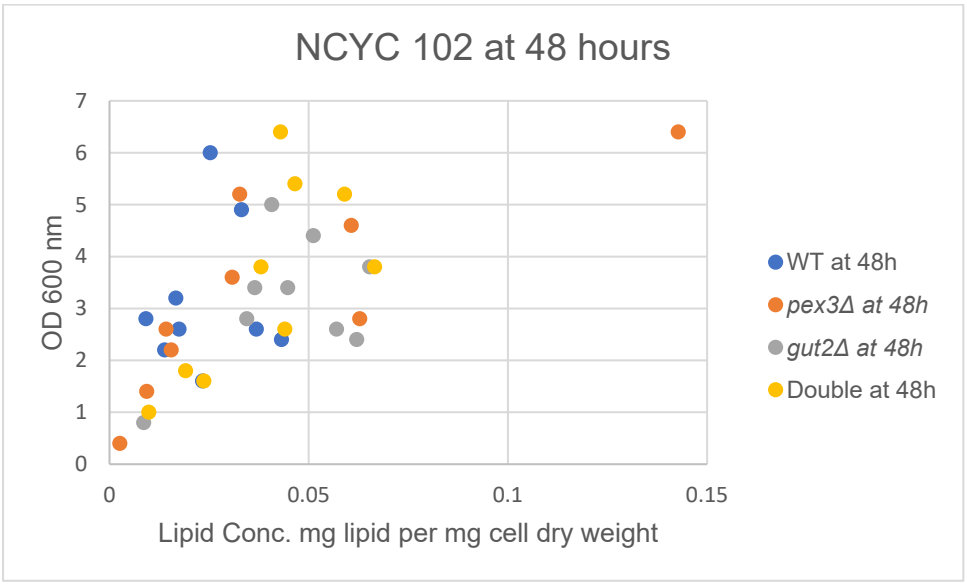

Figure 58. the relationship between the OD and the lipid concentration in the NCYC 102 strain at 48 hours for the WT, pex3Δ, gut2Δ, pex3Δ/gut2Δ cells. The lipid concentration is determined as mg Triolein equivalents per mg dry weight of yeast cells; this is because Triolein was used as standard curve.

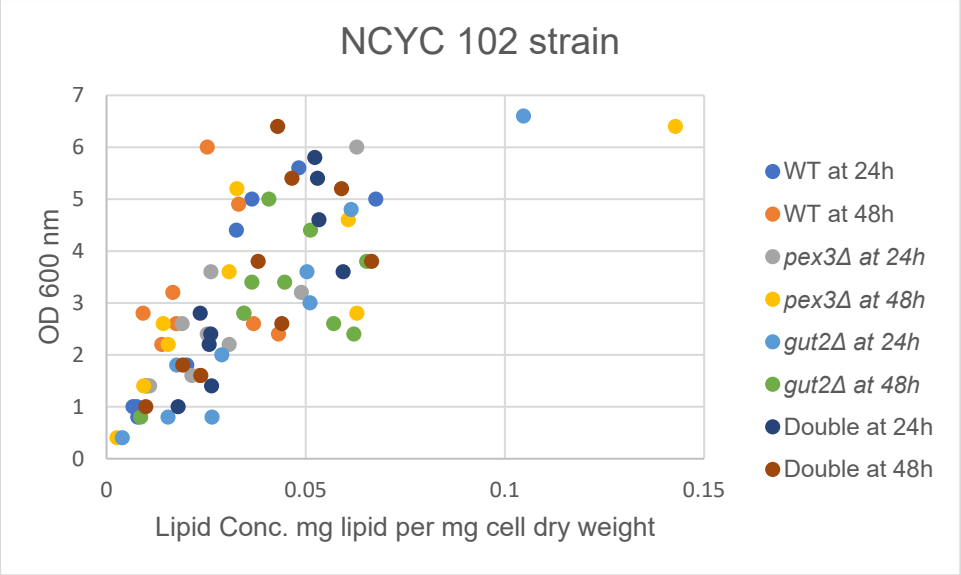

Figure 59 the relationship between the OD and the lipid concentration in the NCYC 102 strain at 24 hours and 48 hours for the WT, pex3Δ, gut2Δ, pex3Δ/gut2Δ cells. The lipid concentration is determined as mg Triolein equivalents per mg dry weight of yeast cells; this is because Triolein was used as standard curve.

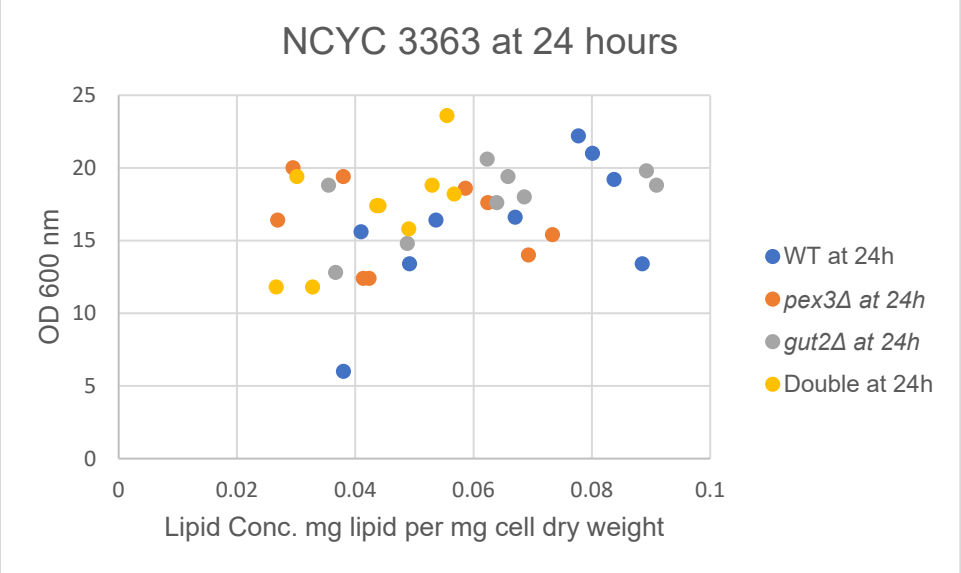

Figure 60 the relationship between the OD and the lipid concentration in the NCYC 3363 strain at 24 hours for the WT, pex3Δ, gut2Δ, pex3Δ/gut2Δ cells. The lipid concentration is determined as mg Triolein equivalents per mg dry weight of yeast cells; this is because Triolein was used as standard curve.

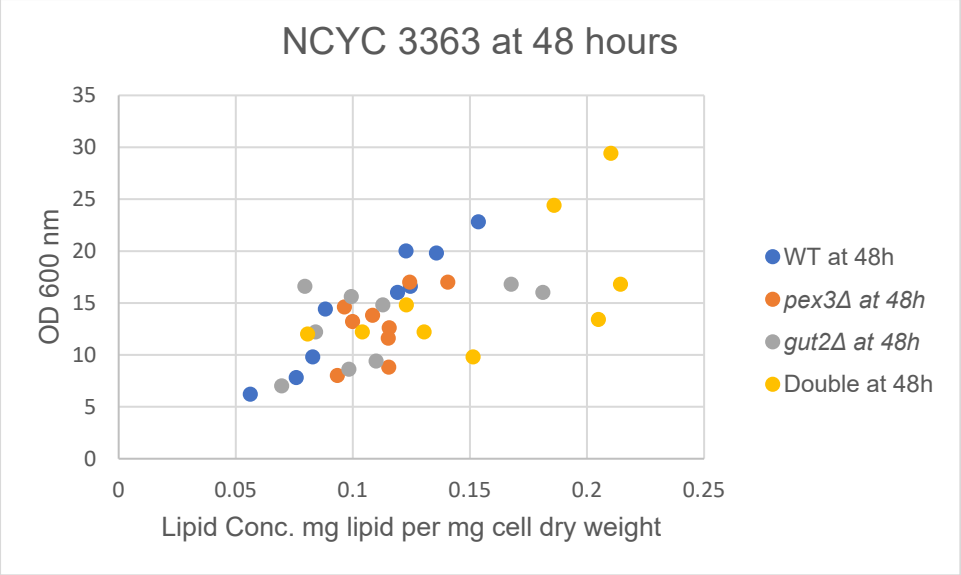

Figure 61 the relationship between the OD and the lipid concentration in the NCYC 3363 strain at 48 hours for the WT, pex3Δ, gut2Δ, pex3Δ/gut2Δ cells. The lipid concentration is determined as mg Triolein equivalents per mg dry weight of yeast cells; this is because Triolein was used as standard curve.

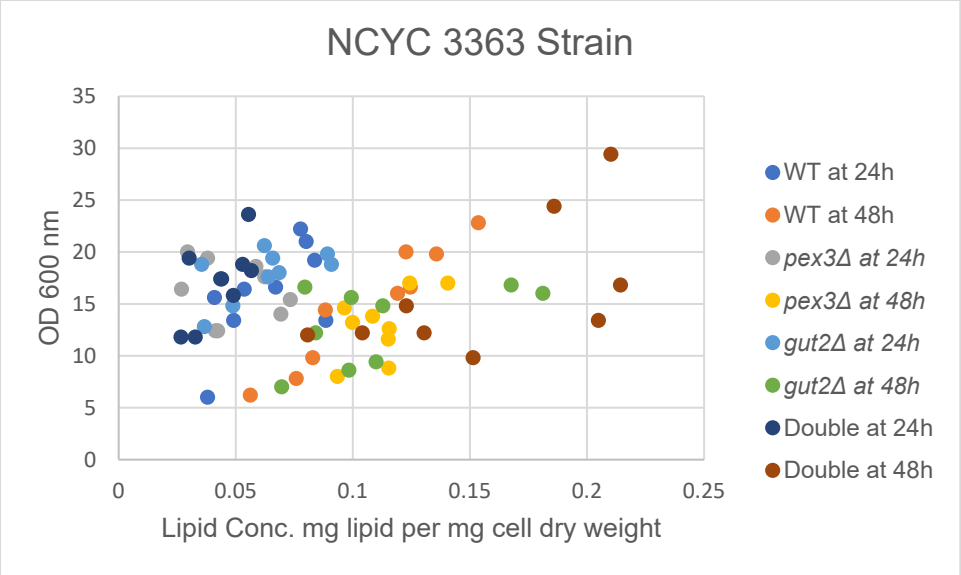

Figure 62 the relationship between the OD and the lipid concentration in the NCYC 3363 strain at 24 hours and 48 hours for the WT, pex3Δ, gut2Δ, pex3Δ/gut2Δ cells. The lipid concentration is determined as mg Triolein equivalents per mg dry weight of yeast cells; this is because Triolein was used as standard curve.

The NCYC102 chart in Figure 56 shows a high standard deviation in the mutants this is because first the cells struggle to grow on starvation media, second the results were not consistent each time a different result was obtained.

Once the *pex3Δ* mutant was higher, second time the *gut2Δ* mutant was higher, and another result, the double *pex3/gut2Δ* mutant was higher, in all 9 times the mutants were higher than the WT. While in NCYC 3363 strain the results were consistent each time the *pex3/gut2Δ* double mutant was higher than the WT and the other mutants. It was expected that the *pex3/gut2Δ* mutant gives high amount of lipid because *pex3Δ* prevents efficient fatty acids break down and the *gut2Δ* increases the levels of G3P which gives more TAG. So, the yeast cells will be making more TAG that's what was seen in the NCYC 3363 strain. Our results prove our hypothesis that the double mutant will give more natural lipid. The NCYC 3363 strain might be a promising strain to produce more lipid, but it needs further investigation to get the correct conditions. In addition, all genes investigated so far are present as single copy, while the NCYC 102 has at least many of the genes in diploid; the difference between the strains is shown in Table 19.

Factors/strains	**NCYC102**	**NCYC 3363**
genes	Diploid has 2 copies of *ARG1* and *FOX2,* but single copy for *GUT2* and *PEX3.*	Haploid for every gene we have tested in the lab including *ARG1*, *GUT2*, *PEX3* and *FOX2.*
growth	Struggles to grow on starvation media.	Grows on starvation media but slowly.
HR	Difficult to knock out both genes	Easy to knockout genes

Table 19 the difference between NCYC 102 and NCYC 3363 strains.

5.7 Fluorescence images:

The Nile red stained cells were imaged using two fluorescence channels (Red and Green, excitation 586nm and emission 603nm (AAT Bioquest Spectrum [Texas Red] 2021), excitation 490nm and emission 525nm (ThermoFisher Scientific fluorescein (FITC), respectively). The Red channel shows the whole cell stained with red because Nile red stains all the lipids in cells such as lipid bodies, membranes, phospholipids, phosphatidylcholine, and lipoprotein. Basically, it stains all lipids either at low or high density. While the green channel shows fluorescent signal from Nile Red that only occurs when it is in a high density lipid environment such as lipid bodies (Greenspan and Fowler, 1985). Figures 63, 64, 65, and 66 show the images for both strains NCYC 102 and NCYC 3363; for WT, *pex3Δ*, *gut2Δ*, and *pex3/gut2Δ* double mutants at 24 hours and 48 hours. The images show the Bright field, green channel, red channel, and the merged between the red and green channels.

First NCYC 3363 strain:

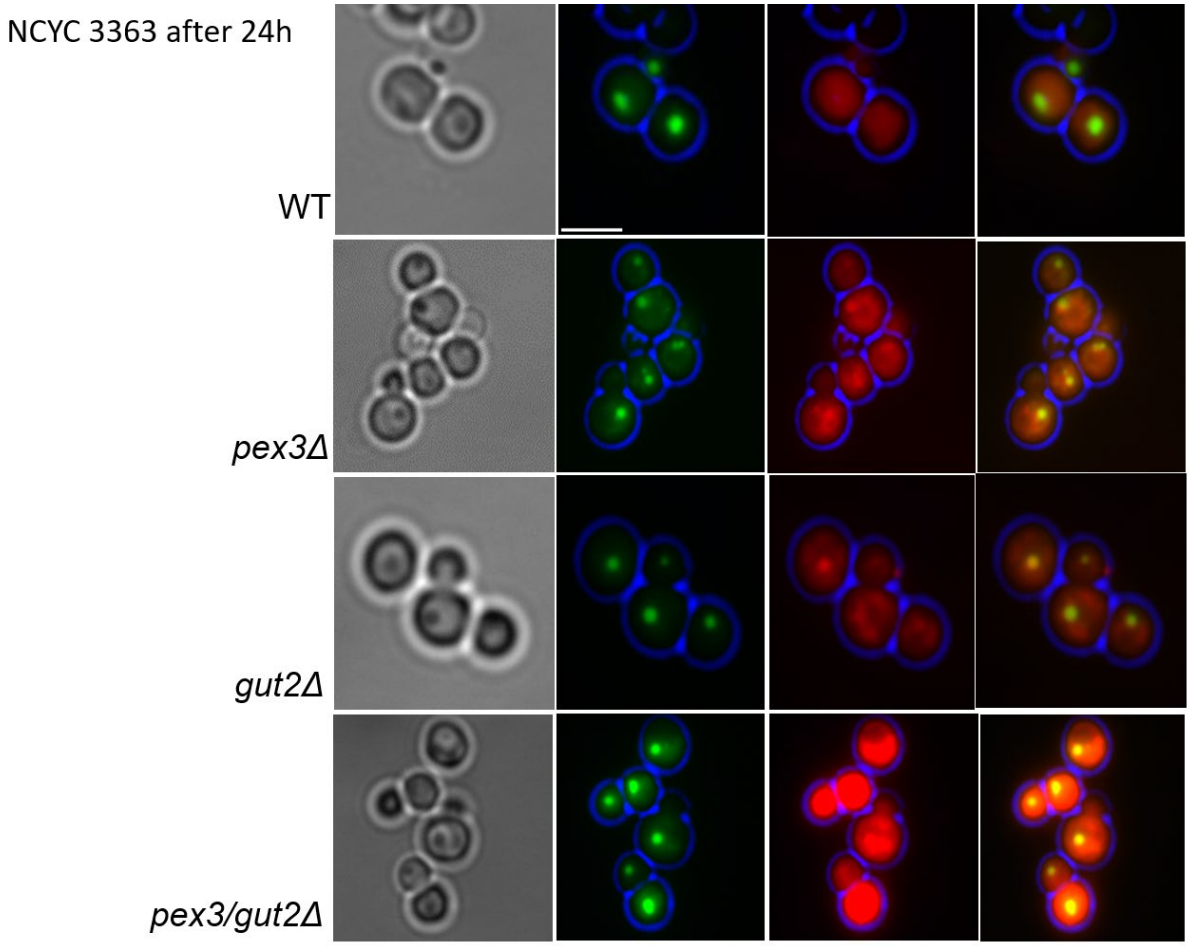

Figure 63 Fluorescence microscopy images for the NCYC 3363 strain. WT, pex3Δ, gut2Δ, and pex3/gut2Δ cells were imaged after being stained with Nile red for 7 minutes; and grown in YM1 starvation media for 24hours at 25°C. The images show the brightfield, green, and red channels, and the merged image between green and red channels. Bar 5μm.

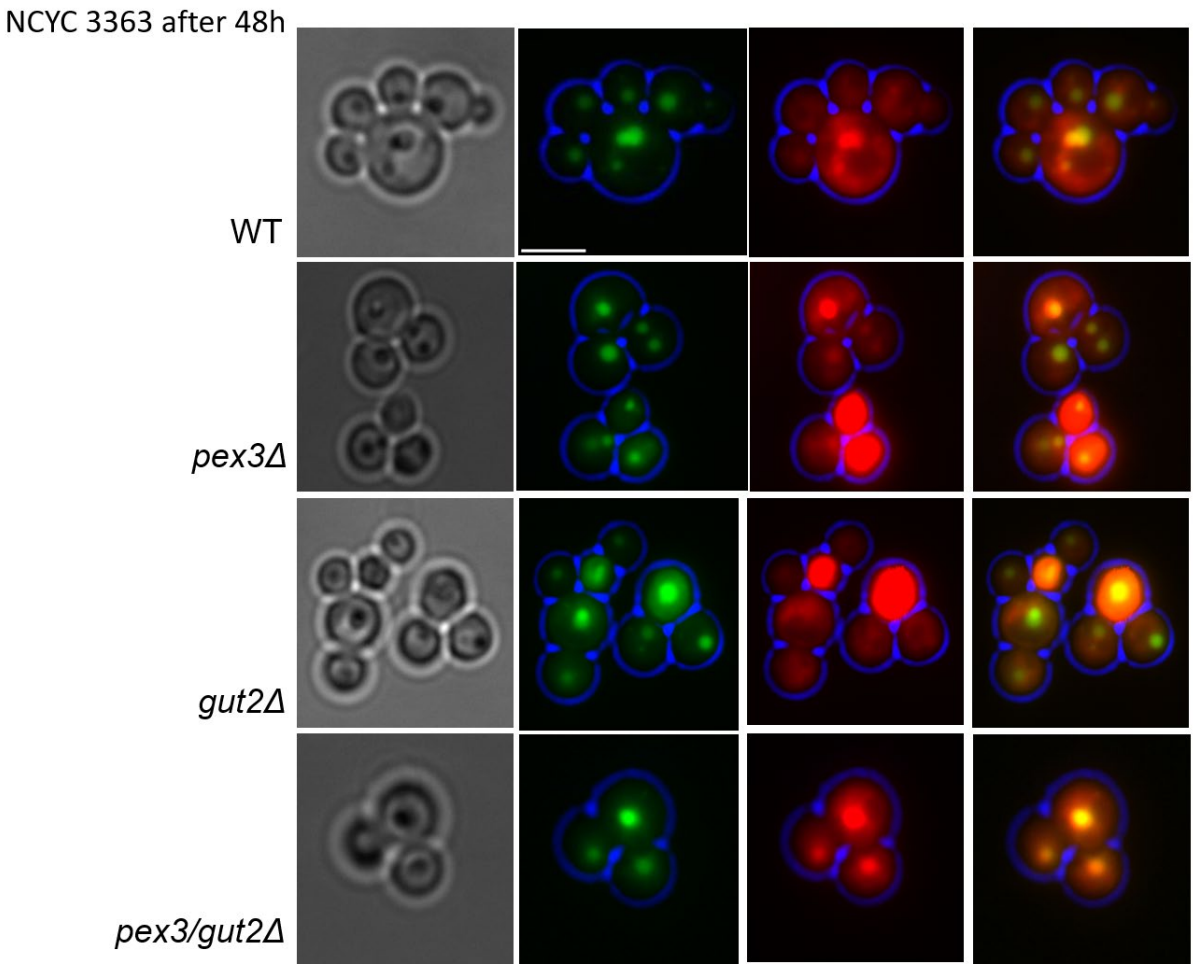

Figure 64 Fluorescence microscopy images for the NCYC 3363 strain. WT, pex3Δ, gut2Δ, and pex3/gut2Δ cells were imaged after being stained with Nile red for 7 minutes; and grown in YM1 starvation media for 48hours at 25°C. The images show the brightfield, green, and red channels, and the merged image between green and red channels. Bar 5µm.

Second NCYC102 strain:

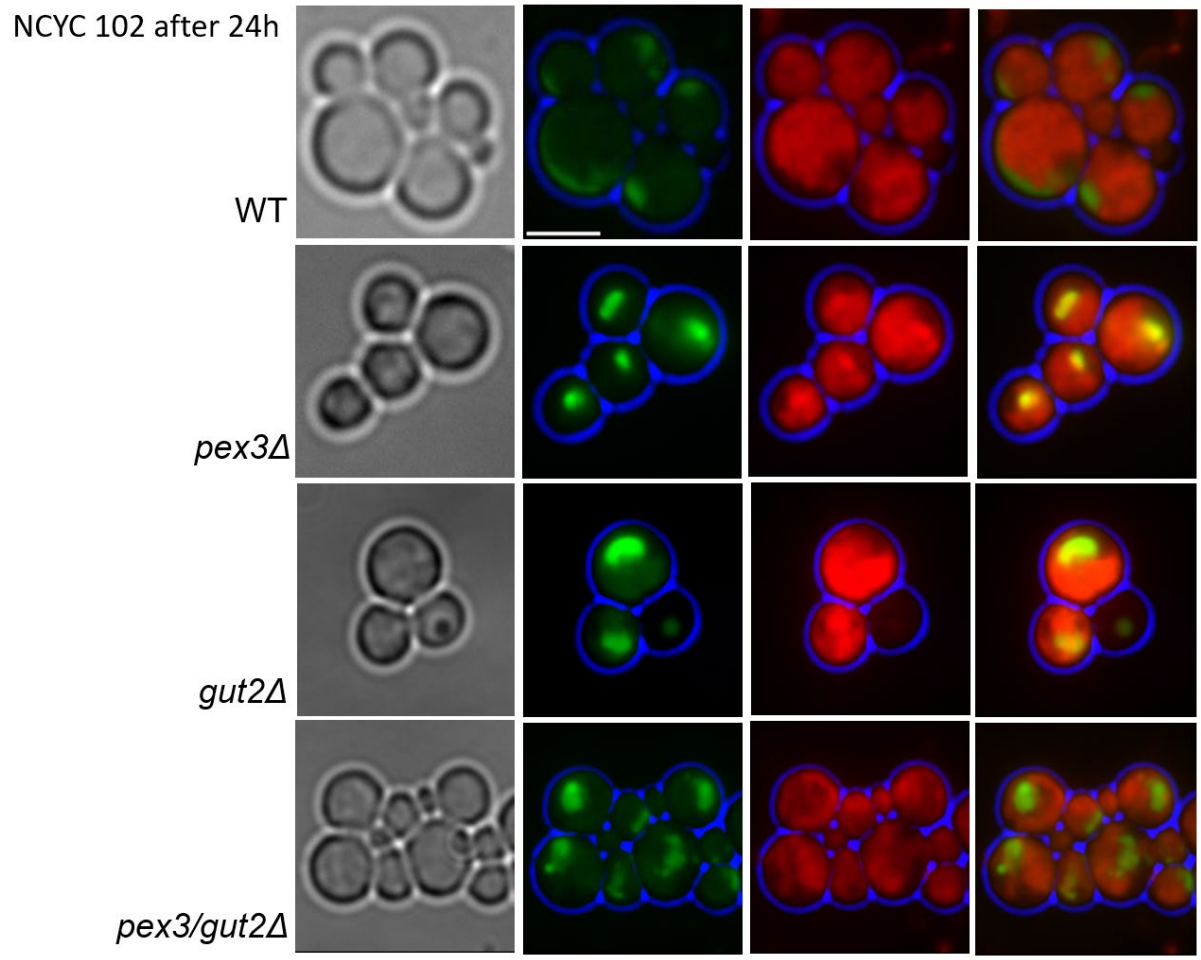

Figure 65 Fluorescence microscopy images for the NCYC 102 strain. WT, pex3Δ, gut2Δ, and pex3/gut2Δ cells were imaged after being stained with Nile red for 7 minutes; and grown in YM1 starvation media for 24hours at 25°C. The images show the brightfield, green, and red channels, and the merged image between green and red channels. Bar 5μm.

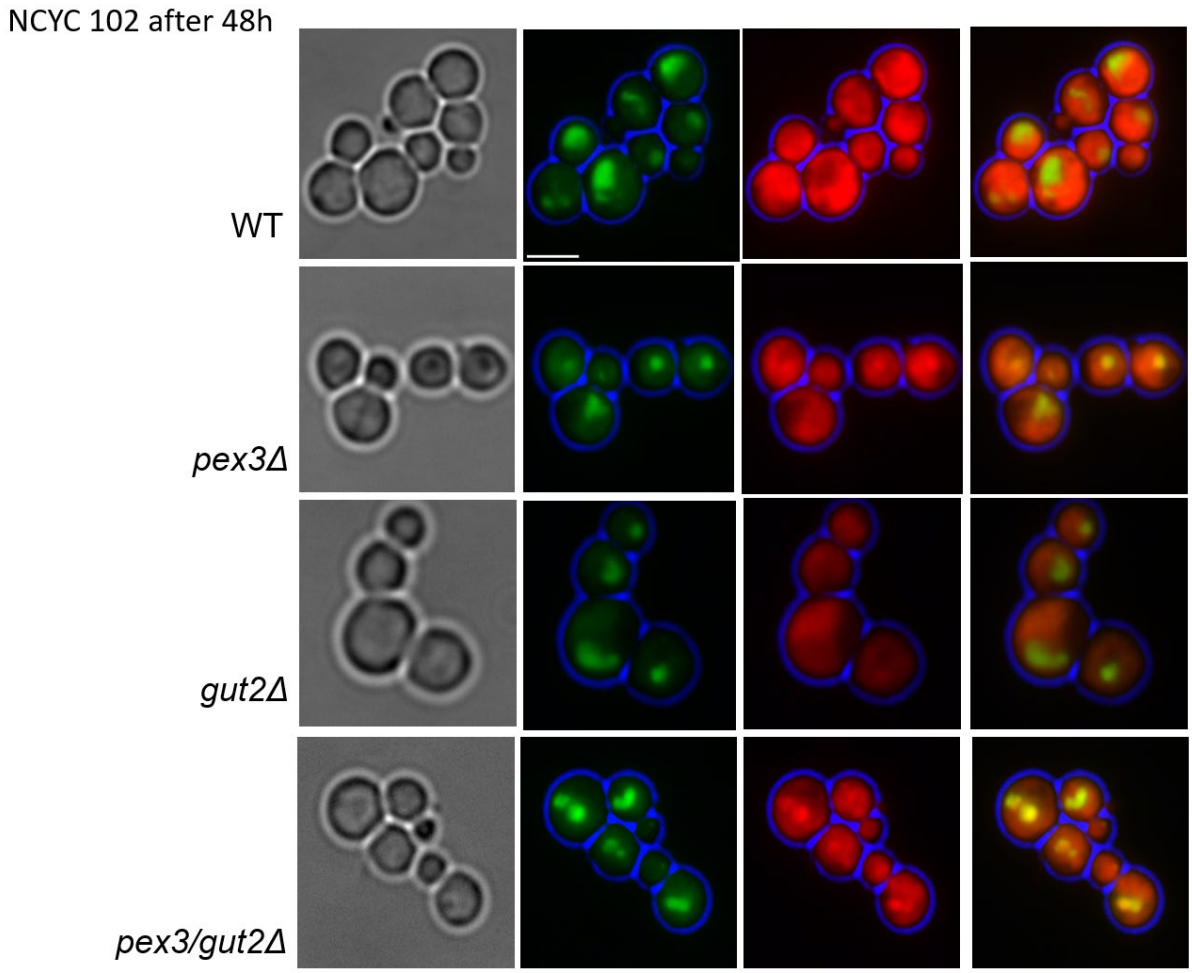

Figure 66 Fluorescence microscopy images for the NCYC 102 strain. WT, pex3Δ, gut2Δ, and pex3/gut2Δ cells were imaged after being stained with Nile red for 7 minutes; and grown in YM1 starvation media for 48hours at 25°C. The images show the brightfield, green, and red channels, and the merged image between green and red channels. Bar 5um.

The cells were imaged at the same exposure time for both strains. The NCYC 102 and NCYC 3363 *pex3/gut2Δ double* knock out showed high fluorescence under the microscope compared the other mutants. The WT in both strains had low fluorescence, while the *pex3Δ* and *gut2Δ* single mutants had medium fluorescence. The difference was clear between the *pex3/gut2Δ* double mutant and the other mutants.

5.8 Discussion:

A number of studies (Hettema *et al.*, 2000; Fang *et al.*, 2004; Munck *et al.*, 2009; Motley, Nuttall and Hettema, 2012; Yamashita *et al.*, 2014) demonstrates that Pex3 is involved in peroxisomes membrane biosynthesis, peroxisomes isolation, and

peroxisome degradation. *PEX3* was knockout from the genome of *D. hansenii* using the SAT1 marker, under the control of *C. albicans ACT1* promoter and *C. albicans URA3* terminator with 1kb flank upstream and 1kb downstream. The knockout was done using the pBluescirpt SK(+) plasmid under the nourseothricin resistance marker (SAT1). The *PEX3* gene was deleted in both strains NCYC 102 and NCYC 3363; both strains have one single copy of the gene. The *PEX3* gene was knocked out to block the fatty acid β-oxidation pathway. *Pex3Δ* mutants are not able to grow on oleate; growth curves were conducted to show the phenotype of *pex3Δ* explained in Chapter 4. GFP-PTS1 was expressed in the NCYC 102 *pex3Δ* and WT cells using HygroB as a selectable marker, targeting it to a safe landing site in the *ARG1* locus. This proved that the *pex3Δ* was correct since the GFP-PTS1 was mislocalized to the cytosol, while in the WT it was localized in the peroxisomes.

The next gene that was deleted in *D. hansenii* was *GUT2,* it was deleted in both strains NCYC 102 and NCYC 3363. In the NCYC 102, it was deleted using SAT1 marker, while in the NCYC 3363 it was deleted using the HygroB marker. *Gut2Δ* mutants are not able to grow on glycerol; the deletion of the *GUT2* gene results in increases G3P production; this shifts the pathway to TAG formation. Then, a *pex3Δ/gut2Δ* double mutant was generated; in the same *pex3Δ* strain that was conducted earlier, the *gut2Δ* was deleted. The double mutant is not able to grow on both glycerol and oleate media. The double mutant was expected to accumulate more lipids because the *pex3Δ* knockout produces fatty acids and *gut2Δ* knockout produces G3P. This produces more TAG for the cells to accumulate.

Thierry and Jean-Marc, (2011) declares that increasing the G3P levels increases the TAG synthesis, however, it is not enough to increase total lipid accumulation in *Y. lipolytica.* Higher lipid accumulation can be achieved by combining the G3P with

increased free fatty acids (FFA) levels available due to blocking the β-oxidation pathway. Our results correlate with this since the NCYC 3363 strain *pex3/gut2*Δ double mutant gave a higher amount of lipid than the other mutants; where the *pex3Δ* blocks the β-oxidation pathway and the *gut2Δ* increased the G3P levels. Moreover, Beopoulos *et al.*, (2008) describes that the *gut2Δ* mutant and *gut2Δ*/pox1-6 mutant (pox1-6 mutants that block fatty acid β-oxidation) increased the accumulation of lipids in *Y. lipolytica* yeast; our results correlates with this paper the double mutant increased the lipid in the NCYC 3363 strain while the *gut2Δ* mutant increased the lipid in the NCYC102 strain. In addition, Alwan, (2017) states that the *gut2Δ* mutant gave more lipid than the WT in the NCYC 102 strain. Although, our results agree with her that the *gut2Δ* gave high amount of lipid in the NCYC 102, but the amount we obtained was lower than Alwan's because different growth conditions were used in the experiment, since the same conditions of Alwan's were used but higher amounts of lipid were not detected.

The significant key is the higher the OD the higher amount of lipid the cells give; correspondingly Gientka *et al.*, (2017) cites that high lipid concentration can be achieved if high productivity and high cell density are achieved during the growth phase. Gientka *et al.*, (2017) also states the lipid composition depends mainly on the yeast strain and the carbon source used. It should be evident from the results mentioned above that the NCYC 3363 strain accumulates more lipids than NCYC 102 strain. NCYC 3363 and NCYC 102 are extremely two different strains of *D. hansenii* which was clear from the way they reacted in the lipid assay.

Moreover, the results were consistent in NCYC 3363 in all 9 times the *pex3/gut2Δ* mutant gave the higher amount of lipid. However, the NCYC 102 is a partial diploid strain which has two copies of *FOX2* and *ARG1* genes. This suggests that the strain

might break down the lipids instead of accumulating them. Also, the results were not consistent each time one of the mutants gave a high amount of lipids, the overall result was the *gut2Δ* mutant gave a higher amount of lipids. In summary, more investigation into NCYC 3363 strain to get the appropriate conditions could give this strain a strong potential in Biotechnology and metabolic engineering.

Chapter6:

6.1 General Discussion

D. hansenii is a halotolerant, osmotolerant stress resistance yeast which can tolerate salt up to 4M NaCl while S. cerevisiae tolerates 1.7M NaCl (Larsson et al., 1990; Minhas et al., 2009). Prista et al., (2016) claimed that *D. hansenii* strains are highly heterogeneous genetically and biochemically. From a biotechnological point of view, they contribute directly and indirectly to the flavour of the foods in which they grow. The food industry's interest in *D. hansenii* is strongly associated with the salt tolerance qualities of this yeast (Prista *et al.*, 2016). In addition, it can utilize different carbon sources such as glucose, galactose, glycerol, and oleate. It can generate toxic chemicals that kill other yeasts, and which are important for the prospective control of yeast infections. Moreover, *D. hansenii* is one of the oleaginous yeasts which can store more than 20% of its biomass as neutral lipids (Gientka *et al.*, 2017). All these aspects are an interest in biotechnology. This study was conducted to investigate whether *D. hansenii* is amenable to genetic modification and genetic engineering.

The vast majority of the work in this area has focused on the halotolerant of *D. hansenii*, however, the lack of molecular tools was the main limitation when working with this yeast. Therefore, the development of new molecular tools for gene disruption was the primary step. Since *D. hansenii* is one of the CTG clade yeasts, which reads CTG (leucine) as serine, the CTG codons were modified in our heterologous selection cassettes in the way that they were translated to leucine instead of serine. First, auxotrophic markers were constructed, and it was found that

a 50bp flank can be used to direct the selection cassettes to the desired genomic location and delete the target gene through homologous recombination (HR) in *D. hansenii*. Since little is known about *D. hansenii*, some factors affecting *D. hansenii* growth were examined, and finally, after metabolic engineering whether the yeast could produce more fatty acids was investigated.

In brief**,** to work with *D. hansenii,* Kanamycin and Hygromycin B cassettes, were created as genetic tools. The cassette contained the ORF for bacterial aminoglycoside phosphotransferase (kan^r), which gives resistance in eukaryotes to geneticin (G418). A similar cassette was created using the ORF for a kinase that phosphorylates hygromycin B, and thereby inactivates this antibiotic; these cassettes were cloned in the pUC19 MCS. These cassettes can be used in any CTG clade yeast.

The *ARG1* gene was effectively removed using the HygroB marker in the NCYC102 strain, but unfortunately, there were at least two copies of the *ARG1* gene, whereas strains NCYC 3981 and NCYC 3363 had only one single copy. Initial attempts at gene deletion of *ARG1* were performed using a 1kb flanking region of the *ARG1* gene. Subsequently, we set out to shorten the flanks; this was inspired by previous work in *S. cerevisiae* and *S. pombe* were accomplished with 30–50 bp, and 80–100 bp flanks, respectively (Hegemann et al., 2014). The flanks are included in oligonucleotides that are used to PCR amplify the selection cassettes such and KanR or HygrB. The PCR product contains now the short flanks that will direct the selection cassette to its target site in genome after transformation (Baudin et al., 1993; Kaur et al., 1996) This is a quick and economic method to generate gene deletion mutants and it would be desirable if the same can be achieved with *D. hansenii*. Starting with 1kb flanks, the flanks were further truncated and even 50bp

still resulted in targeted gene deletions at high frequency. Whereas the whole gene of *ARG1* was deleted in the above experiments, we also found that deletion the *ARG1* ORF could be mediated by 50bp flanks.

Previously, to create a knockout in *D. hansenii* various steps are involved. First, the *D. hansenii* DNA was isolated. PCR was then performed to amplify the region of interest using primers designed in the Snap Gene program, to anneal both the start and the end of the region of interest. First, the upstream flank was inserted into the plasmid, then the PCR product was then purified to obtain pure DNA. The plasmid was transformed into *E. coli*, then mini prepped. After that, a restriction digest was then performed to cleave the plasmid and DNA. Gel extraction, ligation, and *E. coli* transformation were then performed. Mini prep and restriction digest were performed to ensure the insert was correct. The sequences were submitted for sequencing, as per the previous section 2.6.8. Restriction digest, gel extraction, and ligation were performed on the plasmid to insert the downstream flank. Then *E. coli* transformation, colony PCR, miniprep and another restriction digest were completed to check the insert was correct, and this was proven to be the case. The samples were than sequenced (section 2.6.8). Finally, the plasmid was cut into linear DNA by PCR and transformed to *D. hansenii* see Figure 24*. D. hansenii* colonies were checked for gene deletion using replica plate technique. Cells were then grown on selective media plates with high antibiotics to obtain pure colonies. This method was difficult to implement and took a long time to complete, however, now it has become easier to get a gene deletion in *D. hansenii* with the new 50bp flank method just PCR and then transform to *D. hansenii*, it saves time and material.

A key factor for the knockout to work was the concentration of DNA, high concentrations of DNA required precipitation of the PCR products. DNA precipitation

also improved knockout efficiency. This study was the first to find that using PCR amplification with 50bp flanks works in *D. hansenii* indeed this method provides a rapid and effective strategy for cloning using HR. In Chapter 3, the cloning of DNA was improved by HR in *D. hansenii* by using a 50 bp flank PCR method. This will no doubt encourage other researchers to use *D. hansenii*, saving them time and materials. It also improves the molecular tools used to manipulate this yeast. This will be the building block for biotechnology to work with *D. hansenii.* The new PCR mediated technique can be used to tag genes in the genome by introducing new promoters to mediate overexpression of the antibiotic to give the cells resistance to it. We used the technique to tag GFP-PTS1 under the control of *ACT1* promoter in the *pex3Δ* knockout cells, to target heterologous genes for metabolic engineering to the *ARG1* locus, and to proof that the *pex3Δ* was correct.

We tested 13 different *D. hansenii* strains for cloning and gene disruption. Unfortunately, eleven of strains had a second copy of *ARG1* gene, this might be because the sources of the strains were different. The 11 different strains of *D. hansenii*: CBS 13215, CBS 767, CBS 7848, CBS 13202, CBS 1102, CBS 5139, CBS 5307, CBS 13195, CBS 1142, CBS 1099, and NCYC 102. The sources of strains are different: Zooplankton, Carlsberg laboratories, Takuan Japanese salted pickle, Southern Ocean seawater 497M, beef-pork sausage, skin of man, stomach of fish, Southern Ocean seawater 4509M, sake-moto, cheese, and Carlsberg laboratories respectively. While NCYC 3363, and NCYC 3981 have only one copy of *ARG1* gene. Their sources were soy sauce, the Netherlands, and a lagoon in Greenwich Island, Antarctica, respectively. It is essential to have a haploid strain to work with because it makes gene disruption in yeast simpler. The NCYC 3363 seems to be a promising

strain to work with in *D. hansenii*. The strains can be tested to know if they are haploid or not by using the new modified PCR technique.

The research design involved studying the factors affecting the growth of *D. hansenii*. It is generally accepted knowledge that *D. hansenii* can grow in 4M NaCl (Larsson et al., 1990; Minhas et al., 2009; Navarrete, C., and Martínez, 2020), but these results were different because the maximum amount of salt that the cells could grow in was 3M NaCl, and none of the strains tested in the lab was able to grow in 4M NaCl. Manzanares-Estreder et al. (2017) found evidence in *S. cerevisiae* the peroxisomal function is crucial for the salt stress adaptation under sugar restriction. Our results in *D. hansenii* are inconsistent with this study because the mutants *pex3Δ* and *fox2Δ* cells proliferated under small low levels of glucose at different salt concentrations. However, *D. hansenii* responds differently to salt tolerances than *S. cerevisiae.* The *pex3Δ* mutant in *D. hansenii* and *S. cerevisiae* were able to grow like the WT in all different media with different amounts of glucose and salt. This experiment was performed several times: the same result was achieved in all experiments. This was discussed earlier in the thesis see Chapter 4 page 94. Salt tolerance is an important feature in *D. hansenii* because it indicates that the yeast is tough and can tolerate different stress conditions used in industry. So, it is a capable yeast to use in biotechnology.

Temperature has been tested as one of the factors affecting the growth of *D. hansenii*; different strains of *D. hansenii* were tested; this was done to better understand the yeast environment. Studying the factors that influence the growth of *D. hansenii* is important because it provides a clear picture of the yeast and its metabolism. Navarrete, C., and Martínez (2020) acknowledge the fact that *D. hansenii* can grow over a wide temperature range from 20^{o}C to 35^{o}C*,* and the results

suggest that at 30ºC they were not able to grow for the strains tested in the lab. The optimum temperature for *D. hansenii* was 25ºC, but there was a clear variation between different strains and the top temperature tolerated.

Then, the growth of *D. hansenii* on different carbon sources was analysed and compared to a range of other yeasts. It clearly showed that *D. hansenii* has the ability to grow strongly on all different carbon sources examined, frequently better than *S. cerevisiae*. Moreover, the peroxisomes biogenesis mutant *pex3Δ* and fatty acid oxidation mutant *fox2Δ* were able to grow on all different carbon sources of glucose, galactose, and glycerol. However, they initially grew slowly on media with the fatty acid as main carbon source before growth ceased. The initial growth is on components in the media other than oleate that can support low level of growth. One of the characteristics of *D. hansenii*: is that it is able to utilise a large variety of carbon sources such as maltose, lactose, arabinose, sucrose, and xylose (Dyerberg, Navarrete and Martínez, 2022) and grows in the presence of certain inhibitors such as vanillin, and methanol. It is an excellent option for working within industrial bioprocesses for both lignocellulosic and non-lignocellulosic biomass materials (Navarrete, Estrada and Martínez, 2022).

Finally, growth curves were performed as a *pex3Δ* phenotype, as described in Chapter 4. The WT and *pex3Δ* can be grown on glucose, galactose, and glycerol as carbon sources. This is because the curves overlap each other, and the *pex3Δ* can utilize the sugars without peroxisomes. On the other hand, *pex3Δ* grows very slowly on oleate, a t-test was performed and the P value=0.0001 was calculated, showing a significant difference between the WT and the *pex3Δ* curves. In Chapter 4, the results gave an overview of *D. hansenii, and* how it responds to different salinity, and different temperatures. It also has the ability to grow on different carbon sources.

Little is known about this yeast, so it was important to study in detail the factors that influence the growth of *D. hansenii*.

Lipid accumulation in strains NCYC 102 and NCYC 3363 strains of *D. hansenii* was then tested. The *PEX3* gene was knocked out to block the fatty acid β-oxidation pathway. *Pex3Δ* mutants cannot grow on oleate: growth curves were performed to demonstrate the phenotype described in Chapter 4. GFP-PTS1 was labelled in the *pex3Δ* and the WT cells using HygroB as a selectable marker to target the safe landing site of the *ARG1* gene. This proved that *pex3Δ* was correct as GFP-PTS1 was mislocalized to the cytosol, whereas in WT it was localized in the peroxisomes. *GUT2* was the next gene that was deleted in *D. hansenii,* it was deleted in both strains NCYC 102 and NCYC 3363. In the NCYC 102, it was deleted using the SAT1 marker, whereas in the NCYC 3363 it was deleted using the HygroB marker. *Gut2Δ* mutants cannot grow on glycerol; deletion of the *GUT2* gene leads to increased G3P production; this shifts the pathway to form more TAG. A *pex3Δ/gut2Δ* double mutant was then generated; in the same *pex3Δ* strain that was performed earlier, the *gut2Δ* was deleted. The double mutant is unable to grow on both glycerol and oleate media. As *pex3Δ* knockout produces fatty acids and the *gut2Δ* knockout produces G3P, it was expected that the double mutant would accumulate more lipids.

Thierry and Jean-Marc, (2011) state that increasing the G3P levels increases the TAG synthesis, but that is not enough to increase total lipid accumulation in *Y. lipolytica*: higher lipid accumulation can be achieved by combining the G3P with increased levels of available free fatty acids (FFA) by blocking the β-oxidation pathway. Our results correlate with this, as the NCYC 3363 strain *pex3/gut2*Δ double mutant resulted in higher lipid levels than the other mutants; where the *pex3Δ* blocks the β-oxidation pathway and the *gut2Δ* increased the G3P levels. Furthermore,

Beopoulos et al., (2008) describe that in *Y. lipolytica* yeast the *gut2Δ* mutant and *gut2Δ*/pox1-6 mutant (pox1-6 mutants that block fatty acid β-oxidation) increased the accumulation of lipids; the results associates with (Beopoulos et al., 2008) that the double mutant increased the lipid in the NCYC 3363 strain and the *gut2Δ* mutant increased the lipid in the NCYC102 strain. In addition, Alwan, (2017) stated that the *gut2Δ* mutant provided more lipids than the WT in the NCYC 102 strain: even though the results agree that the *gut2Δ* did produce large amounts of lipid in the NCYC 102, the amount obtained was lower than Alwan's (2017) study because different growth conditions were used. The main key is that the higher the OD, the more lipids the cells produce. Gientka et al.,(2017) therefore state that high lipid concentrations can be achieved if high productivity and high cell densities are achieved during the growth phase. Gientka et al., (2017) also state that lipid composition mainly depends on the yeast strain and the carbon source used. From the above results, it is thus clear that the NCYC 3363 strain accumulates more lipids than NCYC 102 strain. NCYC 3363 and NCYC 102 are very different strains of *D. hansenii,* as evidenced by their responses in the lipid assay. Furthermore, the results in NCYC 3363 were consistent on all 9 occasions where the *pex3/gut2Δ* mutant provided the higher amounts of lipid. However, the NCYC 102 is partial diploid strain which has two copies of *FOX2* and *ARG1* genes, therefore suggesting that the strain may be degrading lipids rather than accumulating them. Also, the results were not consistent each time one of the mutants gave more lipids, the overall result being that the *gut2Δ* mutant gave more lipids. In conclusion, further investigation into NCYC 3363 strain to obtain suitable conditions may provide this strain with excellent potential in biotechnology and metabolic engineering.

6.2 Possible further investigation

To improve the results in the NCYC 3363 strain some steps need to be taken. The nitrogen conditions need to be optimized first, by growing the cells on different amounts of nitrogen and see what is the finest amount that accumulates more lipids. to obtain an ideal starvation media. Another way to investigate is to knock out other genes such as *POX1 to POX6*, and *FOX3* to try to increase the lipid levels. In addition, the cells could be grown for 72 hours to check if the cells would die or if they might give a higher amount of lipid. After that, the salt tolerance needs to be checked to see if inducing the salt will give more lipids. Gas chromatography-mass spectrometry (GC-MS), and the fatty acid methyl esters (FAME) should be carried out to analyze the fatty acids. Nuclear magnetic resonance (NMR), which allows the visualization of single atoms and molecules would be done too. After that, it would be important to check the pH for the different strains of *D. h*ansenii and it would also be beneficial to plot the growth curve on both the NCYC 3363 and NCYC 3981 strains and to use the *pex3Δ* in all 10 different strains. Then, more molecular tools could be developed to work with this yeast.

References:

AAT Bioquest spectrum [Texas Red] (2021) Available at: https://www.aatbio.com/fluorescence-excitation-emission-spectrum-graph-viewer/texas_red_sulforhodamine_101_sulfonyl_chloride.

Aggarwal, M. and Mondal, A. K. (2009) 'Debaryomyces hansenii: An osmotolerant and halotolerant yeast', in *Yeast Biotechnology: Diversity and Applications*. Dordrecht: Springer Netherlands, pp. 65–84. doi: 10.1007/978-1-4020-8292-4_4.

Al-Saryi, N. A. *et al.* (2017) 'Two NAD-linked redox shuttles maintain the peroxisomal redox balance in Saccharomyces cerevisiae', *Scientific Reports*. Nature Publishing Group, 7(1), p. 11868. doi: 10.1038/s41598-017-11942-2.

Allenbach, L. and Poirier, Y. (2000) 'Analysis of the alternative pathways for the beta-oxidation of unsaturated fatty acids using transgenic plants synthesizing polyhydroxyalkanoates in peroxisomes', *Plant physiology*. American Society of Plant Biologists, 124(3), pp. 1159–1168. doi: DOI 10.1104/pp.124.3.1159.

Almagro, A. *et al.* (2000) 'Effects of salts on Debaryomyces hansenii and Saccharomyces cerevisiae under stress conditions', *International Journal of Food Microbiology*. Elsevier, 56(2–3), pp. 191–197. doi: 10.1016/S0168-1605(00)00220-8.

Alwan, Z. H. O. (2017) 'Neutral lipid production by the yeast Debaryomyces hansenii NCYC102 under different stress conditions', Thesis, University of Sheffield.

Baudin, A. *et al.* (1993) 'A simple and efficient method for direct gene deletion in Saccharomyces cerevisiae', *Nucleic Acids Research*, 21(14), pp. 3329–3330. doi: 10.1093/nar/21.14.3329.

Beopoulos, A. *et al.* (2008) 'Control of lipid accumulation in the yeast Yarrowia

lipolytica', *Applied and Environmental Microbiology*. American Society for Microbiology, 74(24), pp. 7779–7789. doi: 10.1128/AEM.01412-08.

Beopoulos, A. *et al.* (2009) 'Yarrowia lipolytica as a model for bio-oil production', *Progress in Lipid Research*. Elsevier Ltd, 48(6), pp. 375–387. doi: 10.1016/j.plipres.2009.08.005.

Cao, M. *et al.* (2018) 'CRISPR–Mediated Genome Editing and Gene Repression in Scheffersomyces stipitis', *Biotechnology Journal*, 13(9), pp. 5–9. doi: 10.1002/biot.201700598.

Coffey, A. G., Daly, C. and Fitzgerald, G. (1994) 'The impact of biotechnology on the dairy industry', *Biotechnology Advances*, 12(4), pp. 625–633. doi: 10.1016/0734-9750(94)90003-5.

Converti, A. and Dominguez, J. M. (2001) 'Influence of temperature and pH on xylitol production from xylose by Debaryomyces hansenii UFV-170', *Process Biochemistry*. John Wiley & Sons, Ltd, 41(3), pp. 675–681. doi: 10.1016/j.procbio.2005.08.019.

Converti, A., Perego, P. and Domínguez, J. M. (1999) 'Xylitol Production from Hardwood Hemicellulose Hydrolysates by Pachysolen tannophilus, Debaryomyces hansenii, and Candida guilliermondii', *Applied Biochemistry and Biotechnology*. Humana Press, 82(2), pp. 141–152. doi: 10.1385/ABAB:82:2:141.

Danner, H. and Braun, R. (1999) 'Biotechnology for the production of commodity chemicals from biomass', *Chemical Society Reviews*. Royal Society of Chemistry, 28(6), pp. 395–405. doi: 10.1039/a806968i.

Domínguez, J. M. *et al.* (1999) 'Xylitol production from wood hydrolyzates by entrapped Debaryomyces hansenii and Candida guilliermondii cells', *Applied*

Biochemistry and Biotechnology - Part A Enzyme Engineering and Biotechnology. Humana Press, 81(2), pp. 119–130. doi: 10.1385/ABAB:81:2:119.

Dujon, B. *et al.* (2004) 'Genome evolution in yeasts', *Nature*. Nature Publishing Group, 430(6995), pp. 35–44. doi: 10.1038/nature02579.

Durá, M. A., Flores, M. and Toldrá, F. (2004) 'Effect of Debaryomyces spp. on the proteolysis of dry-fermented sausages', *Meat Science*. Elsevier, 68(2), pp. 319–328. doi: 10.1016/j.meatsci.2004.03.015.

Dyerberg, A. S. B., Navarrete, C. and Martínez, J. L. (2022) 'High-throughput screening of a Debaryomyces hansenii library for potential candidates with improved stress tolerance and wider carbon utilisation capabilities'. BioRxiv. https://doi.org/10.1101/2022.03.24.485636.

Esser, K. *et al.* (2004) 'The mitochondrial IMP peptidase of yeast: Functional analysis of domains and identification of Gut2 as a new natural substrate', *Molecular Genetics and Genomics*, 271(5), pp. 616–626. doi: 10.1007/s00438-004-1011-y.

Fakas, S. (2017) 'Lipid biosynthesis in yeasts: A comparison of the lipid biosynthetic pathway between the model nonoleaginous yeast Saccharomyces cerevisiae and the model oleaginous yeast Yarrowia lipolytica', *Engineering in Life Sciences*, 17(3), pp. 292–302. doi: 10.1002/elsc.201600040.

Fang, Y. *et al.* (2004) 'PEX3 functions as a PEX19 docking factor in the import of class I peroxisomal membrane proteins', *Journal of Cell Biology*. Rockefeller University Press, 164(6), pp. 863–875. doi: 10.1083/jcb.200311131.

Flores, M. *et al.* (2017) 'Screening of Debaryomyces hansenii Strains for Flavor Production under a Reduced Concentration of Nitrifying Preservatives Used in Meat

Products', *Journal of Agricultural and Food Chemistry*, 65(19), pp. 3900–3909. doi: 10.1021/acs.jafc.7b00971.

Gálvez-López, D. *et al.* (2019) 'The metabolism and genetic regulation of lipids in the oleaginous yeast Yarrowia lipolytica', *Brazilian Journal of Microbiology*. Brazilian Journal of Microbiology, 50(1), pp. 23–31. doi: 10.1007/s42770-018-0004-7.

Gedvilaite, A. and Sasnauskas, K. (1994) 'Control of the expression of the ADE2 gene of the yeast Saccharomyces cerevisiae', *Current Genetics*, 25(6), pp. 475–479. doi: 10.1007/BF00351665.

Gientka, I. *et al.* (2017) 'Identification and Characterization of Oleaginous Yeast Isolated from Kefir and Its Ability to Accumulate Intracellular Fats in Deproteinated Potato Wastewater with Different Carbon Sources', *BioMed Research International*. Hindawi Limited, 2017. doi: 10.1155/2017/6061042.

Gil-Mascarell, R. *et al.* (1999) 'The Arabidopsis HAL2-like gene family includes a novel sodium-sensitive phosphatase', *Plant Journal*, 17(4), pp. 373–383. doi: 10.1046/j.1365-313X.1999.00385.x.

Gírio, F. M. *et al.* (2000) 'Polyols production during single and mixed substrate fermentations in Debaryomyces hansenii', *Bioresource Technology*. Elsevier, 71(3), pp. 245–251. doi: 10.1016/S0960-8524(99)00078-4.

Gould, S. G., Keller, G. A. and Subramani, S. (1987) 'Identification of a peroxisomal targeting signal at the carboxy terminus of firefly luciferase.', *The Journal of cell biology*. Rockefeller University Press, 105(6 Pt 2), pp. 2923–31. doi: 10.1083/JCB.105.6.2923.

Gould, S. J. *et al.* (1989) 'A conserved tripeptide sorts proteins to peroxisomes',

Journal of Cell Biology. Rockefeller University Press, 108(5), pp. 1657–1664. doi: 10.1083/jcb.108.5.1657.

Gould, S. J. *et al.* (1990) 'Peroxisomal protein import is conserved between yeast, plants, insects and mammals.', *The EMBO Journal*. John Wiley & Sons, Ltd, 9(1), pp. 85–90. doi: 10.1002/j.1460-2075.1990.tb08083.x.

Gould, S. J., Keller, G. A. and Subramani, S. (1988) 'Identification of peroxisomal targeting signals located at the carboxy terminus of four peroxisomal proteins.', *The Journal of cell biology*. Rockefeller University Press, 107(3), pp. 897–905. doi: 10.1083/JCB.107.3.897.

Greenspan, P. and Fowler, S. D. (1985) 'Spectrofluorometric studies of the lipid probe, nile red', *Journal of Lipid Research*. Â© 1985 ASBMB. Currently published by Elsevier Inc; originally published by American Society for Biochemistry and Molecular Biology., 26(7), pp. 781–789. doi: 10.1016/s0022-2275(20)34307-8.

Greenspan, P., Mayer, E. P. and Fowler, S. D. (1985) 'Nile red: A selective fluorescent stain for intracellular lipid droplets', *Journal of Cell Biology*, 100(3), pp. 965–973. doi: 10.1083/jcb.100.3.965.

Guerrero, C. A. *et al.* (2005) 'Salt-dependent expression of ammonium assimilation genes in the halotolerant yeast, Debaryomyces hansenii', *Current Genetics*, 47(3), pp. 163–171. doi: 10.1007/s00294-004-0560-2.

Güneşer, O. *et al.* (2015) 'Bioflavour production from tomato and pepper pomaces by Kluyveromyces marxianus and Debaryomyces hansenii', *Bioprocess and Biosystems Engineering*. Springer Berlin Heidelberg, 38(6), pp. 1143–1155. doi: 10.1007/s00449-015-1356-0.

Hegemann, J. H. *et al.* (2014) ‘Targeted gene deletion in Saccharomyces cerevisiae and Schizosaccharomyces pombe’, in *Methods in Molecular Biology*, pp. 45–73. doi: 10.1007/978-1-4939-0799-1_5.

Hettema, E. H. *et al.* (1996) ‘The ABC transporter proteins Pat1 and Pat2 are required for import of long-chain fatty acids into peroxisomes of Saccharomyces cerevisiae.’, *The EMBO Journal*, 15(15), pp. 3813–3822. doi: 10.1002/j.1460-2075.1996.tb00755.x.

Hettema, E. H. *et al.* (2000) ‘Saccharomyces cerevisiae Pex3p and Pex19p are required for proper localization and stability of peroxisomal membrane proteins’, *The EMBO Journal*. EMBO Press, 19(2), pp. 223–233. doi: 10.1093/emboj/19.2.223.

Hettema, E. H. *et al.* (2014) ‘Evolving models for peroxisome biogenesis’, *Current Opinion in Cell Biology*. Elsevier Ltd, 29(1), pp. 25–30. doi: 10.1016/j.ceb.2014.02.002.

Hettema, E. H. and Tabak, H. F. (2000) ‘Transport of fatty acids and metabolites across the peroxisomal membrane’, *Biochimica et Biophysica Acta (BBA) - Molecular and Cell Biology of Lipids*. Elsevier, 1486(1), pp. 18–27. doi: 10.1016/S1388-1981(00)00045-7.

Hiltunen, J. K. *et al.* (1992) ‘Peroxisomal multifunctional β-oxidation protein of Saccharomyces cerevisiae. Molecular analysis of the FOX2 gene and gene product’, *Journal of Biological Chemistry*, 267(10), pp. 6646–6653. doi: 10.1016/s0021-9258(19)50476-8.

Hoepfner, D. *et al.* (2005) ‘Contribution of the Endoplasmic Reticulum to Peroxisome Formation’, *Cell*. Cell Press, 122(1), pp. 85–95. doi: 10.1016/J.CELL.2005.04.025.

Jacques, N. *et al.* (2010) ‘Population polymorphism of nuclear mitochondrial dna insertions reveals widespread diploidy associated with loss of heterozygosity in debaryomyces hansenii’, *Eukaryotic Cell*, 9(3), pp. 449–459. doi: 10.1128/EC.00263-09.

Jacques, N. *et al.* (2015) ‘Increased diversity in the genus Debaryomyces from Arctic glacier samples’, *Antonie van Leeuwenhoek, International Journal of General and Molecular Microbiology*, 107(2), pp. 487–501. doi: 10.1007/s10482-014-0345-7.

Jacques, N., Mallet, S. and Casaregola, S. (2009) ‘Delimitation of the species of the Debaryomyces hansenii complex by intron sequence analysis’, *International Journal of Systematic and Evolutionary Microbiology*, 59(5), pp. 1242–1251. doi: 10.1099/ijs.0.004325-0.

Jeffries, T. W. and Cregg, J. M. (2010) ‘Protein Expression in Nonconventional Yeasts’, *Genetics, Strain improvement and Recombinant Proteins*, (64), pp. 302–311. Available at: https://www.fpl.fs.fed.us/documnts/pdf2010/fpl_2010_jeffries001.pdf (Accessed: 7 January 2019).

Jiru, T. M. and Abate, D. (2014) ‘Oleaginous microorganisms, diversity, lipid biosynthesis pathway and strain improvement’, *WebPub Journal of Scientific Research*, 2(6), pp. 55–65. Available at: http://www.researchwebpub.org/wjsr.

Johnson, E. A. and Echavarri-Erasun, C. (2011a) ‘Debaryomyces - an overview’, in Kurtzman, C. P., W, F. J., and Teun, B. (eds) *The Yeasts*. fifth, pp. 21–44. Available at: https://www.sciencedirect.com/topics/immunology-and-microbiology/debaryomyces (Accessed: 11 January 2019).

Johnson, E. A. and Echavarri-Erasun, C. (2011b) 'Yeast biotechnology', in *The Yeasts*. Elsevier, pp. 21–44. doi: 10.1016/B978-0-444-52149-1.00003-3.

Jones, J. M., Morrell, J. C. and Gould, S. J. (2004) 'PEX19 is a predominantly cytosolic chaperone and import receptor for class 1 peroxisomal membrane proteins.', *The Journal of cell biology*. Rockefeller University Press, 164(1), pp. 57–67. doi: 10.1083/jcb.200304111.

Joshi, A. S. *et al.* (2018) 'Lipid droplet and peroxisome biogenesis occur at the same ER subdomains', *Nature Communications*. Nature Publishing Group, 9(1), p. 2940. doi: 10.1038/s41467-018-05277-3.

Kalish, J. E. *et al.* (1996) 'Characterization of a novel component of the peroxisomal protein import apparatus using fluorescent peroxisomal proteins.', *The EMBO journal*. John Wiley & Sons, Ltd, 15(13), pp. 3275–85. doi: 10.1016/S1388-2457(01)00739-8.

Kamineni, A. *et al.* (2021) 'Increasing lipid yield in Yarrowia lipolytica through phosphoketolase and phosphotransacetylase expression in a phosphofructokinase deletion strain', *Biotechnology for Biofuels*. BioMed Central, 14(1), pp. 1–14. doi: 10.1186/s13068-021-01962-6.

Kao, Y.-T., Gonzalez, K. L. and Bartel, B. (2017) 'Peroxisome function, biogenesis, and dynamics in plants', *Plant Physiology*. American Society of Plant Biologists, 176(1), p. pp.01050.2017. doi: 10.1104/pp.17.01050.

Kaur, R., Ingavale, S. S. and Bachhawat, A. K. (1996) 'PCR-Mediated Direct Gene Disruption in Schizosaccharomyces Pombe', *Nucleic Acids Research*, 25(5), pp. 1080–1081. doi: 10.1093/nar/25.5.1080.

Kim, P. K. and Hettema, E. H. (2015) ‘Multiple pathways for protein transport to peroxisomes’, *Journal of Molecular Biology*. Elsevier, pp. 1176–1190. doi: 10.1016/j.jmb.2015.02.005.

Kuzminov, A. (2011) ‘Homologous Recombination-Experimental Systems, Analysis and Significance’, *EcoSalplus*, 4(2). doi: 10.1128/ecosalplus.7.2.6.

Larsson, C. *et al.* (1990) ‘Osmoregulation of the salt-tolerant yeast Debaryomyces hansenii grown in a chemostat at different salinities’, *Journal of Bacteriology*. American Society for Microbiology Journals, 172(4), pp. 1769–1774. doi: 10.1128/jb.172.4.1769-1774.1990.

Larsson, C. *et al.* (1998) ‘The importance of the glycerol 3-phosphate shuttle during aerobic growth of Saccharomyces cerevisiae’, *Yeast*, 14(4), pp. 347–357. doi: 10.1002/(SICI)1097-0061(19980315)14:4<347::AID-YEA226>3.0.CO;2-9.

Lassmann T., F. O. and S. E. L. (2009) ‘Kalign2: high-performance multiple alignment of protein and nucleotide sequences allowing external features.’, *Nucleic Acids Research*, 37(3), pp. 858–65. doi: 10.1093/nar/gkn1006.

Leathers, T. D. and Gupta, S. C. (1997) ‘Xylitol and riboflavin accumulation in xylose-grown cultures of Pichia guilliermondii’, *Applied Microbiology and Biotechnology*, 47(1), pp. 58–61. doi: 10.1007/s002530050888.

Ledesma-Amaro, R. and Nicaud, J. M. (2016) ‘Yarrowia lipolytica as a biotechnological chassis to produce usual and unusual fatty acids’, *Progress in Lipid Research*. The Authors, 61, pp. 40–50. doi: 10.1016/j.plipres.2015.12.001.

Lodhi, I. J. and Semenkovich, C. F. (2014) ‘Peroxisomes: A nexus for lipid metabolism and cellular signaling’, *Cell Metabolism*. NIH Public Access, pp. 380–

392. doi: 10.1016/j.cmet.2014.01.002.

López-Linares, J. C. *et al.* (2018) 'Xylitol production by Debaryomyces hansenii and Candida guilliermondii from rapeseed straw hemicellulosic hydrolysate', *Bioresource Technology*. Elsevier, 247(July 2017), pp. 736–743. doi: 10.1016/j.biortech.2017.09.139.

Manzanares-Estreder, S. *et al.* (2017) 'Multilayered control of peroxisomal activity upon salt stress in *S accharomyces cerevisiae*', *Molecular Microbiology*. Blackwell Publishing Ltd, 104(5), pp. 851–868. doi: 10.1111/mmi.13669.

Mattanovich, D., Sauer, M. and Gasser, B. (2014) 'Yeast biotechnology: teaching the old dog new tricks', *Microbial Cell Factories*. BioMed Central, 13(1), p. 34. doi: 10.1186/1475-2859-13-34.

McKay, L. L. and Baldwin, K. A. (1990) 'Applications for biotechnology: present and future improvements in lactic acid bacteria', *FEMS Microbiology Letters*. No longer published by Elsevier, 87(1–2), pp. 3–14. doi: 10.1111/j.1574-6968.1990.tb04876.x.

Miesfeld, R. L. and McEvoy, M. M. (2017) 'Biochemistry', in Twitchell, B. (Carla L. T. (ed.) *Biochemistry*. First Edit. W.W.Norton & company, pp. 447–451.

Minhas, A., Biswas, D. and Mondal, A. K. (2009) 'Development of host and vector for high-efficiency transformation and gene disruption in *Debaryomyces hansenii*', *FEMS Yeast Research*. Oxford University Press, 9(1), pp. 95–102. doi: 10.1111/j.1567-1364.2008.00457.x.

Mishra, S. and Baranwal, R. (2009) *Yeast biotechnology: Diversity and applications*, *Yeast Biotechnology: Diversity and Applications*. doi: 10.1007/978-1-4020-8292-4.

Motley, A. M. and Hettema, E. H. (2007) ‘Yeast peroxisomes multiply by growth and division’, *Journal of Cell Biology*. Rockefeller University Press, 178(3), pp. 399–410. doi: 10.1083/jcb.200702167.

Motley, A. M., Nuttall, J. M. and Hettema, E. H. (2012) ‘Pex3-anchored Atg36 tags peroxisomes for degradation in Saccharomyces cerevisiae’, *EMBO Journal*. Nature Publishing Group, 31(13), pp. 2852–2868. doi: 10.1038/emboj.2012.151.

Munck, J. M. *et al.* (2009) ‘A dual function for Pex3p in peroxisome formation and inheritance’, *Journal of Cell Biology*, 187(4), pp. 463–471. doi: 10.1083/jcb.200906161.

Navarrete, C.,and Martínez, J. L. (2020) ‘Non-conventional yeasts as superior production platforms for sustainable fermentation based bio-manufacturing processes’, *AIMS Bioengineering*, 7(4), pp. 289–305. doi: 10.3934/bioeng.2020024.

Navarrete, C. *et al.* (2009) ‘Oxidative stress sensitivity in Debaryomyces hansenii’, *FEMS Yeast Research*, 9(4), pp. 582–590. doi: 10.1111/j.1567-1364.2009.00500.x.

Navarrete, C. *et al.* (2022) ‘DebaryOmics: an integrative –omics study to understand the halophilic behaviour of Debaryomyces hansenii’, *Microbial Biotechnology*, 15(4), pp. 1133–1151. doi: 10.1111/1751-7915.13954.

Navarrete, C., Estrada, M. and Martínez, J. L. (2022) ‘Debaryomyces hansenii : an old acquaintance for a fresh start in the era of the green biotechnology’, *World Journal of Microbiology and Biotechnology*. Springer Netherlands, pp. 1–10. doi: 10.1007/s11274-022-03280-x.

Nett, J. H. *et al.* (2005) ‘Cloning and disruption of the Pichia pastoris ARG1, ARG2, ARG3, HIS1, HIS2, HIS5, HIS6 genes and their use as auxotrophic markers’, *Yeast*,

22, pp. 295–304. doi: 10.1002/yea.1202.

NOUT, M. J. R. (2003) ‘Traditional fermented products from Africa, Latin America and Asia’, in *Yeasts in Food*. Woodhead Publishing Ltd, pp. 451–473. doi: 10.1533/9781845698485.451.

Padilla, B., Manzanares, P. and Belloch, C. (2014) ‘Yeast species and genetic heterogeneity within Debaryomyces hansenii along the ripening process of traditional ewes’ and goats’ cheeses’, *Food Microbiology*. Elsevier Ltd, 38, pp. 160–166. doi: 10.1016/j.fm.2013.09.002.

Papouskova, K. and Sychrova, H. (2007) ‘The co-action of osmotic and high temperature stresses results in a growth improvement of Debaryomyces hansenii cells’, *International Journal of Food Microbiology*, 118(1), pp. 1–7. doi: 10.1016/j.ijfoodmicro.2007.04.005.

Petersen, K. M. and Jespersen, L. (2004) ‘Genetic diversity of the species Debaryomyces hansenii and the use of chromosome polymorphism for typing of strains isolated from surface-ripened cheeses’, *Journal of Applied Microbiology*, 97, pp. 205–213. doi: 10.1111/j.1365-2672.2004.02293.x.

Poirier, Y. *et al.* (2006) ‘Peroxisomal β-oxidation-A metabolic pathway with multiple functions’, *Biochimica et Biophysica Acta - Molecular Cell Research*. Elsevier, pp. 1413–1426. doi: 10.1016/j.bbamcr.2006.08.034.

Prista, C. *et al.* (2005) ‘Mechanisms underlying the halotolerant way of Debaryomyces hansenii’, *FEMS Yeast Research*. Oxford University Press, pp. 693–701. doi: 10.1016/j.femsyr.2004.12.009.

Prista, C. *et al.* (2016) ‘The halotolerant Debaryomyces hansenii, the Cinderella of

non-conventional yeasts', *Yeast*. John Wiley & Sons, Ltd, 33(10), pp. 523–533. doi: 10.1002/yea.3177.

Qiao, K. *et al.* (2017) 'Lipid production in Yarrowia lipolytica is maximized by engineering cytosolic redox metabolism', *Nature Biotechnology*. Nature Publishing Group, 35(2), pp. 173–177. doi: 10.1038/nbt.3763.

Ramírez-Orozco, M., Hernández-Saavedra, N. Y. and Ochoa, J. L. (2001) 'Debaryomyces hansenii growth in nonsterile seawater ClO2 - Peptone-containing medium', *Canadian Journal of Microbiology*, 47(7), pp. 676–679. doi: 10.1139/cjm-47-7-676.

Ramos, J. *et al.* (2017) 'Debaryomyces hansenii strains from Valle de los pedroches Iberian dry meat products: Isolation, identification, characterization, and selection for starter cultures', *Journal of Microbiology and Biotechnology*, 27(9), pp. 1576–1585. doi: 10.4014/jmb.1704.04045.

Reuß, O. *et al.* (2004) 'The SAT1 flipper, an optimized tool for gene disruption in Candida albicans', *Gene*, 341(1–2), pp. 119–127. doi: 10.1016/j.gene.2004.06.021.

Rivas, B. *et al.* (2003) 'Carbon Material and Bioenergetic Balances of Xylitol Production from Corncobs by Debaryomyces hansenii', *Biotechnology Progress*. American Chemical Society (ACS), 19(3), pp. 706–713. doi: 10.1021/bp025794v.

van Roermund, C. W. T. *et al.* (2003) 'Fatty acid metabolism in Saccharomyces cerevisiae', *Cellular and Molecular Life Sciences (CMLS)*. Birkhäuser-Verlag, 60(9), pp. 1838–1851. doi: 10.1007/s00018-003-3076-x.

Van Roermund, C. W. T. *et al.* (2012) 'Peroxisomal Fatty Acid Uptake Mechanism in Saccharomyces cerevisiae *', *Journal of Biological Chemistry*, 287(24), pp. 20144-

20153. doi: 10.1074/jbc.M111.332833.

Sánchez, N. S. *et al.* (2006) ‘Glycolytic sequence and respiration of Debaryomyces hansenii as compared to Saccharomyces cerevisiae’, *Yeast*. John Wiley & Sons, Ltd, 23(5), pp. 361–374. doi: 10.1002/yea.1360.

Seiler, H. and Busse, M. (1990) ‘The yeasts of cheese brines’, *International Journal of Food Microbiology*, 11(3–4), pp. 289–303. doi: 10.1016/0168-1605(90)90022-W.

Sibirny, A. A. (2016) ‘Yeast peroxisomes: Structure, functions and biotechnological opportunities’, *FEMS Yeast Research*. Edited by J. Nielsen. Oxford University Press, pp. 1–14. doi: 10.1093/femsyr/fow038.

Smulian, A. G. *et al.* (2007) ‘Expression of hygromycin phosphotransferase alters virulence of Histoplasma capsulatum’, *Eukaryotic Cell*, 6(11), pp. 2066–2071. doi: 10.1128/EC.00139-07.

Sørensen, B. B. (1997) ‘Lipolysis of pork fat by the meat starter culture Debaryomyces hansenii at various environmental conditions’, *International Journal of Food Microbiology*. Elsevier, 34(2), pp. 187–193. doi: 10.1016/S0168-1605(96)01183-X.

Spasskaya, D. S. *et al.* (2021) ‘CRISPR/Cas9-Mediated Genome Engineering Reveals the Contribution of the 26S Proteasome to the Extremophilic Nature of the Yeast Debaryomyces hansenii’, *ACS Synthetic Biology*, 10(2), pp. 297–308. doi: 10.1021/acssynbio.0c00426.

Steiner, S. and Philippsen, P. (1994) ‘Sequence and promoter analysis of the highly expressed TEF gene of the filamentous fungus Ashbya gossypii’, *MGG Molecular & General Genetics*. Springer-Verlag, 242(3), pp. 263–271. doi: 10.1007/BF00280415.

Strucko, T. *et al.* (2021) ‘A CRISPR/Cas9 method facilitates efficient oligo-mediated gene editing in Debaryomyces hansenii’, *Synthetic Biology*, 6(1), pp. 1–9. doi: 10.1093/synbio/ysab031.

Subramani, S. (1992) ‘Targeting of proteins into the peroxisomal matrix’, *The Journal of Membrane Biology*. Springer-Verlag, pp. 99–106. doi: 10.1007/BF00233350.

Swinkels, B. W. *et al.* (1992) ‘A novel, cleavable peroxisomal targeting signal at the amino-terminus of the rat 3-ketoacyl-coA thiolase’, *Trends in Cell Biology*. Rockefeller University Press, 2(2), p. 38. doi: 10.1016/0962-8924(92)90153-E.

Van Den Tempel, T. and Jakobsen, M. (2000) ‘The technological characteristics of Debaryomyces hansenii and Yarrowia lipolytica and their potential as starter cultures for production of Danablu’, *International Dairy Journal*. Elsevier, 10(4), pp. 263–270. doi: 10.1016/S0958-6946(00)00053-4.

Thierry, D. and Jean-marc, N. (2011) ‘Involvement of the G3P shuttle and b - oxidation pathway in the control of TAG synthesis and lipid accumulation in Yarrowia lipolytica’, *Metabolic Engineering*. Elsevier, 13(5), pp. 482–491. doi: 10.1016/j.ymben.2011.05.002.

Thomé, P. E. (2007) ‘Cell wall involvement in the glycerol response to high osmolarity in the halotolerant yeast Debaryomyces hansenii’, *Antonie van Leeuwenhoek, International Journal of General and Molecular Microbiology*. Kluwer Academic Publishers, 91(3), pp. 229–235. doi: 10.1007/s10482-006-9112-8.

Thomé, P. E. and Trench, R. K. (1999) ‘Osmoregulation and the genetic induction of glycerol-3-phosphate dehydrogenase by NaCl in the euryhaline yeast Debaryomyces hansenii’, *Marine Biotechnology*. Springer-Verlag, 1(3), pp. 230–238. doi:

10.1007/PL00011772.

Vieira Gomes, A. *et al.* (2018) ‘Comparison of Yeasts as Hosts for Recombinant Protein Production’, *Microorganisms*. Multidisciplinary Digital Publishing Institute (MDPI), 6(2), p. 38. doi: 10.3390/microorganisms6020038.

Vigliotta, G. *et al.* (2007) ‘Nitrite metabolism in Debaryomyces hansenii TOB-Y7, a yeast strain involved in tobacco fermentation’, *Applied Microbiology and Biotechnology*. Springer-Verlag, 75(3), pp. 633–645. doi: 10.1007/s00253-007-0867-2.

Visser, W. F. *et al.* (2007) ‘Metabolite transport across the peroxisomal membrane.’, *The Biochemical journal*. Portland Press Limited, 401(2), pp. 365–75. doi: 10.1042/BJ20061352.

Wanders, R. J. A. (2004) ‘Peroxisomes, lipid metabolism, and peroxisomal disorders’, *Molecular Genetics and Metabolism*. Academic Press, 83(1–2), pp. 16–27. doi: 10.1016/J.YMGME.2004.08.016.

Wanders, R. J. A. *et al.* (2010) ‘Peroxisomes, lipid metabolism and lipotoxicity’, *Biochimica et Biophysica Acta (BBA) - Molecular and Cell Biology of Lipids*. Elsevier, 1801(3), pp. 272–280. doi: 10.1016/J.BBALIP.2010.01.001.

Wanders, R. J. A. and Waterham, H. R. (2006) ‘Biochemistry of Mammalian Peroxisomes Revisited’, *The annual Review of Biochemistry*, 75, pp. 295-332. doi: 10.1146/annurev.biochem.74.082803.133329.

Yaguchi, A., Rives, D. and Blenner, M. (2017) ‘New kids on the block: emerging oleaginous yeast of biotechnological importance’, *AIMS Microbiology*, 3(2), pp. 227–247. doi: 10.3934/microbiol.2017.2.227.

Yamashita, S. ichi *et al.* (2014) ‘The membrane peroxin PEX3 induces peroxisome-ubiquitination-linked pexophagy’, *Autophagy*, 10(9), pp. 1549–1564. doi: 10.4161/auto.29329.

Zhang, K. *et al.* (2015) ‘Genomic reconstruction to improve bioethanol and ergosterol production of industrial yeast Saccharomyces cerevisiae’, *Journal of Industrial Microbiology and Biotechnology*, 42(2), pp. 207–218. doi: 10.1007/s10295-014-1556-7.